

THE DIVERSITY OF CARBON IN COMETARY REFRACTORY DUST PARTICLES

IR spectroscopy of comets, and
the Story of the “The Diversity of Primitive Refractory Grains”

Diane H. Wooden (NASA Ames), with contributions from:

- *comet observations team: Mike Kelley (UMD), David Harker (UCSD/CASS),
Chick Woodward (UMN)*
- *review article ‘WIZ2017’ : Wooden, Hope Ishii, Mike Zolensky*
- *discussions with Stardust team members, including Rhonda Stroud*

PHILOSOPHICAL
TRANSACTIONS A

rsta.royalsocietypublishing.org

Research



Cometary Dust: The Diversity
of Primitive Refractory Grains

D. H. Wooden¹, H. A. Ishii² and M. E.
Zolensky³

¹NASA Ames Research Center, Moffett Field, CA
94035-0001, USA

An Idea to consider

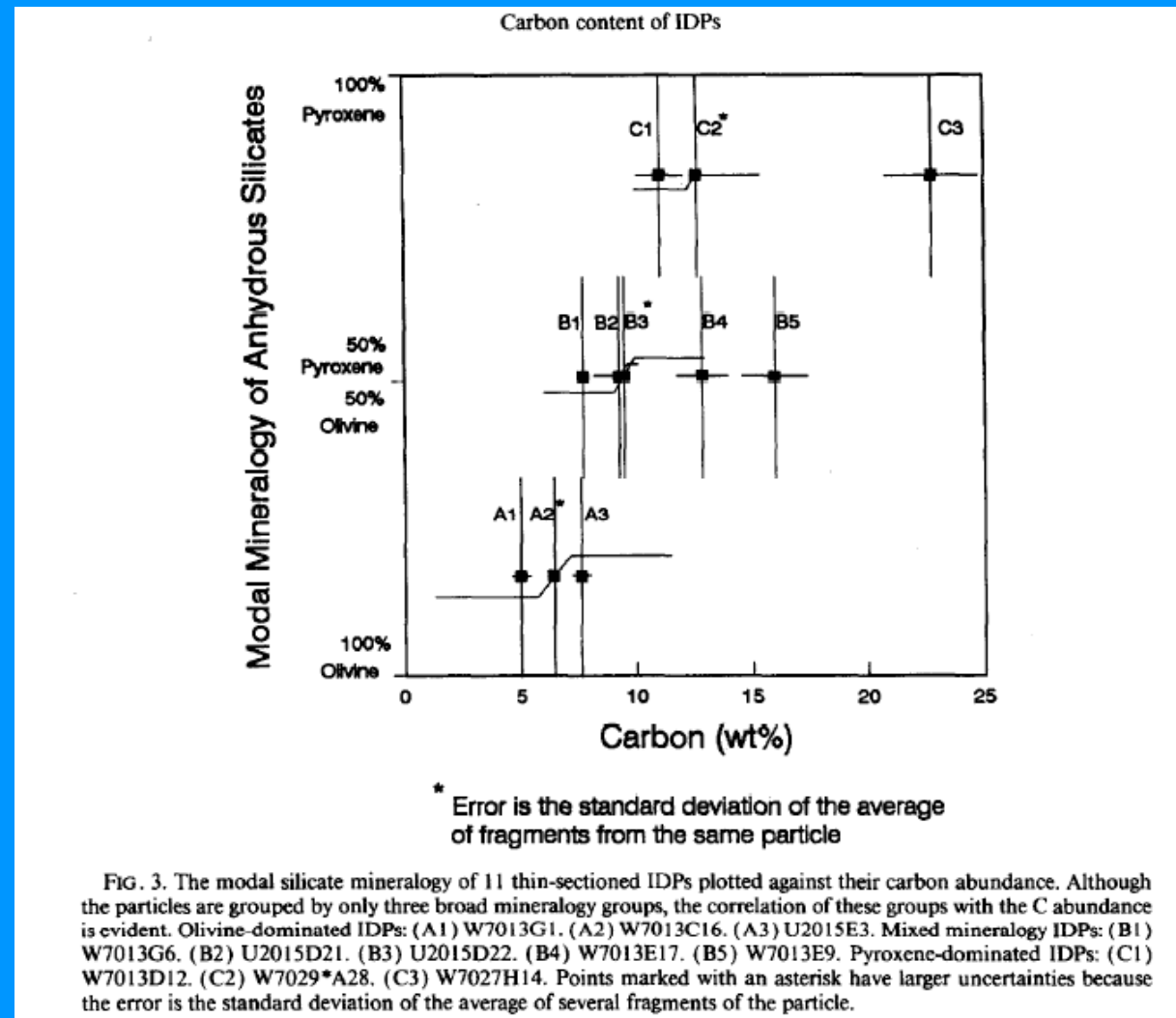
- » In the solid state refractory materials ...
- » More Primitive is related to greater diversity and on smaller scales (nanoscale to submicron scale)

Thomas+92-94 studies showed Carbon content of cometary 'anhydrous IDPs' can have 5 wt%–25 wt% C or as high as 45 wt% (90 vol%)

- » pyroxene- (Enstatite-) dominated IDPs have systematically higher C abundances
- » 2-3x to 13x CI abundances
- » up to 90 vol% C
- » acts as matrix holding mineral grains

IDPs). We performed point-count analyses of thin sections of two pyroxene-dominated IDPs: W7027H14 and L2006B23. Results show that W7027H14 contains 40–50 vol% carbonaceous material, which is in good agreement with an estimate of ~40 vol%, assuming a particle diameter of 10 μm , a particle density of 1 g cm^{-3} [9], and ~23 wt% C (bulk). L2006B23 has ~45 wt% C, the highest reported bulk C of any IDP. The volume percent of C is ~90, determined by point counting, and agrees with the theoretical estimate of 90 vol% based on a particle diameter of 15 μm , density of 1 g cm^{-3} [9], 45 wt% C (bulk), and ~50% porosity.

The nature of the carbonaceous material in anhydrous IDPs is poorly known. We have not observed graphitized C (i.e., 0.34 nm spacings) in any particles, nor have we observed C in the form of carbonates. Rather, the carbonaceous material could be poorly graphitized or amorphous. The C-rich phases in L2006B23 have a vesicular texture, indicating the loss of volatiles, probably hydrocarbons. It seems plausible that several C phases could co-exist in anhydrous IDPs.



Stardust & IDPs: Near-IR transmission spectra

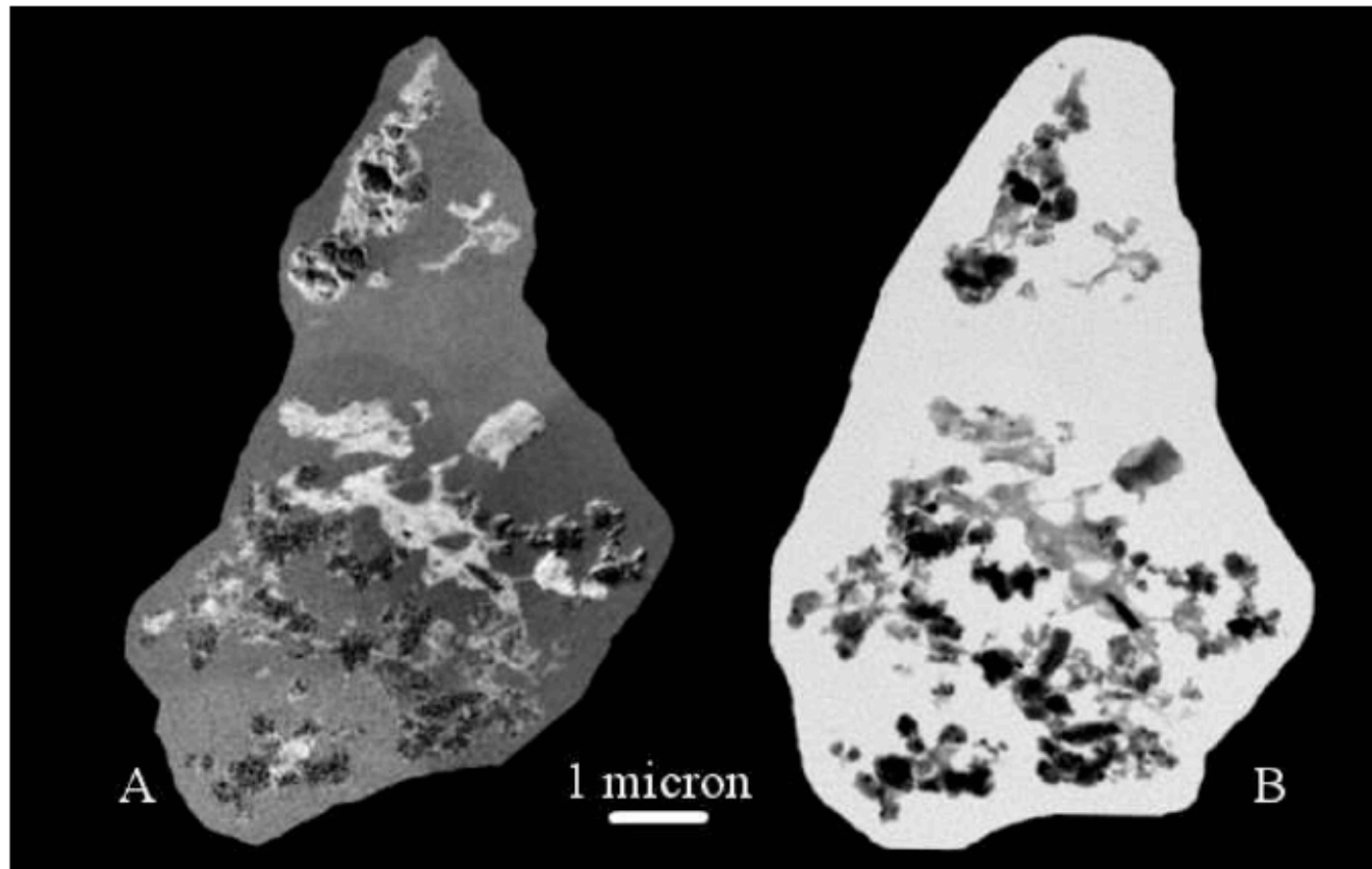


Figure 1. Transmission electron micrograph of IDP GS. (A) Carbon map of the particle. The bright areas are C-rich. (B) Bright field image of the particle.

» IDP GS = 26P/Grigg-Skjellerup collection (Earth running through stream)

THE ASTROPHYSICAL JOURNAL, 765:145 (18pp), 2013 March 10

THE ORIGIN OF THE $3.4\ \mu\text{m}$ FEATURE IN WILD 2 COMETARY PARTICLES
AND IN ULTRACARBONACEOUS INTERPLANETARY DUST PARTICLES

G. MATRAJT¹, G. FLYNN², D. BROWNLEE³, D. JOSWIAK³, AND S. BAJT³

Stardust & IDPs: Near-IR transmission spectra

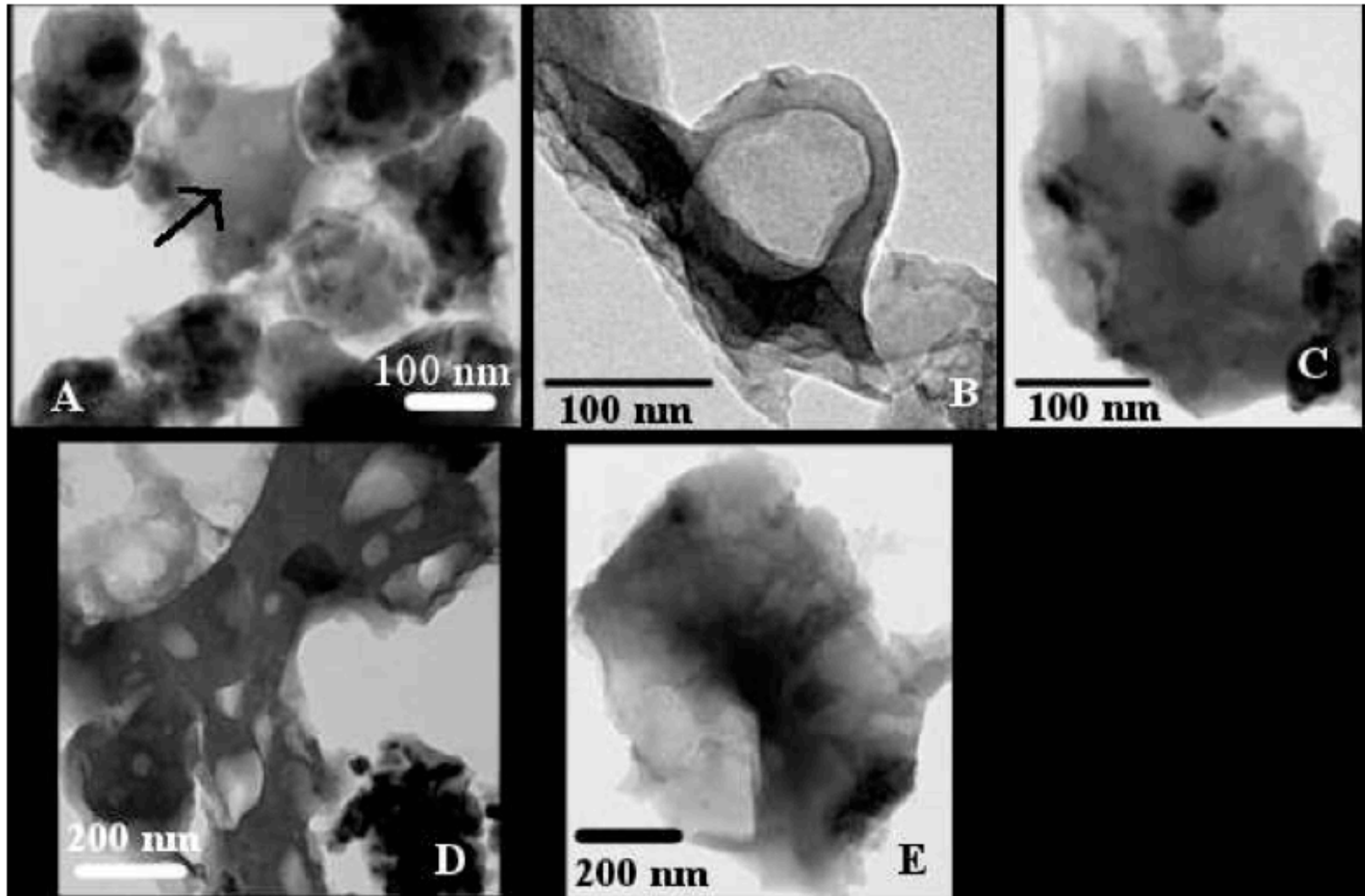


Figure 2. Micrographs of IDP GS showing the different textures for the carbonaceous materials. (A) Vesicular. The arrow points to the small vesicles. (B) Globular. (C) Dirty. (D) Spongy. (E) Smooth.

Stardust & IDPs: Near-IR transmission spectra

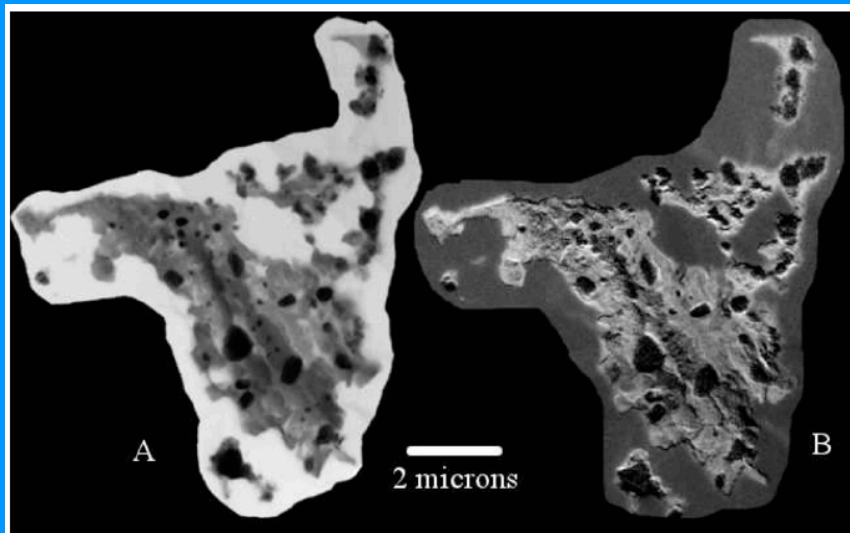


Figure 5. Micrograph of IDP Chocha. (A) Bright field image of the particle. (B) Carbon map of particle.

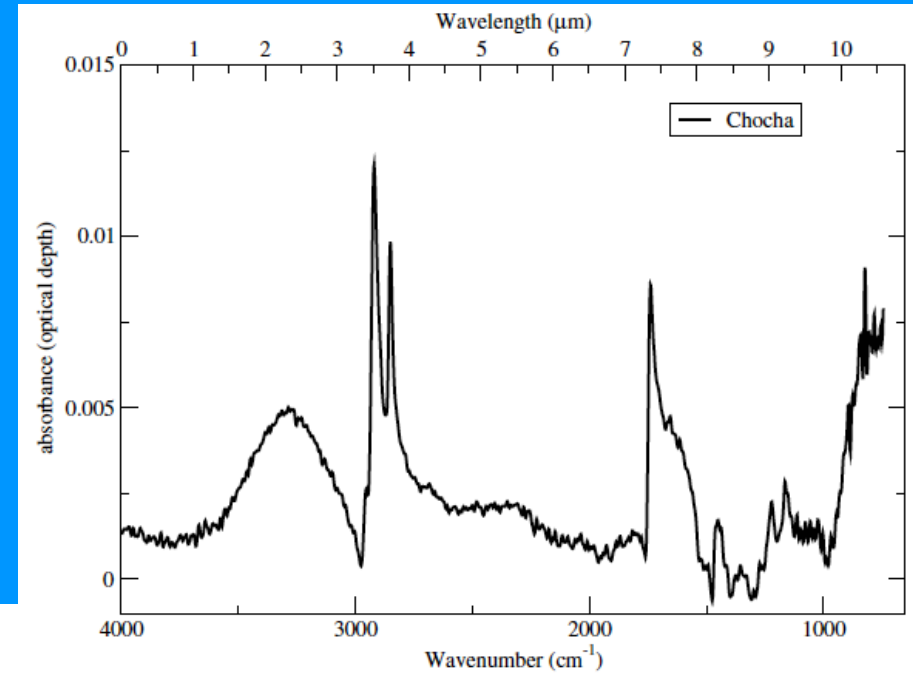


Figure 7. IR spectrum of particle Chocha.

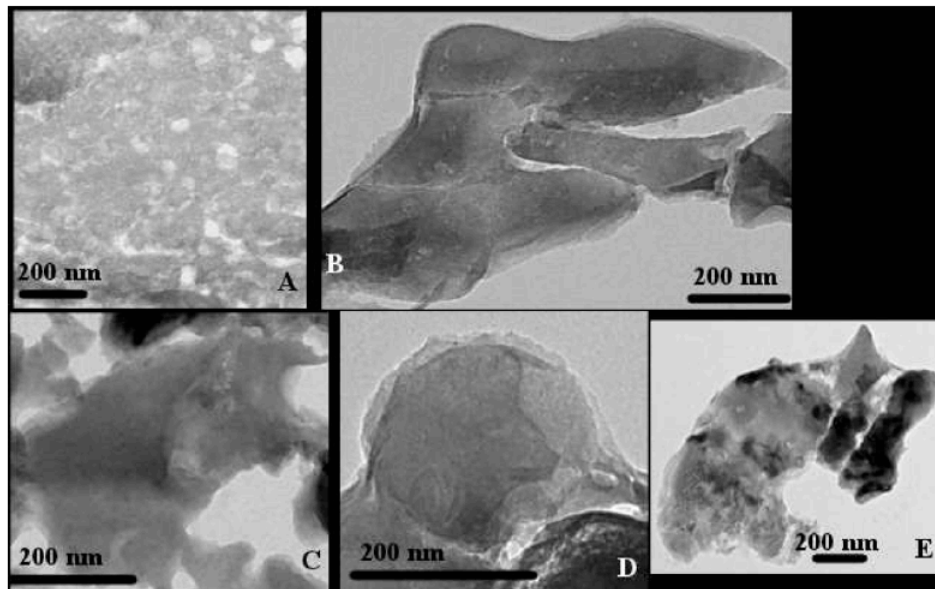


Figure 6. Micrographs of IDP Chocha showing the different textures of the carbonaceous materials. (A) Spongy. (B) Vesicular. (C) Smooth. (D) Globular (note that this is a filled globule). (E) Dirty.

Chocha
aromatic

Stardust & IDPs: Near-IR transmission spectra

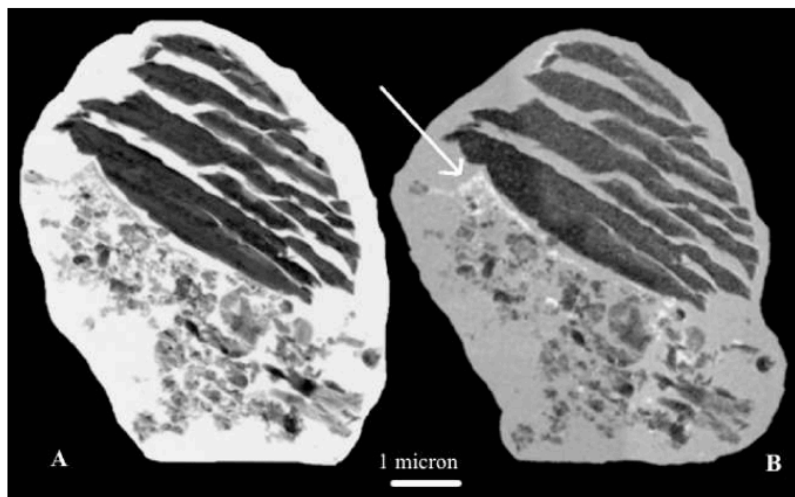
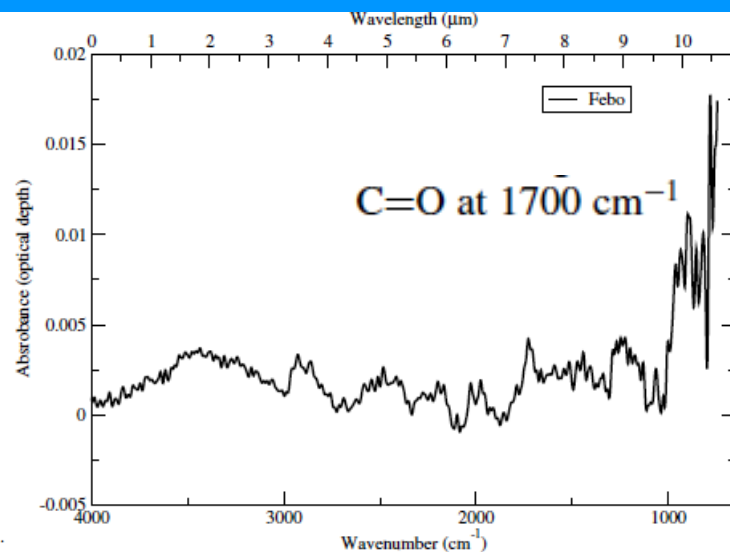


Figure 8. Micrograph of Wild 2 particle Febo. (A) Bright field image of the particle. (B) Carbon map of particle. The arrow points toward the fine-grained material.



Febo
fine-
grained

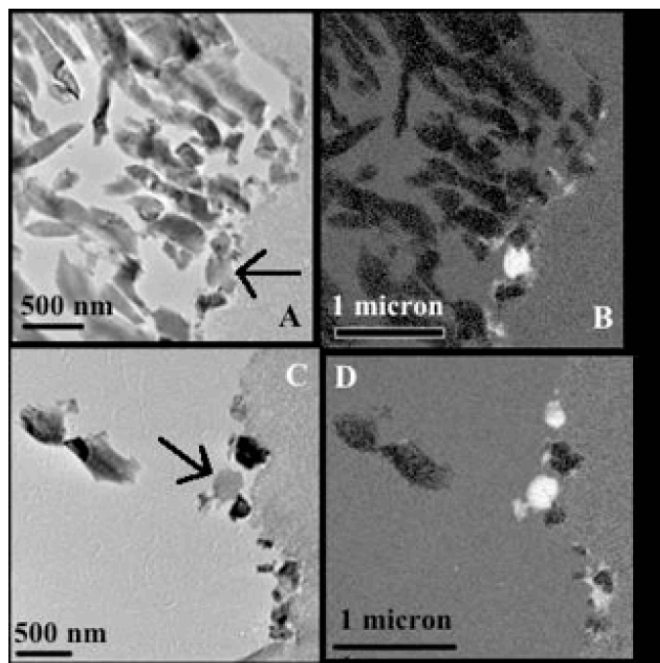


Figure 11. Micrographs of particle Ada. (A) Bright field of an area of the particle. The arrow points to the C-rich globule. (B) Carbon map of the area shown in (A). The bright areas are C-rich. (C) Bright field image of another C-rich area in this particle. The arrow points to a C-rich globule. (D) Carbon map of the area shown in (C).

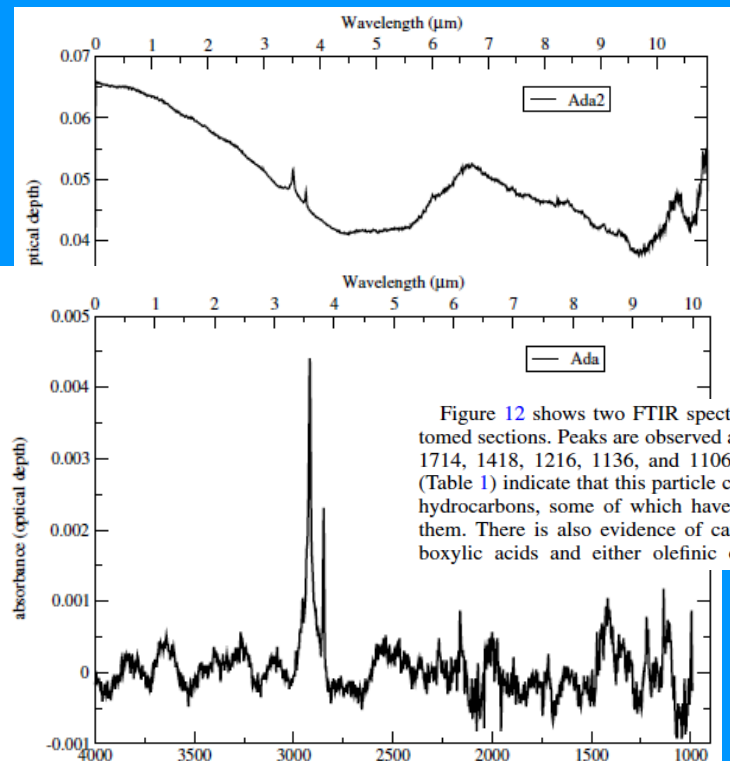


Figure 12 shows two FTIR spectra of two different microtomed sections. Peaks are observed at 2954, 2918, 2847, 2160, 1714, 1418, 1216, 1136, and 1106 cm⁻¹. Peak assignments (Table 1) indicate that this particle contains chains of aliphatic hydrocarbons, some of which have C=C groups attached to them. There is also evidence of carbonyl in ketone and carboxylic acids and either olefinic or aromatic C=C bonds.

Ada
2
regions

flipped by Diane (R → 'absorption')

Stardust & Near-IR transmission spectra

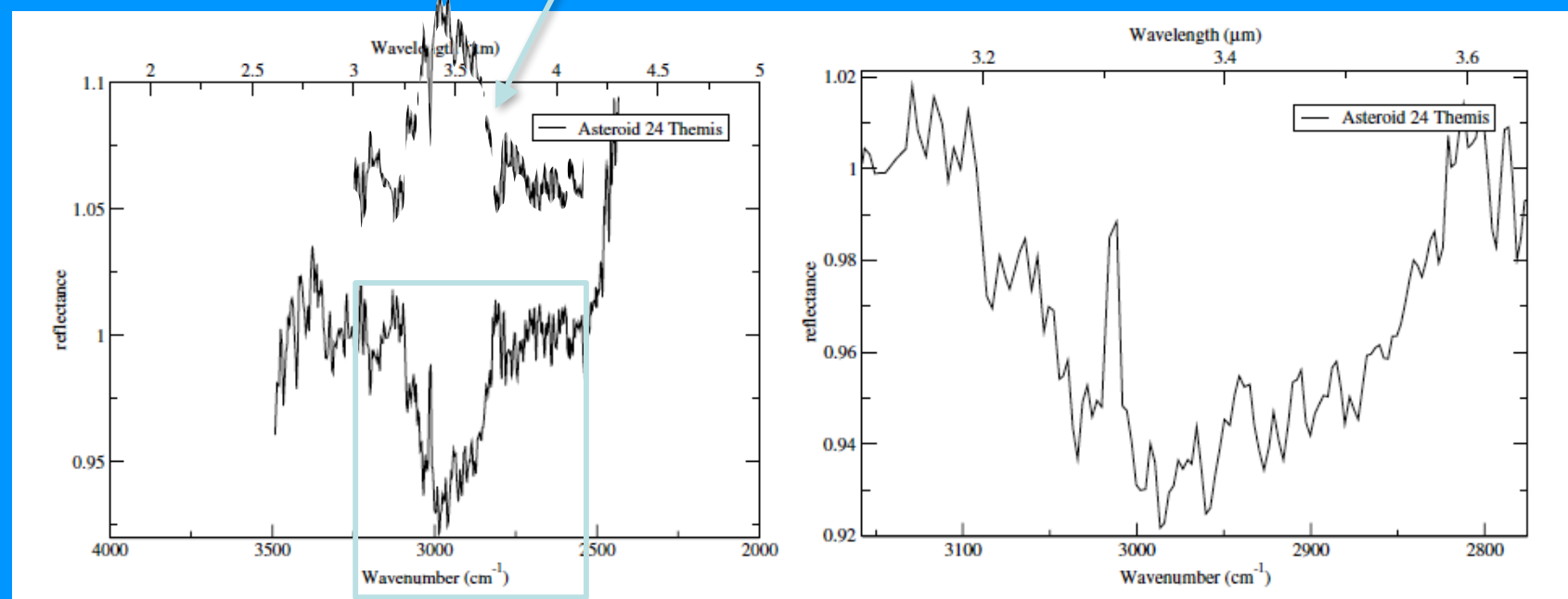


Figure 15. Left panel: IR spectrum of asteroid 24 Themis ratioed to the water-ice model of Rivkin & Emery (2010). Right panel: zoom of the spectrum shown in the left panel. Spectrum reproduced from Rivkin & Emery (2010) and Campins et al. (2010).

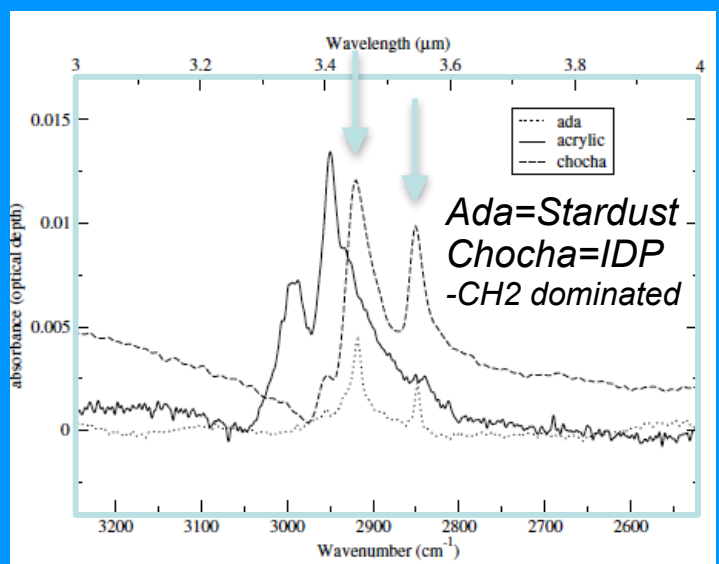


Figure 14. Comparison of particles Ada and Chocha to acrylic.

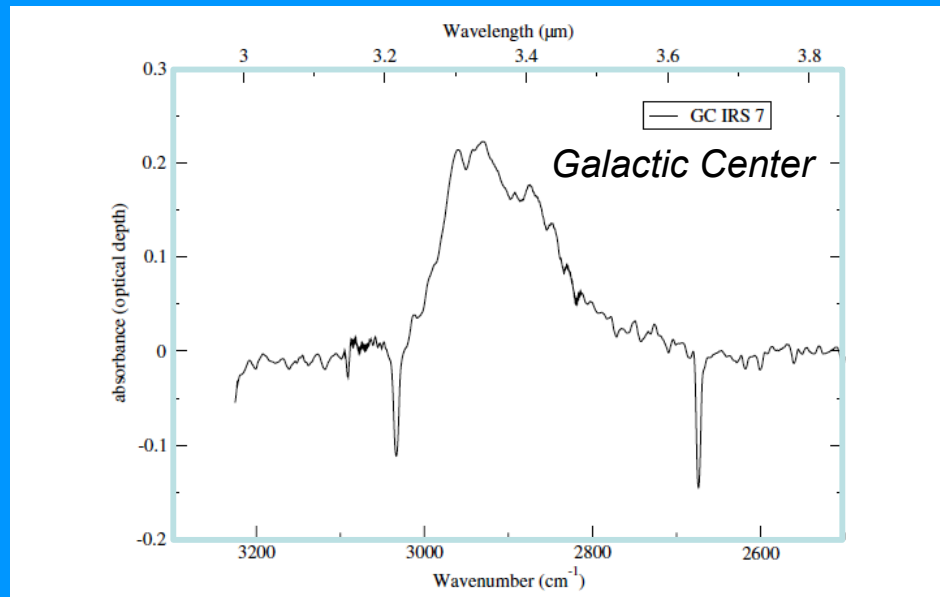


Figure 17. IR spectrum of the galactic center source IRS 7, obtained from the Infrared Space Observatory Data Center.

Stardust & IDPs: Near-IR transmission spectra

THE ASTROPHYSICAL JOURNAL, 765:145 (18pp), 2013 March 10

MATRAJT ET AL.

Table 1
Peak Assignments

Peak Position (in cm^{-1})	Vibration Mode	Interpretation	Sample That Has It
3255, 3270	OH	Water	GS, Chocha
2990	C=C-H	...	Acrylic
2951, 2954, 2950, 2949, 2958	CH ₃ asymmetric stretching	Aliphatic hydrocarbons	GS, Chocha, Febo, Ada, Acrylic, DISM
2920, 2918, 2929, 2925, 2922	CH ₂ asymmetric stretching	Aliphatic hydrocarbons	GS, Chocha, Febo, Ada, DISM
2896, 2870, 2860, 2874	CH ₃ symmetric stretching	Aliphatic hydrocarbons	GS, Febo, DISM
2845, 2847, 2855	CH ₂ symmetric stretching	Aliphatic hydrocarbons	GS, Chocha, Febo, Ada, DISM
2160	C=C stretching	...	Ada
1740	C=O carbonyl	Esters	Chocha
1730, 1717, 1700, 1714, 1727	C=O carbonyl	Ketone, carboxylic acid	Febo, Ada, acrylic
1685	H-O-H	Water	Febo
1654, 1650	C=C stretching	Aromatics	Chocha, Febo, Ada, acrylic
1545-1455	CO ³⁻	Carbonates	GS
1480	CH ₃ asymmetric bending	Aliphatic hydrocarbons	Chocha, acrylic
1447-1448	CH ₂ asymmetric bending	Aliphatic hydrocarbons	Chocha, acrylic
1418, 1435	C=C stretching	Aromatics	Chocha, Febo, Ada, acrylic
1350, 1386	CH ₃ symmetric bending	Aliphatic hydrocarbons	Acrylic
1240, 1270	C-O-C	Esters	Acrylic
1220	CH ₂ symmetric bending	Aliphatic hydrocarbons	Chocha
1147, 1190	Unknown
1160	CH ₂ twisting	Aliphatic hydrocarbons	Chocha
1065	C-OH	Secondary cyclic alcohols	Acrylic
987, 970, 910	CH=CH bending	...	Acrylic
1070, 1060, 952	Si-O	Pyroxene	GS, Febo
1216, 1136, 1106, 1010, 930	Si-O	Silicates	Febo, Ada
880	Si-O	Olivine	Febo

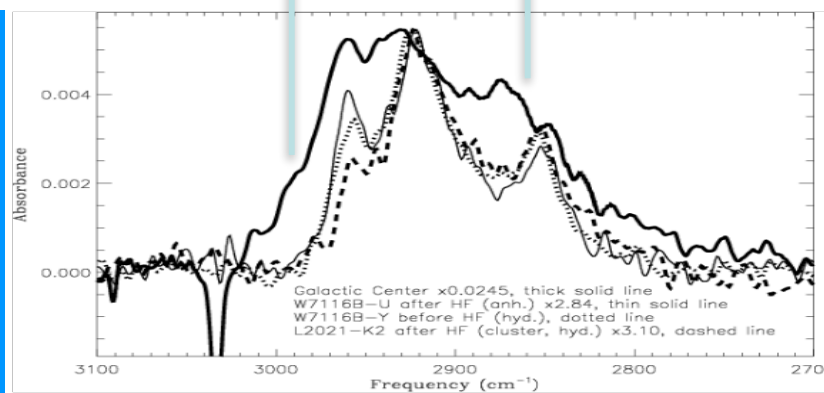
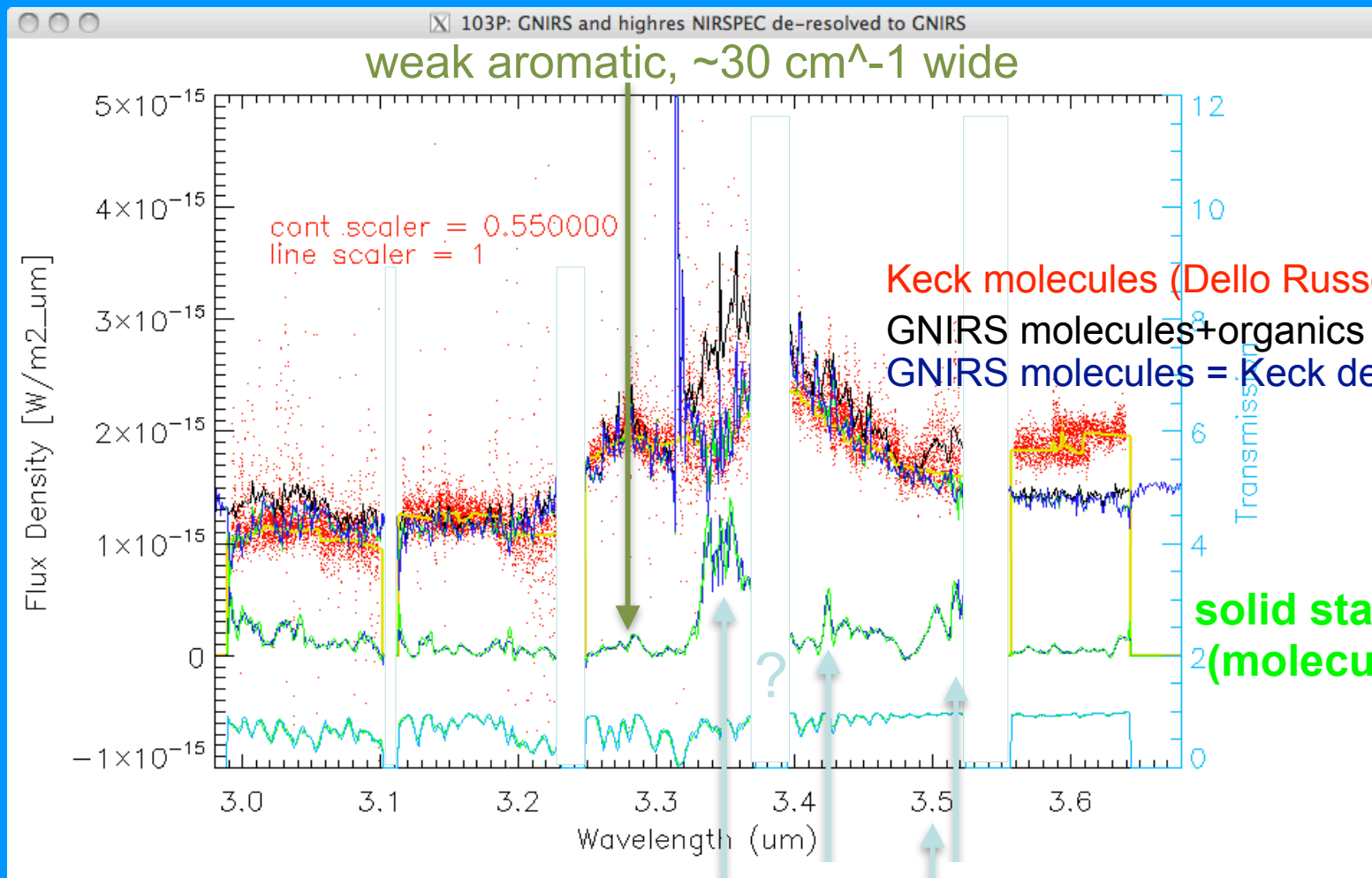
Note. The assignments are based on what was previously reported in the literature (Matrajt et al. 2004, 2005; Muñoz Caro et al. 2006 and references therein).

Stardust & IDPs: Near-IR transmission spectra

Table 2
CH₂/CH₃ Band Depth Ratios

Object/Sample	CH ₂ /CH ₃	Reference
DISM (GC IRS7)	0.96–1.25	Sandford et al. (1991)
DISM (GC IRS7)	0.92–1.2 average 1.06	Pendleton et al. (1994)
Extragalactic ISM (Seyfert 2)	2.0	Dartois et al. (2004)
Tagish Lake	4.36	Matrajt et al. (2004)
IDPs	1.0–5.6 average 2.4	Flynn et al. (2003)
IDPs	1.88–3.69 average 2.47	Matrajt et al. (2005)
Wild 2 samples	1.7–2.8 average 2.15 aerogel 2.15	Muñoz Caro et al. (2008)
Wild 2 samples	2.5	Keller et al. (2006); Sandford et al. (2006)
IOM Murchison	1.5	Ehrenfreund et al. (1991)
IOM Murchison	1.09	Flynn et al. (2003)
IOM Orgueil	1–1.51	Ehrenfreund et al. (1991)
Ultracarbonaceous IDP Chocha	4.6	This study
Ultracarbonaceous IDP GS	1.01	This study
Wild 2 Febo	1.96	This study
Wild 2 Ada	4.3	This study
Comet 103P/Hartley 2 (coma)	No CH ₃ or CH ₂ bands so no ratio calculated	A'Hearn et al. (2011); Wooden et al. (2011)
Asteroid 24 Themis	Not calculated	Campins et al. (2010); Rivkin & Emery (2010)

103P/Hartley 2 (prelim Wooden+11, paper in prep.) aliphatics and aromatics revealed when molecules subtracted



Stardust & IDPs: Other studies



Meteoritics & Planetary Science 47, Nr 4, 525–549 (2012)
doi: 10.1111/j.1945-5100.2011.01310.x

Diverse forms of primordial organic matter identified in interplanetary dust particles

Graciela MATRAJT^{1*}, Scott MESSENGER², Don BROWNLEE¹, and Dave JOSWIAK¹

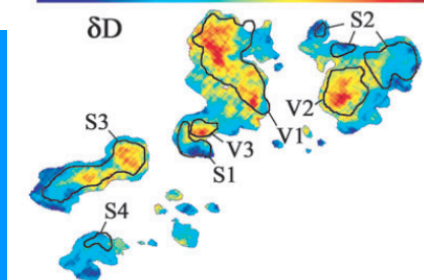
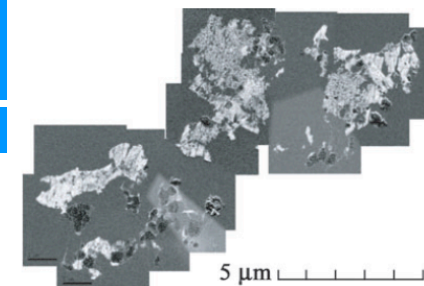


Fig. 14. EFTEM carbon image of an ultramicrotome section of IDP Chocha (top). δD isotopic image of the same section shown above (bottom). The color scale bar corresponds to the δD value in the H isotopic image. The outlines of seven morphologically distinct regions identified by BF and EFTEM images are shown in the δD image, including three spongy regions (V1–V3) and four vesicular regions (S1–S4). The shapes of the carbonaceous morphologies identified in TEM imaging correspond very well to isotopically distinct subregions in the H isotopic image.

Meteoritics & Planetary Science 44, Nr 10, 1611–1626 (2009)

Abstract available online at <http://meteoritics.org>

Organic matter from comet 81P/Wild 2, IDPs, and carbonaceous meteorites; similarities and differences

S. WIRICK^{1*}, G. J. FLYNN², L. P. KELLER³, K. NAKAMURA-MESSENGER³, C. PELTZER¹, C. JACOBSEN¹, S. SANDFORD⁴, and M. ZOLENSKY³

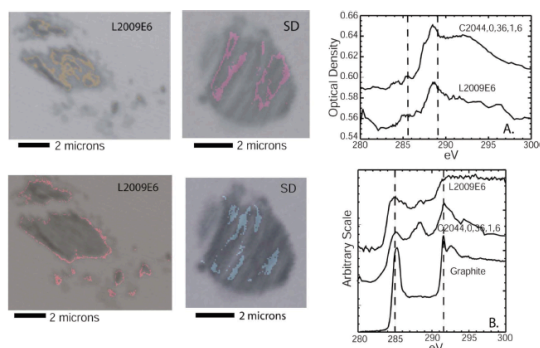


Fig. 4. Comparison of a heated IDP iron sulfide to an 81P/Wild 2 iron sulfide (SD=Stardust). The colored regions are CLUSTER areas with the CLUSTER spectra from these areas plotted in the graphs to the right of the images. The CLUSTER areas were overlaid onto STXM images of both of the particles.

A&A 433, 979–995 (2005)

DOI: 10.1051/0004-6361:20041605

FTIR analysis of the organics in IDPs: Comparison with the IR spectra of the diffuse interstellar medium

G. Matrajt¹, G. M. Muñoz Caro¹, E. Dartois¹, L. d'Hendecourt¹, D. Deboffle¹, and J. Borg¹

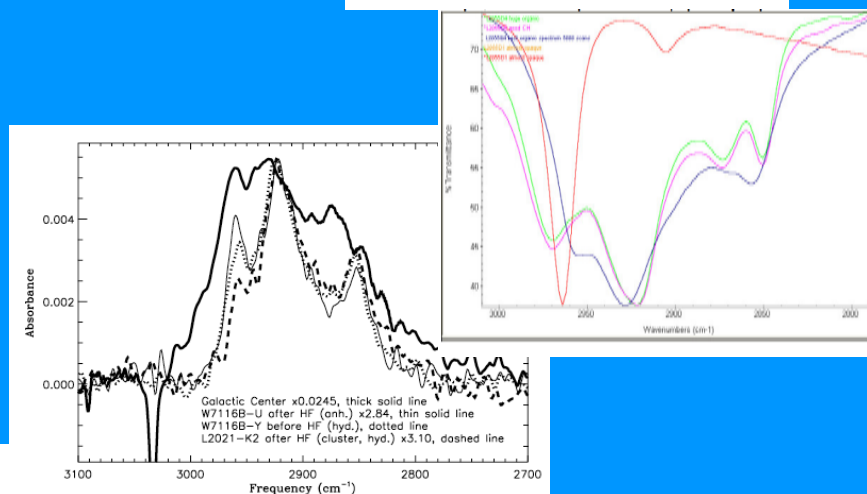


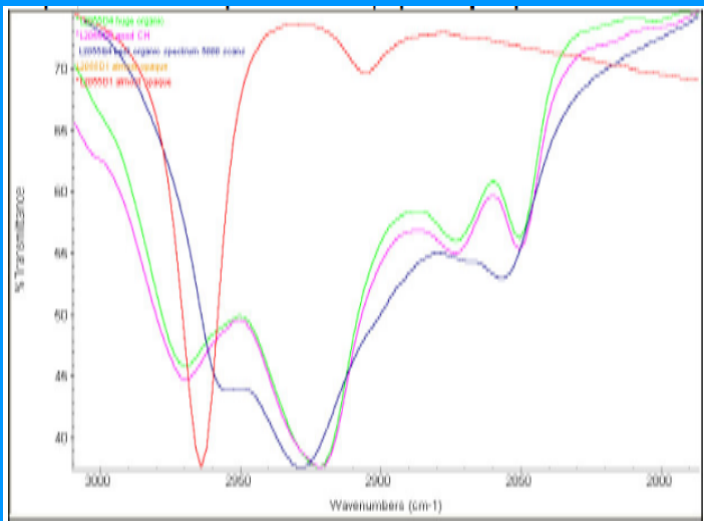
Fig. 9. Comparison of the spectrum of the particles W7116B-Y (hydrated) before HF, L2021-K2 (cluster, hydrated) after HF and W7116B-U (anhydrous) after HF to the IRS 7 source (Galactic Center). Only the 2800–3100 cm^{-1} region is shown. The Galactic Center source spectrum has been obtained from the Infrared Space Observatory (ISO) Data Center.

CP IDPs: Other studies

Comparison of Carbon XANES Spectra from an Iron Sulfide from Comet Wild 2 with an Iron Sulfide Interplanetary Dust Particle. S. Wirick¹, G. J. Flynn², L. P. Keller³, S. A. Sandford⁴, M. E. Zolensky³, K. Nakamura Messenger³, C. Jacobsen¹, ¹Dept. of Physics and Astronomy, SUNY StonyBrook, NY 11794, USA, (swirick@bnl.gov), ²Dept. of Physics, SUNY Plattsburgh, NY 12901 USA, ³NASA Johnson Space Center, Houston, TX, 77058, USA, ⁴NASA AMES Research Center, Moffett Field, CA 94035
Lunar and Planetary Science XXXIX (2008) 1450.pdf

amorphous carbon

ORGANIC ANALYSES OF PARTICLES FROM THE STRATOSPHERIC COLLECTION COINCIDING WITH THE EARTH'S 2003 PASSAGE THROUGH THE DUST TRAIL OF COMET 20P/GRIGG-SKJELLERUP. G. J. Flynn, and S. Wirick, Dept. of Physics, SUNY Plattsburgh, 101 Broad St., Plattsburgh, NY 12901 (George.flynn@plattsburgh.edu).
42nd Lunar and Planetary Science Conference (2011) 1856.pdf



aliphatic carbon in 26P/G-S IDPs

Figure 2: Infrared spectra in the C-H stretching region for L2055D1 (red), L2055D4 (green), L2055D5 (pink), and L2055E4 (blue). The L2055D1 spectrum is dominated by silicone oil, with a large aliphatic C-H₃ absorption, while the other three spectra are dominated by aliphatic C-H₂ absorption features.

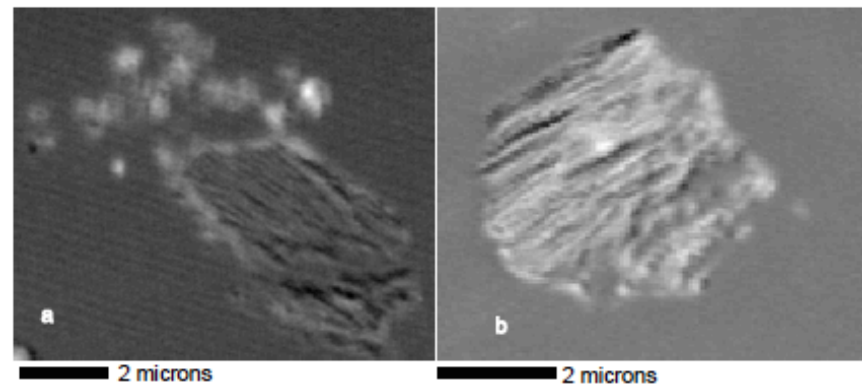


Figure 1. Carbon map of L2099 (a) and Comet Wild 2 particle C2044,0,36,1 (b).

Comet Wild 2 's iron sulfide's carbon map shows more carbon associated with this sulfide than carbon with the IDP iron sulfide. Only one of the 5 sections has carbon XANES spectra similar to the carbon XANES spectra of L2099 shown in Figure 1 where the carbon species is **amorphous** with a carbonyl attached (fig.2).

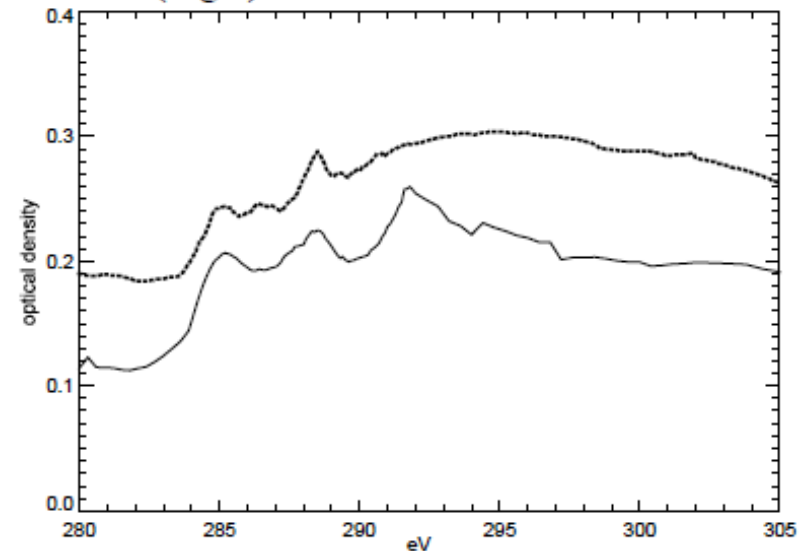


Figure 2. Carbon XANES spectra from iron sulfide in Comet Wild 2 (solid black) and the iron sulfide from IDP L2099 cluster 10.

CP IDPs: Other studies –

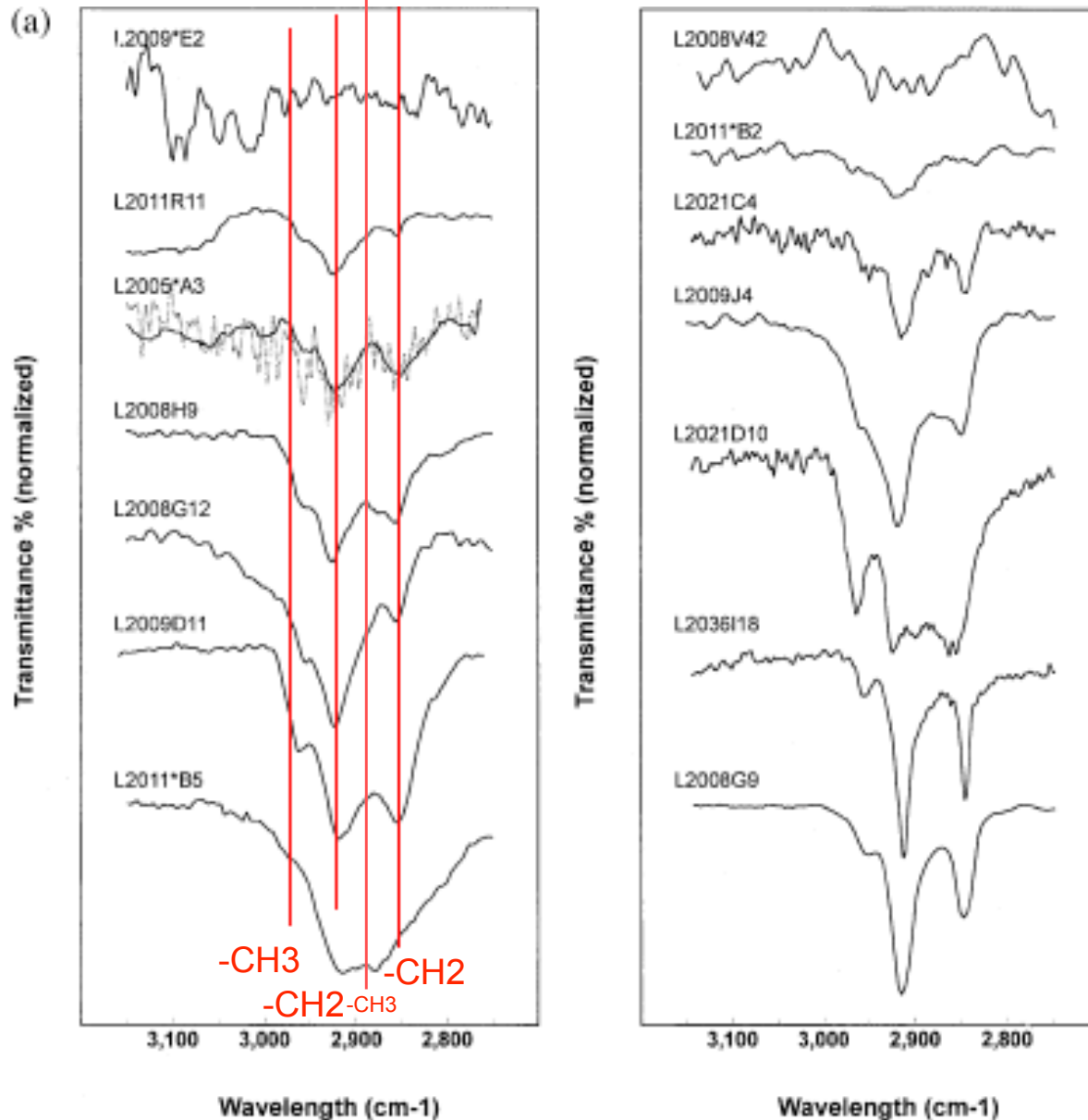
The origin of organic matter in the solar system: Evidence from the interplanetary dust particles

G. J. FLYNN,^{1,*} L. P. KELLER,² M. FESER,³ S. WIRICK,³ and C. JACOBSEN³

Geochimica et Cosmochimica Acta, Vol. 67, No. 24, pp. 4791–4806, 2003

Organic matter in IDPs

Fig. 11. a. FTIR spectra, in the C-H stretching region, of 14 anhydrous IDPs. These data are scaled to have the same Si-O absorption depth. b. FTIR spectra, in the C-H stretching region, of 5 hydrated IDPs. These data are scaled to have the same Si-O absorption depth.



cometary IDPs

left: IR spectra show aliphatic carbon in IDPs, normalized to 10μm Si-O feature

below: C-XANES probes kinds of bonds

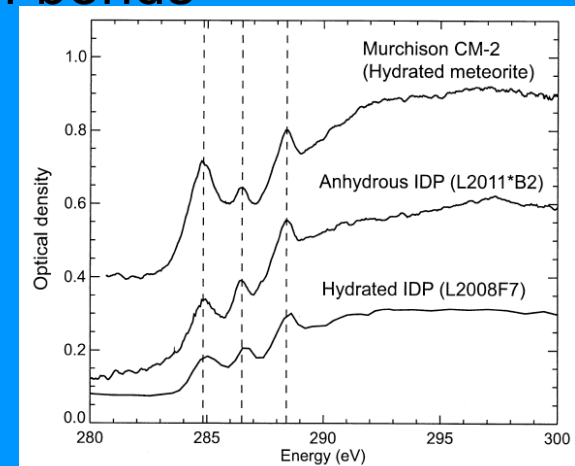
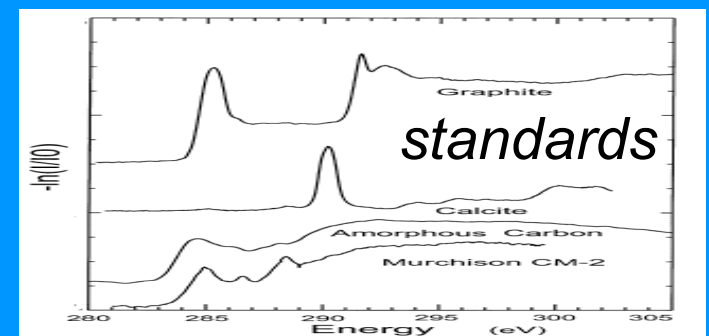


Fig. 4. Carbon K-edge XANES spectra of an organic-rich spot on a microtome section of Murchison, an anhydrous IDP, L2011*B2, and a hydrated IDP, L2008F7.



CP IDPs: Other studies –

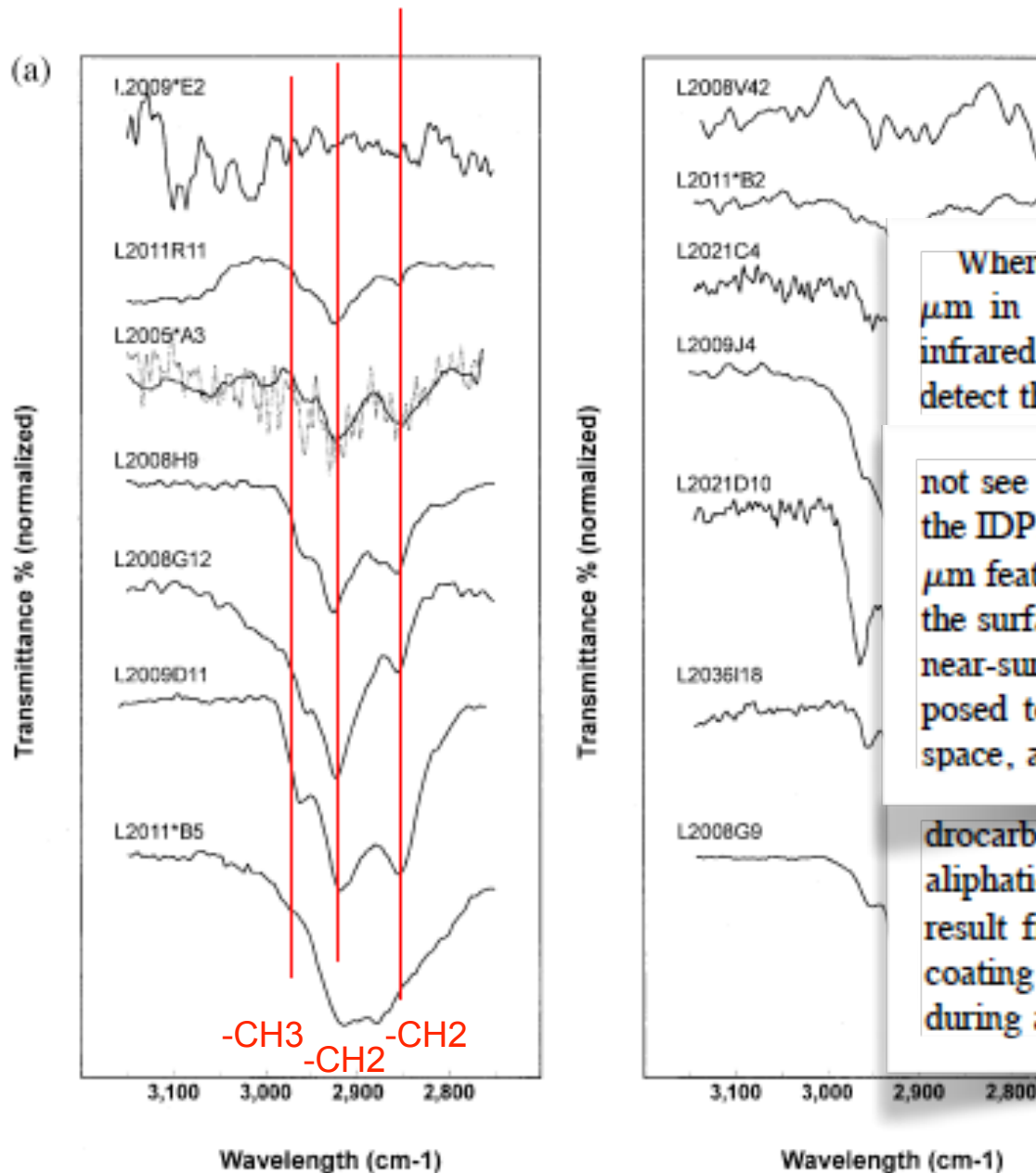
The origin of organic matter in the solar system: Evidence from the interplanetary dust particles

G. J. FLYNN,^{1,*} L. P. KELLER,² M. FESER,³ S. WIRICK,³ and C. JACOBSEN³

Journal of Cosmochemistry Acta, Vol. 67, No. 24, pp. 4791–4806, 2003

cometary IDPs

left: IR spectra - must crush or thin slice the IDP to see feature



When we perform FTIR spectroscopy on whole IDPs (~10 μm in size), which are too thick for good transmission of infrared light through the thickest portion of the particle, we detect the 10 μm silicate absorption features but generally do

not see the ~3.4 μm C-H stretching features. When we crush the IDP, exposing the interior, we detect the 10 μm and the 3.4 μm features, suggesting that organic matter is not present near the surface of the IDP but is present in the interior. The loss of near-surface organic matter would be expected for IDPs exposed to damaging ultraviolet light and particle radiation in space, and this provides some evidence that the aliphatic hy-

drocarbon is indigenous to the IDPs. However, the absence of aliphatic hydrocarbons near the surface of the IDPs might also result from the hexane washing, used to remove the surface coating of silicone oil from the IDPs, or from surface heating during atmospheric entry.

CP IDPs: Other studies

Earth Planets Space, 65, 1159–1166, 2013

Organic grain coatings in primitive interplanetary dust particles: Implications for grain sticking in the Solar Nebula

George J. Flynn¹, Sue Wirick², and Lindsay P. Keller³

the time or mechanism of its production. The individual grains in these CP IDPs are coated by layers of carbonaceous material [3], typically ~100 nm thick, which holds the grains together. We have analyzed these

G. J. FLYNN *et al.*: ORGANIC RIMS ON PRIMITIVE GRAINS

1161

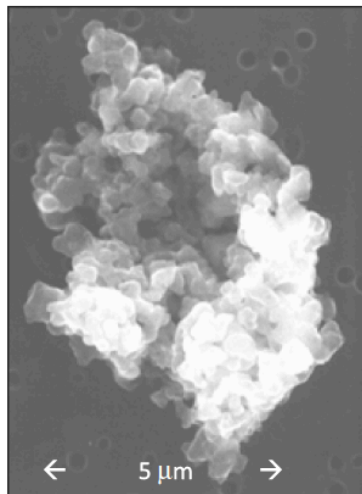


Fig. 1. Scanning electron microscope image of an ~11 μm chondritic IDP collected from the Earth's stratosphere by a NASA aircraft. The individual surface features are micron or submicron grains that have aggregated to form this dust particle. (NASA photo)

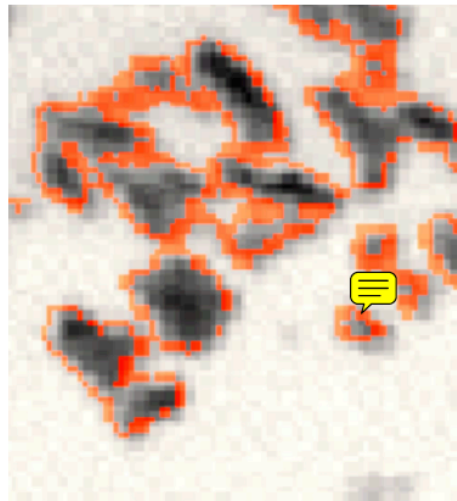


Fig. 2. High-resolution (~25 nm per pixel) x-ray absorption image of part of an ultramicrotome slice of a CP IDP, L2011*B6, showing the individual micron- and submicron-size mineral grains (dark gray). An image of the organic matter selected by cluster analysis (red) is superimposed, showing that the ~100 nm thick rims of organic matter form the contact surfaces between the individual mineral grains. (Field of view ~2.5 μm wide.)

Organic Coatings on Primitive Grains in IDPs: Implications for the Formation of Solar System Organic Matter

Flynn, G. J.; Wirick, S.; Keller, L. P.; Sandford, S.

observations are consistent with the alternative model, that primitive organic matter was produced by irradiation of carbon-bearing ices that condensed on the grain surfaces. References: [1] Ishii, H. A. et al (2008) *Science* 319, 447-450. [2] Flynn, G. J. et al. (2003) *Geochim. Cosmochim. Acta* 67, 4791-4806. [3] Thomas, K. L. et al. (1996) in *Physics, Chemistry and Dynamics of Interplanetary Dust*, ASP Conf. Series, 104, 283-286. [4] Lerotic, M (2005) *Journal of Electron Spectroscopy and Related Phenomena*, 144-147, 1137-1143.

American Geophysical Union, Fall Meeting 2009, abstract #P14A-01

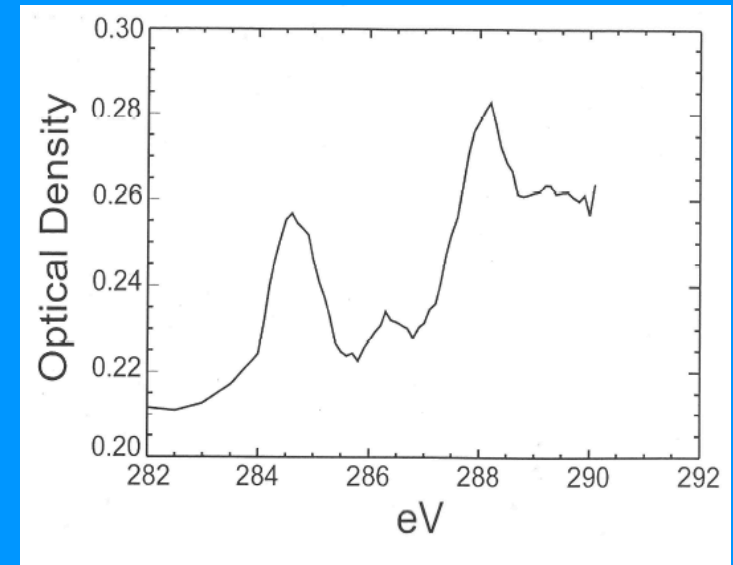


Fig. 4. Carbon-XANES spectrum of the organic rim material in CP IDP L2011*B6, showing the absorption features of C=C (near 285 eV) and C=O (near 288.6 eV).

C-XANES

Stardust C-XANES spectra

Meteoritics & Planetary Science 46, Nr 9, 1376–1396 (2011)

doi: 10.1111/j.1945-5100.2011.01237.x

Correlated microanalysis of cometary organic grains returned by Stardust

Bradley T. DE GREGORIO^{1,2*}, Rhonda M. STROUD¹, George D. CODY³, Larry R. NITTLER⁴,
A. L. DAVID KILCOYNE⁵, and Sue WIRICK⁶

Microanalysis of cometary organic grains

1383

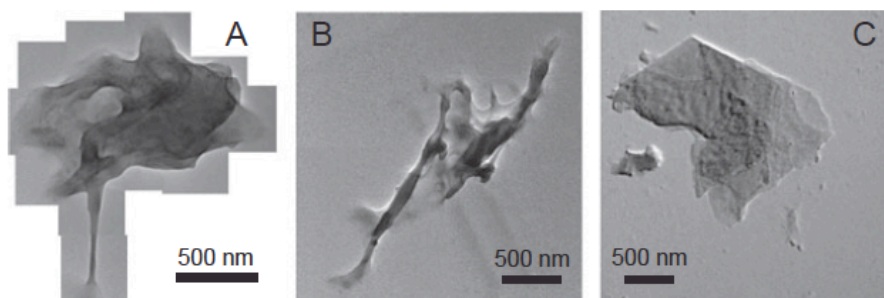


Fig. 2. (A, B) Transmission electron microscopy (TEM) images of two adjacent ultramicrotomed sections from FC9,0,13,1,5 containing dense, lobate, organic matter. (C) A different section of the same particle (FC9,0,13,1,4) only consisted of a single anatase grain (Fe₂O₃) with no associated carbonaceous matter.

contaminants. Only two types of cometary organic matter appear to be relatively unaltered during particle capture. These are (1) **polyaromatic carbonyl-containing organic matter**, similar to that observed in insoluble organic matter (IOM) from primitive meteorites, interplanetary dust particles (IDPs), and in other carbonaceous Stardust samples, and (2) **highly aromatic refractory organic matter**, which primarily constitutes **nanoglobule-like** features. Anomalous isotopic compositions in some of these samples also confirm their cometary heritage. There also appears to be a significant labile aliphatic component of Wild 2 organic matter, but this material could not be clearly distinguished from carbonaceous contaminants known to be present in the Stardust aerogel collector.

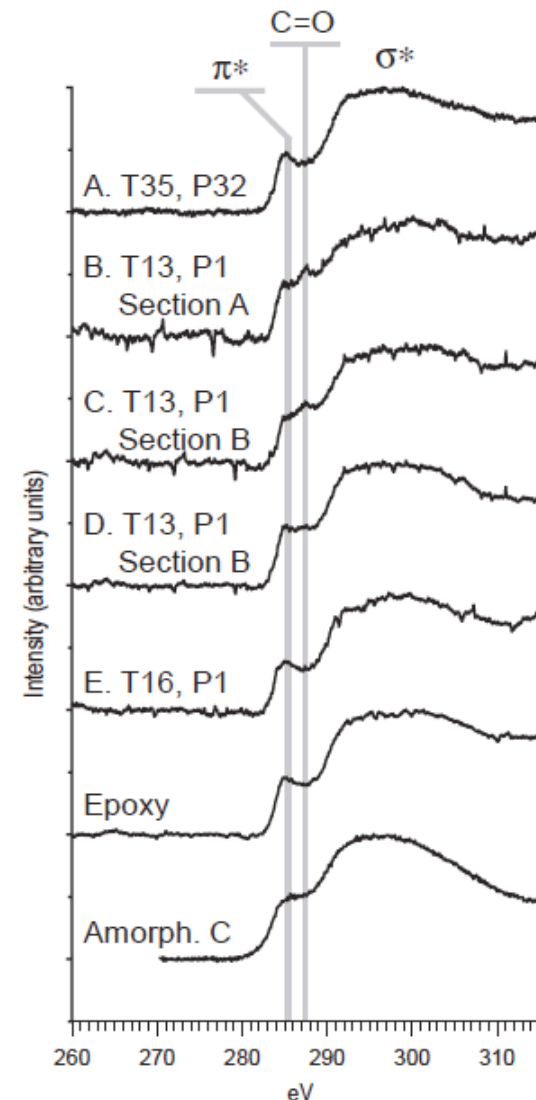


Fig. 3. Electron energy loss spectroscopy (EELS) spectra of organic matter from the Stardust Preliminary Examination. (A) Organic matter in compressed aerogel from sample C2054,0,35,32,10 (Fig. 1A). (B, C, D) Solitary organic matter in sample FC9,0,13,1,5. Spectrum B was acquired from the organic matter shown in Fig. 2A, while Spectra C and D were acquired from the organic matter shown in Fig. 2B. (E) Epoxy and organic mixture from sample FC12,0,16,1,10. (F) Pure epoxy in sample FC12,0,16,1,10. (G) Laboratory-produced amorphous carbon film.

Stardust C-XANES spectra

Meteoritics & Planetary Science 46, Nr 9, 1376–1396 (2011)

doi: 10.1111/j.1945-5100.2011.01237.x

Correlated microanalysis of cometary organic grains returned by Stardust

Bradley T. De GREGORIO^{1,2*}, Rhonda M. STROUD¹, George D. CODY³, Larry R. NITTLER⁴,
A. L. DAVID KILCOYNE⁵, and Sue WIRICK⁶

Diversity - wide variation in functional groups and texture

section. The XANES spectrum of this section (Fig. 7A) contain photoabsorptions due to aromatic carbon-carbon bonding, aromatic ketones, and carboxyl functional groups (Table 2), similar to XANES spectra from the organic matter from Track 13 (Fig. 7B, and Spectra 7 and 8 from Fig. 1 of Cody et al. 2008a). These spectra imply that the cometary organic matter in this particle consists of complex polyaromatic domains modified by oxygenic functional groups and interconnected by short aliphatic chains (Cody et al. 2008a; De Gregorio et al. 2010).

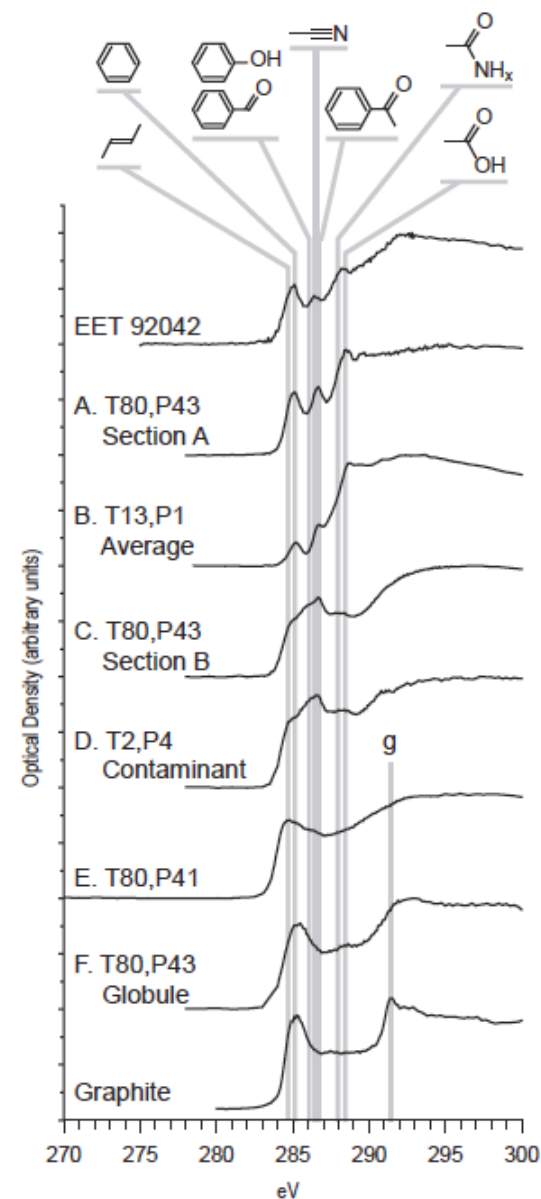


Fig. 7. Carbon-X-ray absorption near-edge structure spectroscopy (C-XANES) spectra of (A) sample C2092,6,80,43,2A (Fig. 6A), (B) an average of adjacent organic ultramicrotome sections from sample FC9,0,13,1,5 (modified from Cody et al. 2008a), (C) sample C2092,6,80,43,2B (Fig. 6B), (D) a possible organic contaminant from sample FC3,0,2,4,5 (De Gregorio et al. 2010), (E) sample C2092,6,80,41,1, and (F) a cometary organic globule from sample C2092,6,80,43,2 (De Gregorio et al. 2010), compared with spectra of graphite and IOM from the primitive meteorite EET 92042. The position of the characteristic graphite exciton photoabsorption is denoted by “g.”

UCAMMs: chocked full of organics, GEMS and olivine (crystals) with ranges of Mg-Fe contents from Fo100–Fo60 (mineral compositions similar to Stardust and some Giant IDPs)

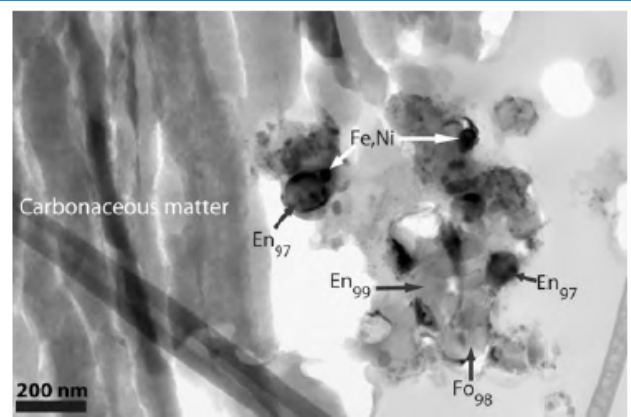
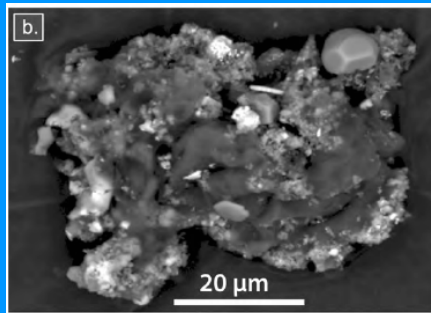


Fig. 3. Bright field transmission electron microscope (TEM) images of one assemblage in ultracarbonaceous micrometeorite (UCAMM) DC02-09-41. The polycrystalline assemblage contains enstatite (En_{97-99}), olivine (Fo_{98}) with a grain size ranging from 100 to 150 nm in diameter and Fe–Ni metal (~ 50 nm).

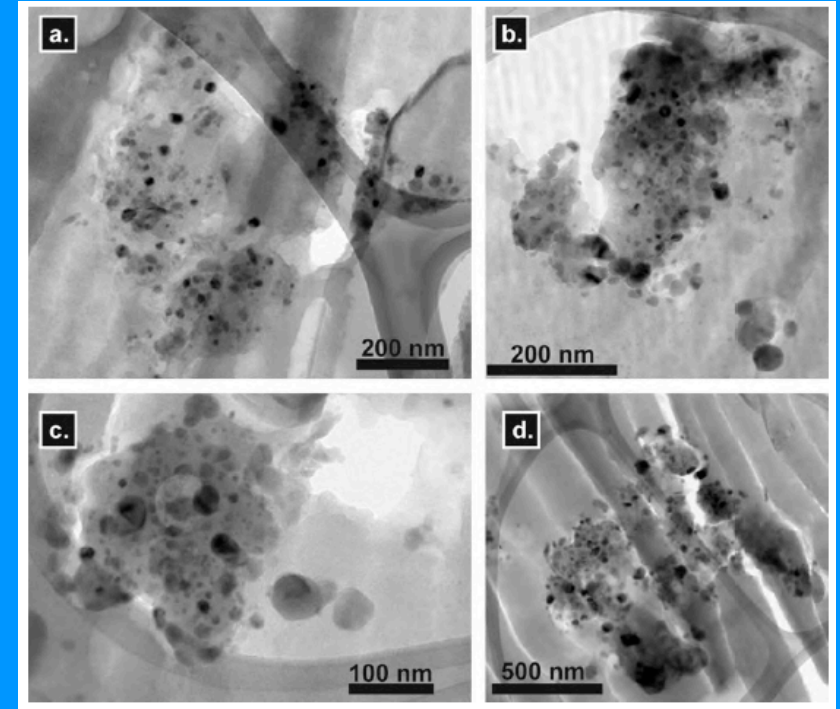


Fig. 8. Bright-field transmission electron microscope (TEM) images of four Glass with Embedded Metal and Sulfides (GEMS) like objects in the ultracarbonaceous micrometeorite DC06-09-19. These objects are embedded in the carbonaceous material. They are composed of nanometer-sized sulfide embedded in a Mg, Si-rich glassy phases.

Geochimica et Cosmochimica Acta 76 (2012) 68–82

Transmission Electron Microscopy of CONCORDIA
UltraCarbonaceous Antarctic MicroMeteorites (UCAMMs):
Mineralogical properties

E. Dobrică^{a,*}, C. Engrand^a, H. Leroux^b, J.-N. Rouzaud^c, J. Duprat^a

UCAMMs are dominated by disordered carbonaceous matter that extends over surfaces of up to $\sim 90\%$ of the particle. Embedded in this carbonaceous matter, we observed small and complex assemblages of fine-grained mineral phases, isolated minerals, glassy phases that resemble Glass with Embedded Metal and Sulfides (GEMS) that were first found in Interplanetary Dust Particles (IDPs), and rounded objects containing both glass and crystalline materials. The mineral assemblages are chondritic in composition, within a factor of 2. Crystalline materials represent at least 25% of mineral phases. This value

Meteoritics & Planetary Science 46, Nr 9, 1363–1375 (2011)
doi: 10.1111/j.1945-5100.2011.01235.x

Raman characterization of carbonaceous matter in CONCORDIA
Antarctic micrometeorites

E. DOBRICĂ^{a,*}, C. ENGRAND^a, E. QUIRICO^b, G. MONTAGNAC^c, and J. DUPRAT^a

Icarus 224 (2013) 243–252

UltraCarbonaceous Antarctic micrometeorites, probing the Solar System beyond
the nitrogen snow-line

E. Dartois^{a,*}, C. Engrand^b, R. Brunetto^a, J. Duprat^b, T. Pino^c, E. Quirico^d, L. Remusat^e, N. Bardin^b,
G. Briani^b, S. Mostefaoui^e, G. Morinaud^a, B. Crane^a, N. Szwec^a, L. Delauche^b, F. Jamme^f, Ch. Sandt^f,
P. Dumas^f

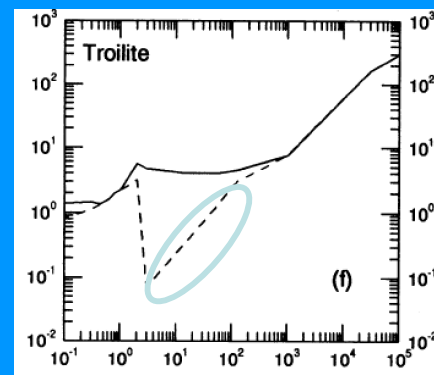
UCAMMs: chance to highlight FeS, which is present in most cometary samples and chondrites

FeS can be primary condensate or alteration product

Table 2

Size and composition range and average of olivines, pyroxenes (low-Ca pyroxene and high-Ca pyroxene) and sulfides in UCAMMs DC06-09-45, DC06-09-19 and DC02-09-41 (*N* is the number of crystals analyzed).

Sample		<i>N</i>	Size variation (nm)	Composition range
DC06-09-45	Olivine	14	40–270 (avg. 170)	Fe _{84–98} (avg. Fe ₉₃)
	Low-Ca pyroxene	57	50–450 (avg. 200)	En _{57–100} (avg. En ₉₂)
	Ca-pyroxene	2	150–160	En _{47.1} Wo _{52.9} Fs ₀ ; En _{48.4} Wo ₄₆ Fs _{5.6}
	Iron sulfide	33	40–1100 (avg. 200)	Fe + Ni:S-50.3:49.7;Ni (at%) 0–38 (avg. 3 at%)
DC06-09-19	Olivine	39	80–495 (avg. 160)	Fe _{59–100} (avg. Fe ₈₇)
	Low-Ca pyroxene	85	50–485 (avg. 220)	En _{76–100} (avg. En ₉₇)
	Ca-pyroxene	1	110	En _{47.1} Wo _{48.3} Fs _{4.7}
	Iron sulfide	105	15–500 (avg. 95)	Fe + Ni:S-53:47;Ni (at%) 0–24 (avg. 2 at%)
DC02-09-41	Olivine	55	60–335 (avg. 170)	Fe _{51–100} (avg. Fe ₈₄)
	Low-Ca pyroxene	114	45–1000 (avg. 260)	En _{62–100} (avg. En ₉₂)
	Ca-pyroxene	1	110	En _{46.5} Wo _{47.7} Fs _{5.8}
	Iron sulfide	44	30–990 (avg. 150)	Fe + Ni:S-49.4:50.6;Ni (at%) 0–4.2 (avg. 0.5 at%)



Pollack+94 FeS complex
index of refraction:
missing data
highly absorptive!

Geochimica et Cosmochimica Acta 76 (2012) 68–82

Transmission Electron Microscopy of CONCORDIA
UltraCarbonaceous Antarctic MicroMeteorites (UCAMMs):
Mineralogical properties

E. Dobrică^{a,*}, C. Engrand^a, H. Leroux^b, J.-N. Rouzaud^c, J. Duprat^a

Cluster IDPs: Other studies - must mention refractory silicates

THE SOLAR NEBULA'S FIRST ACCRETIONARY PARTICLES (FAPs) - ARE THEY PRESERVED IN COLLECTED INTERPLANETARY DUST SAMPLES?

D. E. Brownlee and D.J. Joswiak, Astronomy Dept. 351580, Univ. of Washington, Seattle, WA 98195 - brownlee@astro.washington.edu

Lunar and Planetary Science XXXV (2004)

1944.pdf

We believe that we have seen materials that are strong candidates for being the first (or fundamental) accretionary particles. Some primitive IDPs are made almost entirely of submicron components that are likely to be FAPs. They are generally equant and range from 0.1 to 1 μm across. They average about a quarter of a micron and very few are smaller than 100nm. They are solid materials composed of amorphous silicates, organic material, GEMS, and crystalline materials including Fo, En and Fe sulfides. Some are single mineral phases but most are made of several components. They are solid (non-porous) rocks and we refer to them as "femtorocks" because of their mass and multi-component nature. The femtorocks often contain organic materials and silicates and we believe that they are functionally equivalent to Mayo Greenberg's core-mantle interstellar grain model even though they consist of multiple cores and not a single core surrounded by a single organic mantle. The elemental composition variation among femtorocks is remarkable. As seen in Figure 1, their Fe, Mg and Si compositions vary widely with little modulation due to mineralogical control. They contain minerals but the amorphous components dominate their compositional spread. In the Fe-Mg-Si ternary, the only first order effect is the scarcity of compositions with Mg/Si appreciably greater than unity (enstatite). IDPs made of femtorocks (FAPs?) similar to those seen in figure 1 match CI relative abundances for aggregates larger than 3 microns but at the submicron, fundamental component, level they vary all over the map.

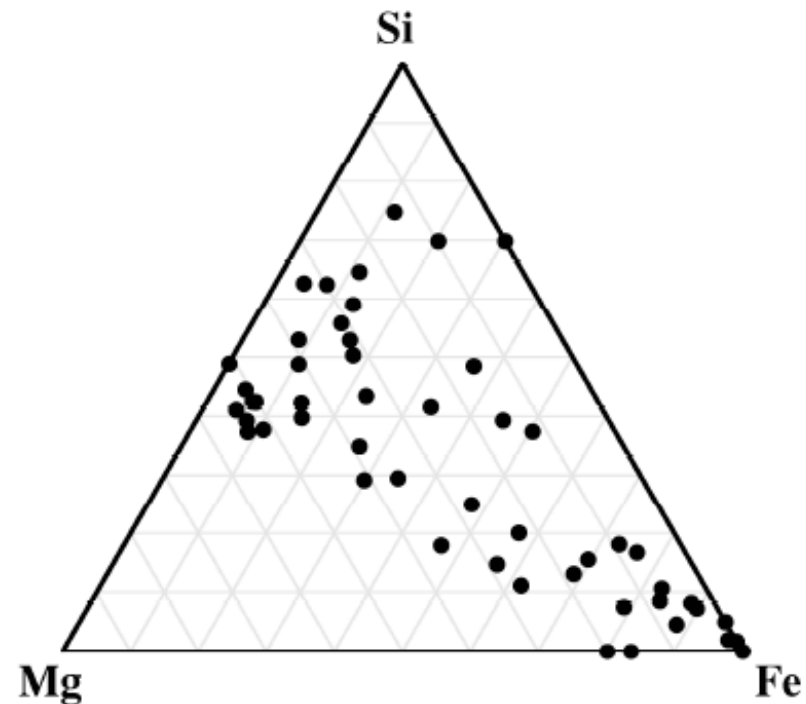
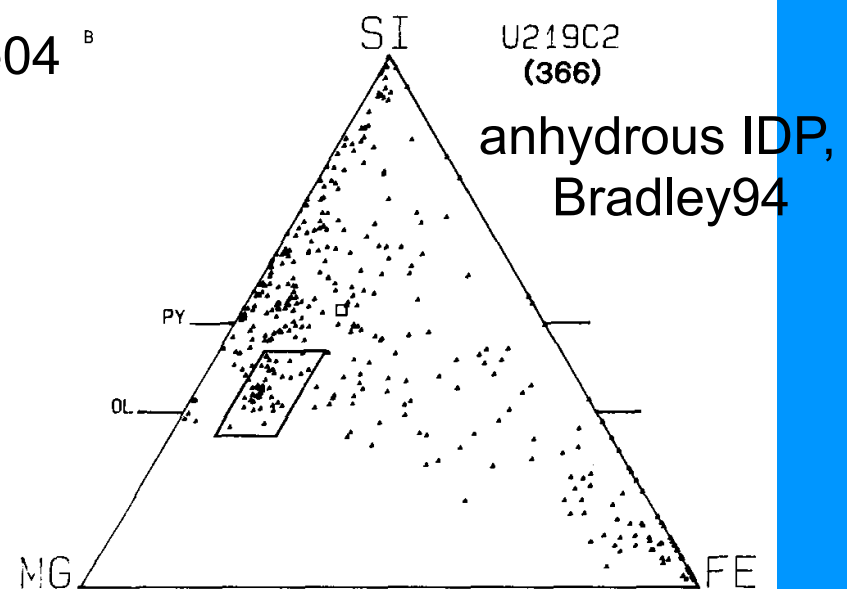
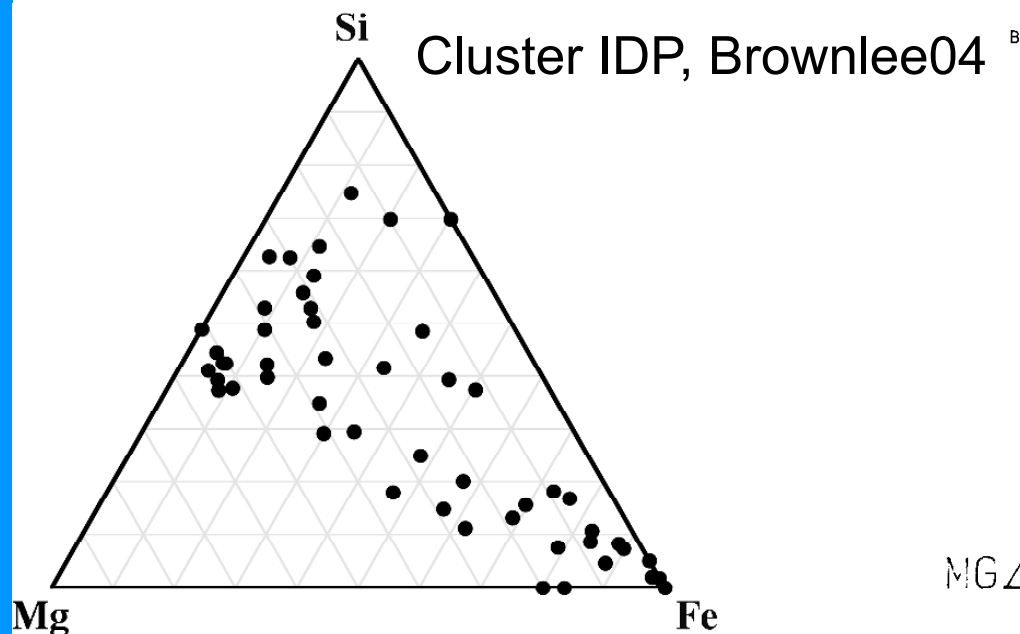
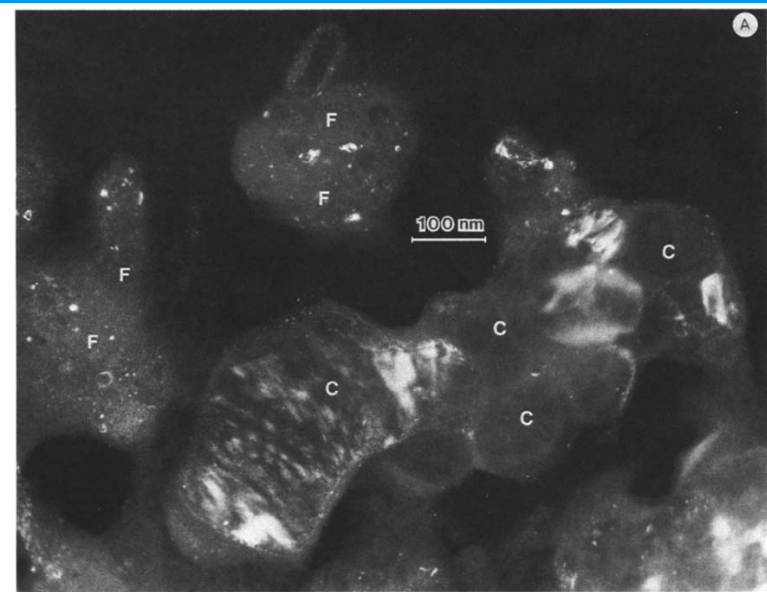
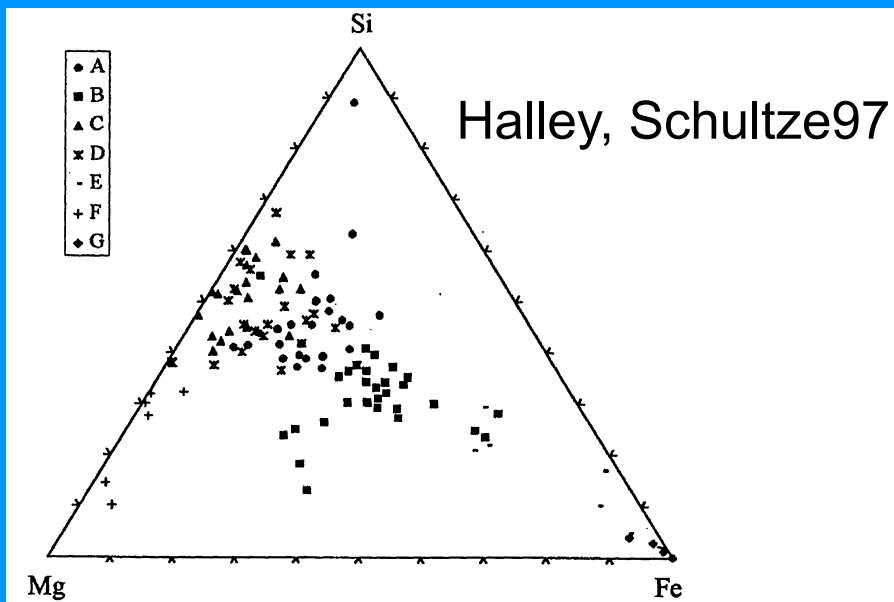


Figure 1 Atom fraction ternary of submicron grains (femtorocks) from U2-20 GCA- a cluster IDP. The large heterogeneity at the submicron scale is remarkable and relatively unconstrained by mineralogical stoichiometry. The large dispersion is similar to data on particle compositions obtained at comet Halley.

Halley & IDPs: Mineralogies show olivine contains Mg and Fe
WIZ2017 Fig.1 - see caption for full citations and for full discussion
of mineralogy (comets, compared to carbonaceous chondrites)



Meteoritic IOM

- » remarkably similar XANES (especially compared to diversity in comets): functional groups similar
- » variations on nano to micron size scales
- » 40% of C is 'lost' in isolation of IOM. What was lost?

The IOM shows tremendous variation in its elemental and isotopic compositions both within and between chondrite groups (Fig. 1). These variations are due, at least in part, to parent body processes, but may also reflect variations in the materials accreted by the different chondrite groups (Section 6). In the chondrites that appear to have experienced the most benign parent body conditions (CIs, CMs and CRs), the bulk compositions of their IOM, normalized to 100 Cs, are in the range $\sim\text{C}_{100}\text{H}_{70-80}\text{O}_{15-20}\text{N}_{3-4}\text{S}_{1-4}$. For comparison, the SOM in the Murchison (CM2) meteorite has an estimated bulk composition of $\sim\text{C}_{100}\text{H}_{155}\text{O}_{20}\text{N}_3\text{S}_3$ (Schmitt-Kopplin et al., 2010) that, except for its H/C, resembles the bulk composition of IOM. However, the abundances of the different compounds in the SOM vary considerably within and between chondrite groups (Table 1). The compositional variations in SOM, at least within a group, appear to be largely determined by parent body processes (e.g., Martins et al., 2007; Aponte et al., 2011; Glavin et al., 2011; Hiltz et al., 2014), with some fraction of the SOM possibly being the product of alteration of IOM by parent body processes (e.g., Sephton et al., 2003; Huang et al., 2007).

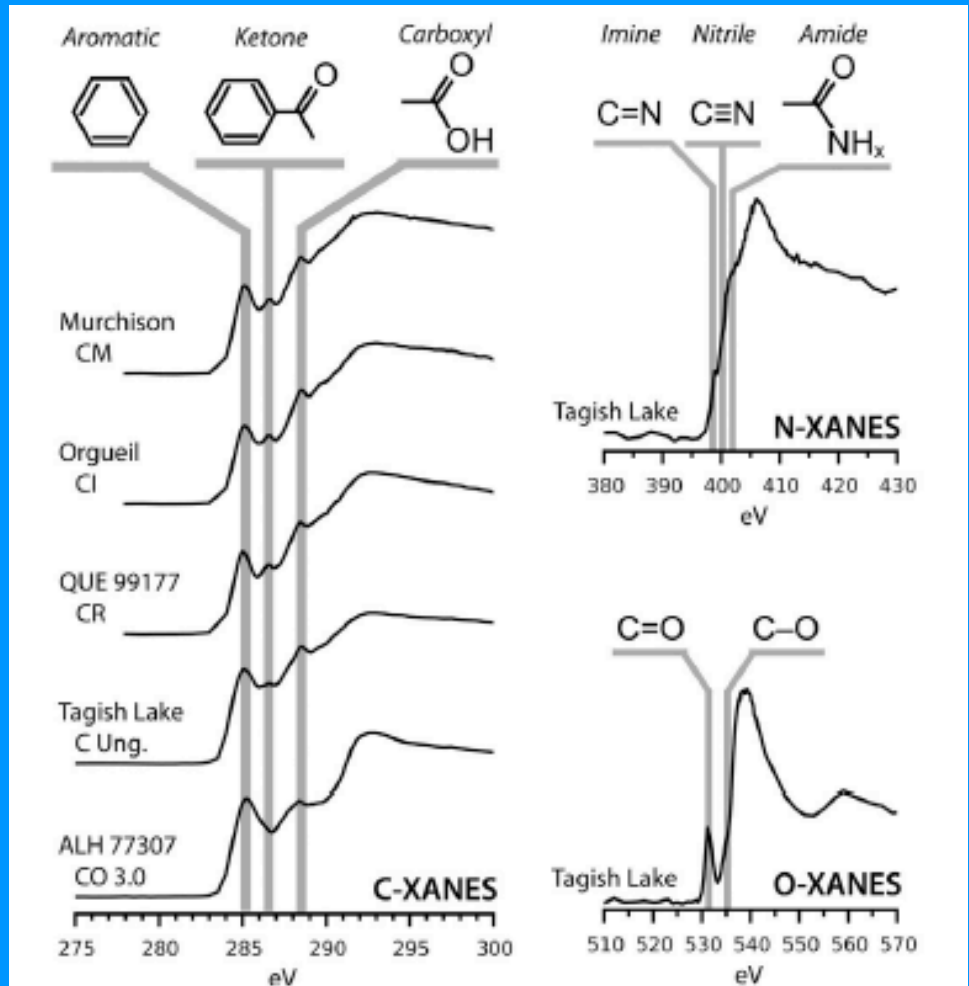


Fig. 9. Average bulk XANES spectra of IOM from several primitive carbonaceous chondrites: Murchison (CM2), Orgueil (CI1), QUE 99177 (CR2), Tagish Lake (C2, lithology 5b) and ALH 77307 (CO3.0). The C XANES spectra show the greatest variation in functional chemistries between different meteorite groups and petrology types, but are still very similar. As shown in the representative spectrum from Tagish Lake, the N XANES spectra from primitive IOM are relatively featureless, only containing minor spectral "shoulders" on the main N absorption edge. In addition, IOM O XANES spectra rarely show spectral features other than the main π^* and σ^* peaks for C=O and C—O bonds, respectively. The C XANES data are taken from De Gregorio et al. (2013), while the data for Tagish Lake are unpublished.

Meteoritic IOM (Alexander+17)

- » different textures, ‘fluffy’, ‘globules’
- » greater diversity on smaller scales
- » differences between chondrite classes
- » aggregate of nanoglobules- texture dominated by fine-grained structure

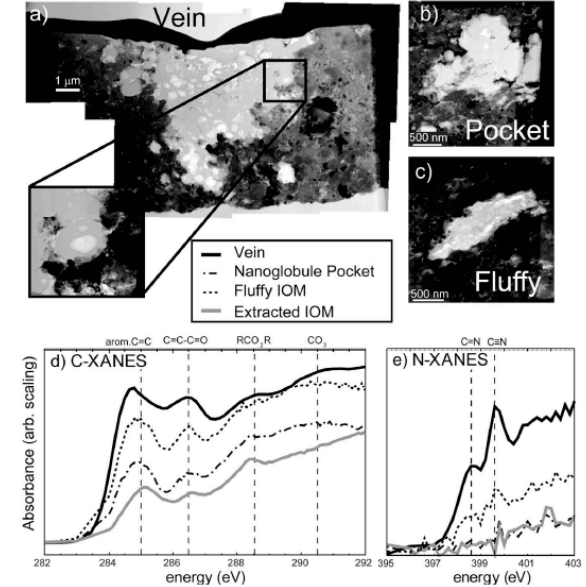


Fig. 3. Coordinated *in situ* microanalyses of organic matter in QUE 99177 (CR2). (a) A bright field STEM image mosaic of a FIB section cut through the organic-rich vein in Fig. 2, which appears to be an aggregate of nanoglobules (see inset). Figures (b) and (c) are bright field STEM images of organic inclusions in another QUE 99177 FIB section, a small aggregate (“pocket”) of nanoglobules and a carbonaceous particle with a fluffy texture, respectively. Figures (d) and (e) are C-XANES and N-XANES spectra, respectively, of organic features indicated in the STEM images compared to the average spectra of IOM extracted from the same meteorite. The XANES measurements reveal heterogeneity in functional-group chemistry on a μm scale. There is a much stronger nitrile peak associated with this vein than in the fluffy IOM and bulk extracted IOM.

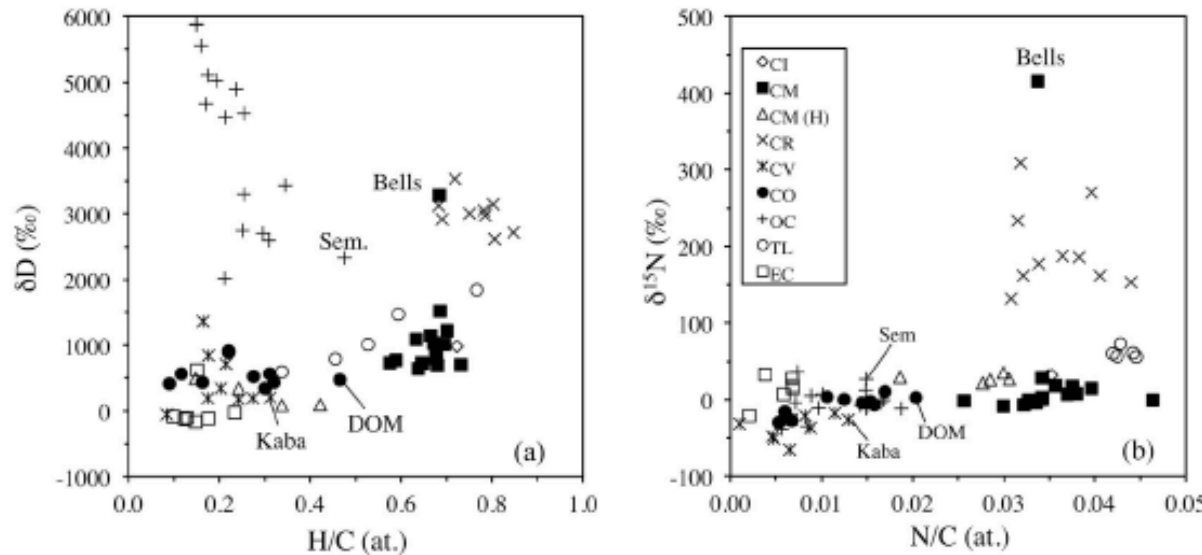


Fig. 1. The variations in bulk IOM H and N elemental and isotopic compositions within and between chondrite groups (updated from Alexander et al., 2007b, 2010). The OC WSG 95300 is not shown in (a) because its δD value is almost 12,000‰ and $\text{H/C} = 0.103$. TL is Tagish Lake, Sem is Semarkona (LL3.00), DOM is DOM 08006 (CO3.00), Kaba is a CV 3.1 and Bells is an anomalous CM2. CM(H) are heated CMs, probably as a result of impacts.

Meteoritic IOM

- » remarkably similar (compared to diversity in comets)
- » variations on nano to micron size scales

Table 1

The abundances of insoluble (IOM) and soluble (SOM) organic components in the least metamorphosed carbonaceous chondrites, including the ungrouped C2 Tagish Lake. For the CMs, all data are from the Murchison CM2 meteorite (updated from Botta and Bada, 2002), unless otherwise noted. The abundances are in $\mu\text{g/g}$ (ppm), except where indicated.

	CI	CM	CR	Tag. Lake
Matrix (vol.%)	100	~50	~30	~80
Bulk C (wt.%) ^a	3.7	2.0	1.2	4.1
C in IOM (wt.%) ^b	2.1	0.96	0.48	1.8
Amino acids	~5 ^c	14–71 ^f	~1–250 ^d	1.9–4.9 ^e
Aromatic hydrocarbons		3 ^f	16 ^g	
Aliphatic hydrocarbons		>35		
Monocarboxylic acids		>300	96 ^g	359–656 ^e
Hydroxy- and dicarboxylic acids		14–15	212 ^g	
Purines and pyrimidines		1.3		
Basic N-heterocycles		7		
Amines	14 ⁱ	5–7 ⁱ	103 ^g	
Alcohols		11		
Aldehydes and ketones		27		
Sulphonic acids		68		
Phosphonic acids		2		
Polyols		>8 ^h		

^a Averages from Alexander et al. (2012).

^b Averages for recovered IOM from Alexander et al. (2007b, 2014b).

^c Average of the abundances in Orgueil and Ivuna (Ehrenfreund et al., 2001).

^d Range of abundances in EET 92042, GRA 95229, and GRO 95577 (Martins et al., 2007).

^e Range for different lithologies of Tagish Lake (Hilts et al., 2014).

^f Abundance in Y-791198 (Naraoka et al., 1988).

^g Abundances in GRA 95229 (Pizzarello et al., 2008).

^h Lower limit for glyceric acid in Murchison (Cooper et al., 2001).

ⁱ From Aponte et al. (2014a, 2015).

Nevertheless, the degradative chemical and pyrolysis techniques both indicate that at least the chemically accessible and thermally labile components of IOM are composed of small aromatic units (typically 1–3 rings, although some larger units are present) that have a high degree of substitution by aliphatic subgroups. The high degree of substitution and the macromolecular nature of IOM indicate that there must be considerable cross-linking by the aliphatic material between the aromatic units that has generated a 3D network. This is consistent with the bulk IOM properties inferred by NMR and FTIR, which also indicate that the aliphatic material must be composed of short chains that are highly branched. Both the chemical degradation and Raman studies suggest that a significant fraction of the cross-linking moieties involve O-bearing functional groups. Relatively little is known about S and N speciation in IOM. XANES shows that S occurs in a number of different functional groups with a range of oxidation states, but at present it is not possible to say anything more quantitative. The N XANES spectra are almost featureless, providing few clues to its speciation, and the difficulty of obtaining ^{15}N NMR spectra from IOM is a puzzle.

Meteoritic IOM in IR

- » large chemical and structural variations between chondrites
- » but note 3.4 μ m band is less diverse than in comet samples

Icarus 223 (2013) 534–543

Mid-infrared study of the molecular structure variability of insoluble organic matter from primitive chondrites

F.-R. Orthous-Daunay^{a,*}, E. Quirico^a, P. Beck^a, O. Brissaud^a, E. Dartois^b, T. Pino^c, B. Schmitt^a

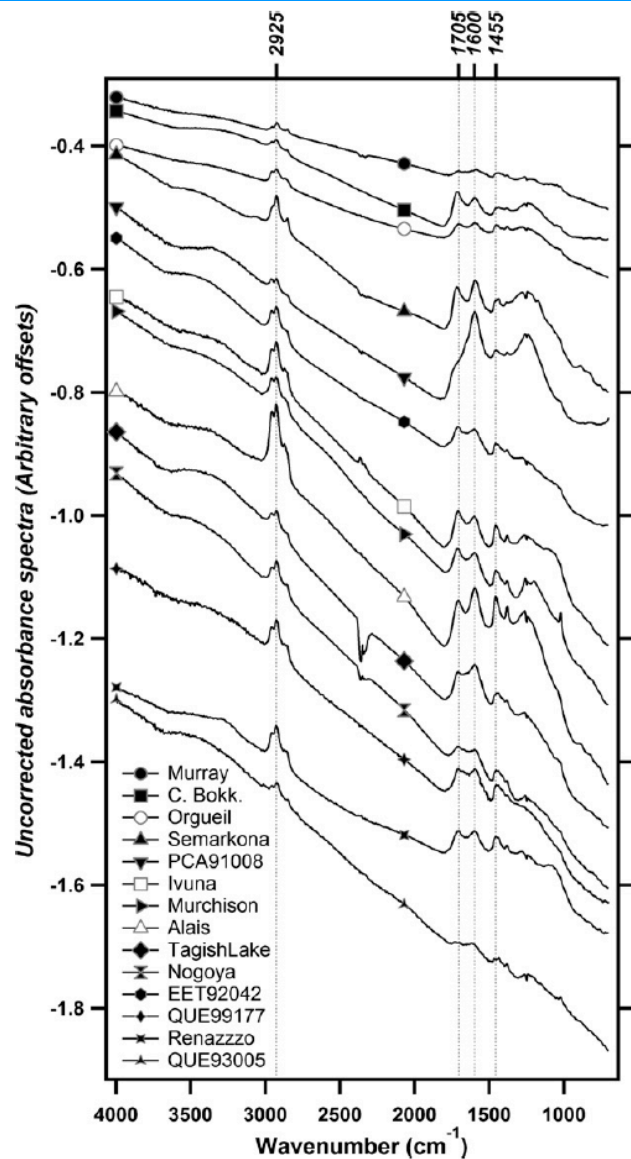


Fig. 1. Raw IR absorbance spectra used in this study. An arbitrary offset is applied for the sake of clarity.

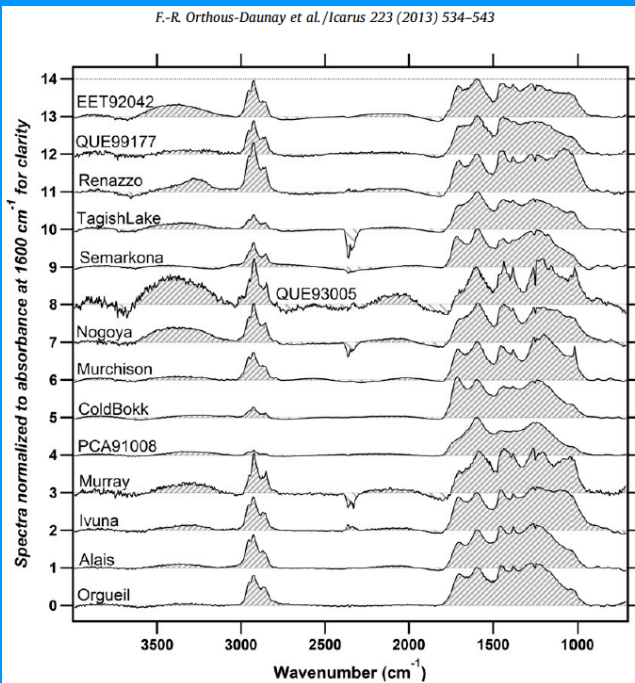
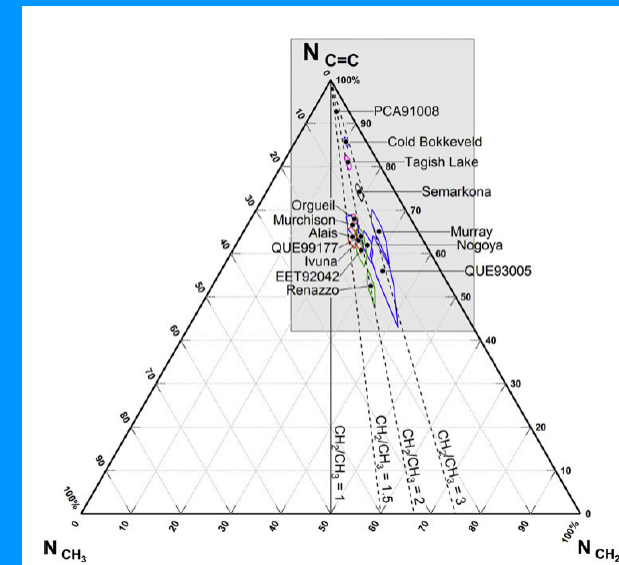
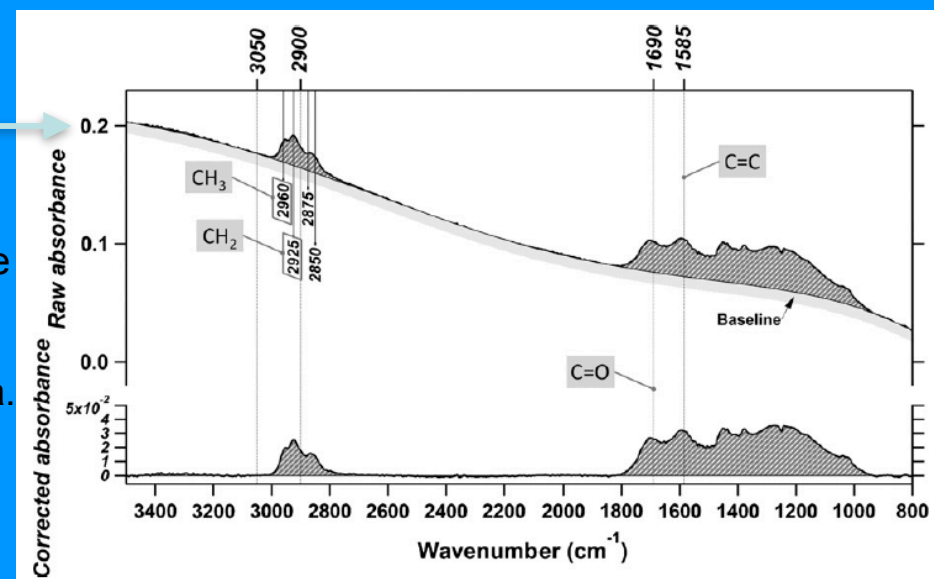


Fig. 2. Corrected and normalized absorbance spectra used for this study prior to Gaussian fitting.



Ternary diagram: one way to see -CH₂, -CH₃, C=C bond ratios

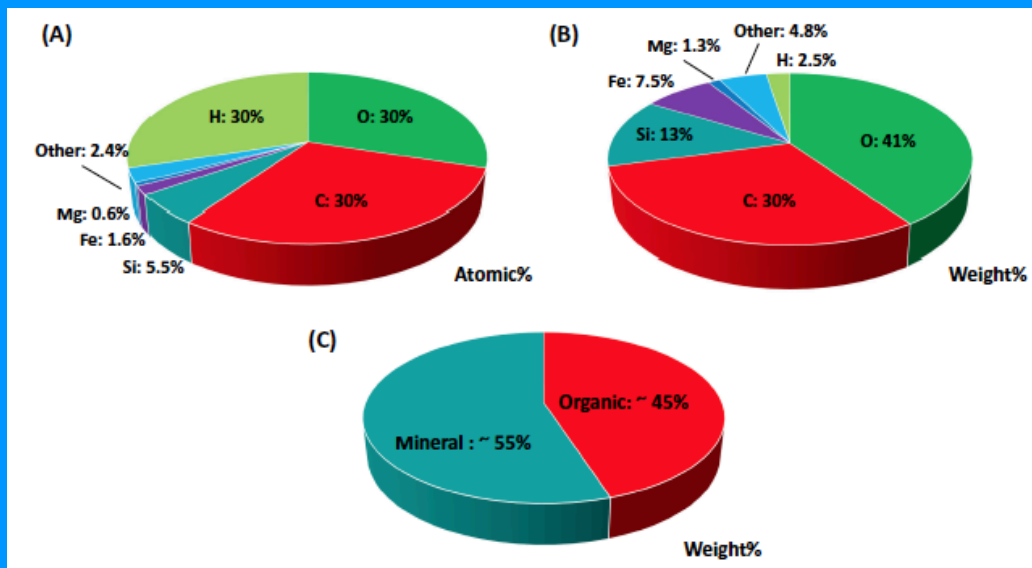
Raw absorbance is about same as Tholin; not 'dark' enough to be cometary highly absorbing grains seen in cometary IR spectra.



also see Derenne & Robert 2010MAPS, on model for IOM

67P/C-G IOM-like organic matter

- » most similar to high molecular weight macromolecular carbon (meteoritic IOM) (Fray+16)
- » higher H/C ratio (Fray+16)
- » higher N/C ratio (Fray+17), but less than in UCAMMs
- » (Bardyn+17)(Fray+17)
- » missing lower molecular weight -COOH (carboxylic)
- » IOM-like material constitutes 50% of C in 67P
- » much more organics than in Stardust



(Bardyn+17)

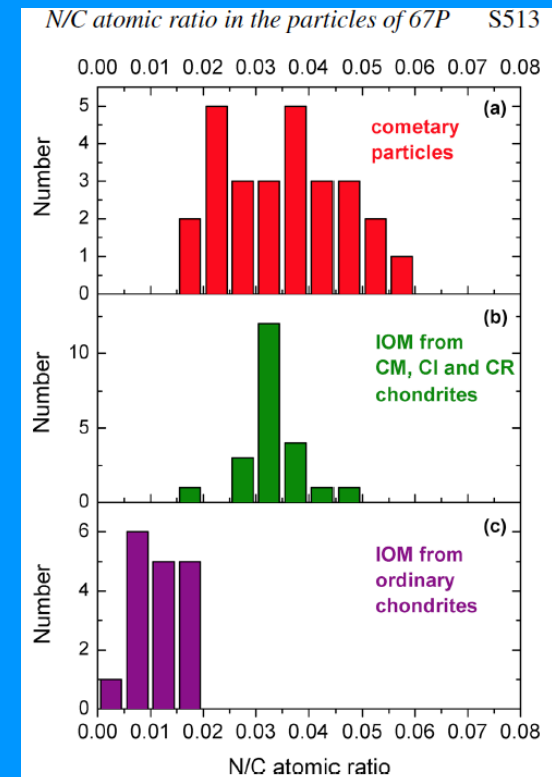


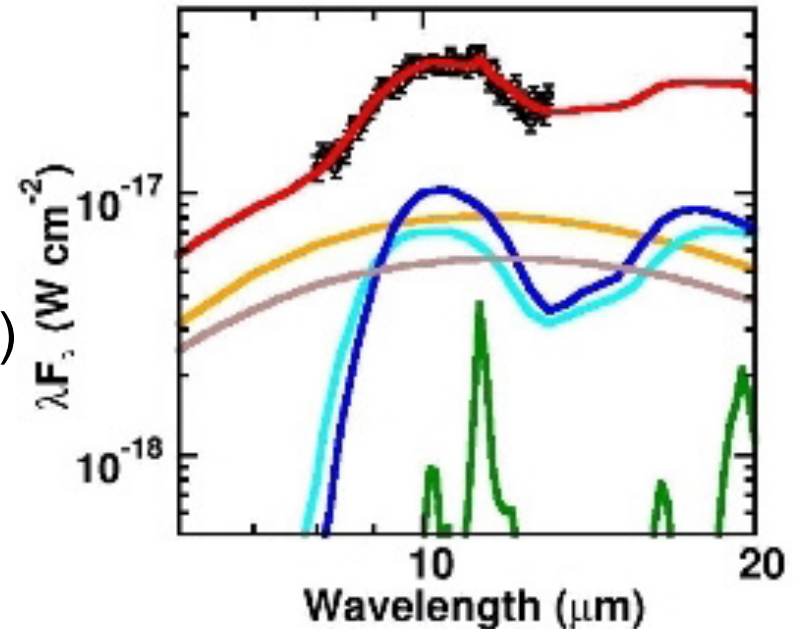
Figure 6. Histograms of the N/C atomic ratios measured in 27 cometary particles of 67P (in red, panel a), in 22 IOM samples of CI, CM and CR carbonaceous chondrites (in green, panel b) and in 17 IOM samples from ordinary chondrites (in purple, panel c). All the N/C atomic ratios of IOM samples of chondrites were found in Alexander et al. (2007).

(Fray+17)

chondrites and IDPs. Thus, the 67P particles and the nucleus are rich in organic matter, as already suggested from indirect observations (Fulle et al. 2016; Herique et al. 2016), and this indicates that comets have been aggregated in an organic-rich region of the protoplanetary disc.

Comet IR spectra have 5 components, which includes warm featureless grains that produce near-IR 'continuum' emission at $>3\mu\text{m}$:

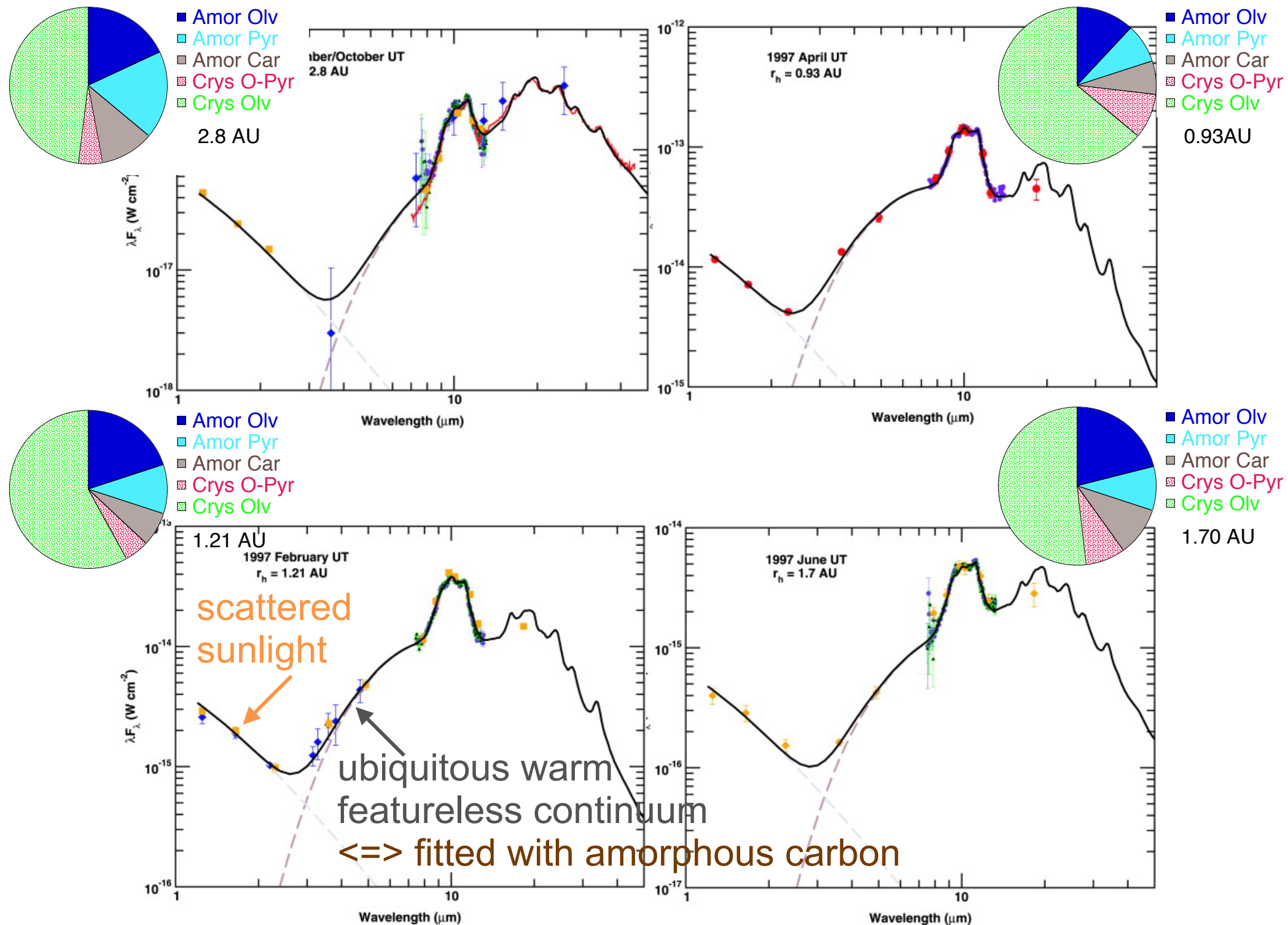
- **Amorphous Mg:Fe silicates**; porous – GEMS-like
- **Amorphous-like olivine** (glassy, disordered)
- **Amorphous-like pyroxene** (glassy, disordered)
- Abundant amorphous carbon-like (n,k)
- **Crystalline silicates** (when detected) are:
 - **Mg-rich $[\text{Mg}/(\text{Mg}+\text{Fe})>0.9]$**



9P/Tempel 1 (Harker, Woodward, Wooden 2005, Science, 310, 278)

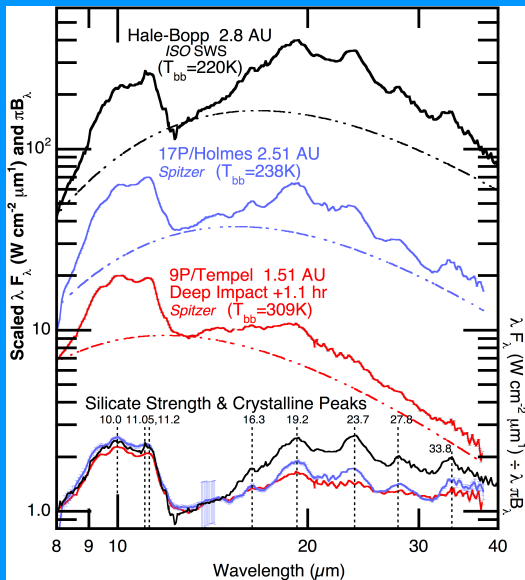
- NO layer-lattice silicates (e.g., Montmorillonite, smectite)
- no spectral detection of Al_2O_3

Intro to Cometary Spectral Energy Distributions: Hale-Bopp & changes with time (rh)

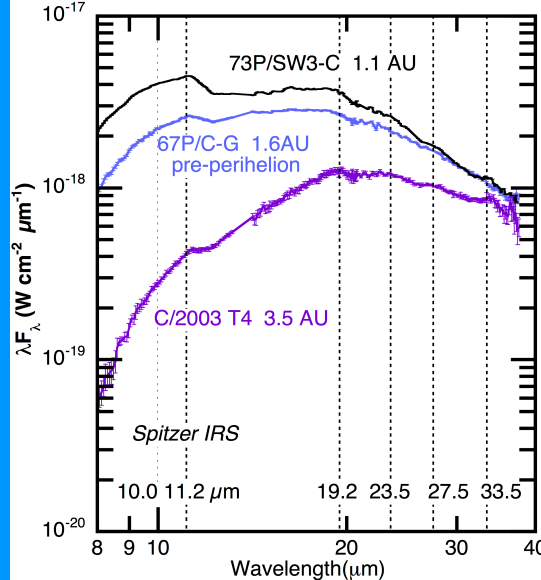


Spitzer spectra of comets show wide range of amorphous carbon-to-silicate ratios and grain size distributions that peak at grain radii varying from $\sim 0.2\mu\text{m}$ to $\sim 1\mu\text{m}$.

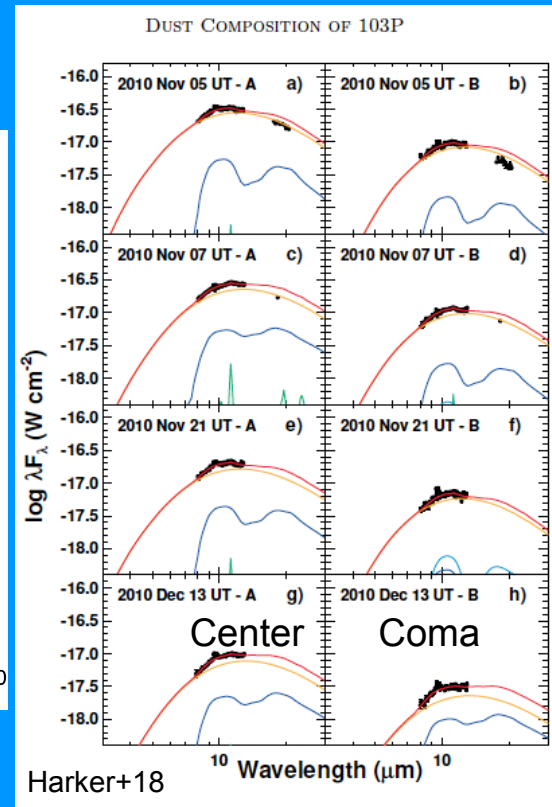
Highest contrast features are *lowest carbon to silicate ratio* and small $\sim 0.2\mu\text{m}$ grains.
 Lowest contrast features are a combination of *higher amorphous carbon* and larger peak grain radii.



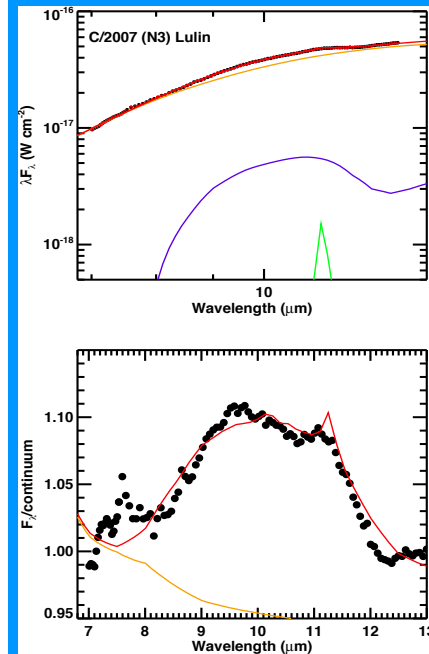
WIZ+17



WIZ+17



Harker+18



Woodward+11

$\sim 0.2\mu\text{m}$ and larger and porous grains, 'low' amorphous carbon relative to silicates (*high sil-to-Acar*)

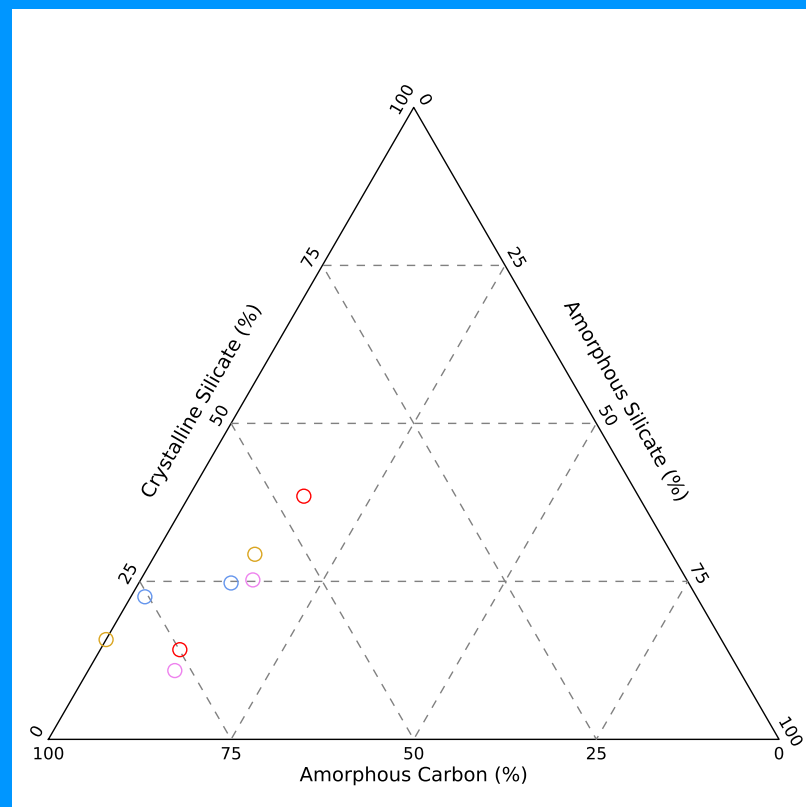
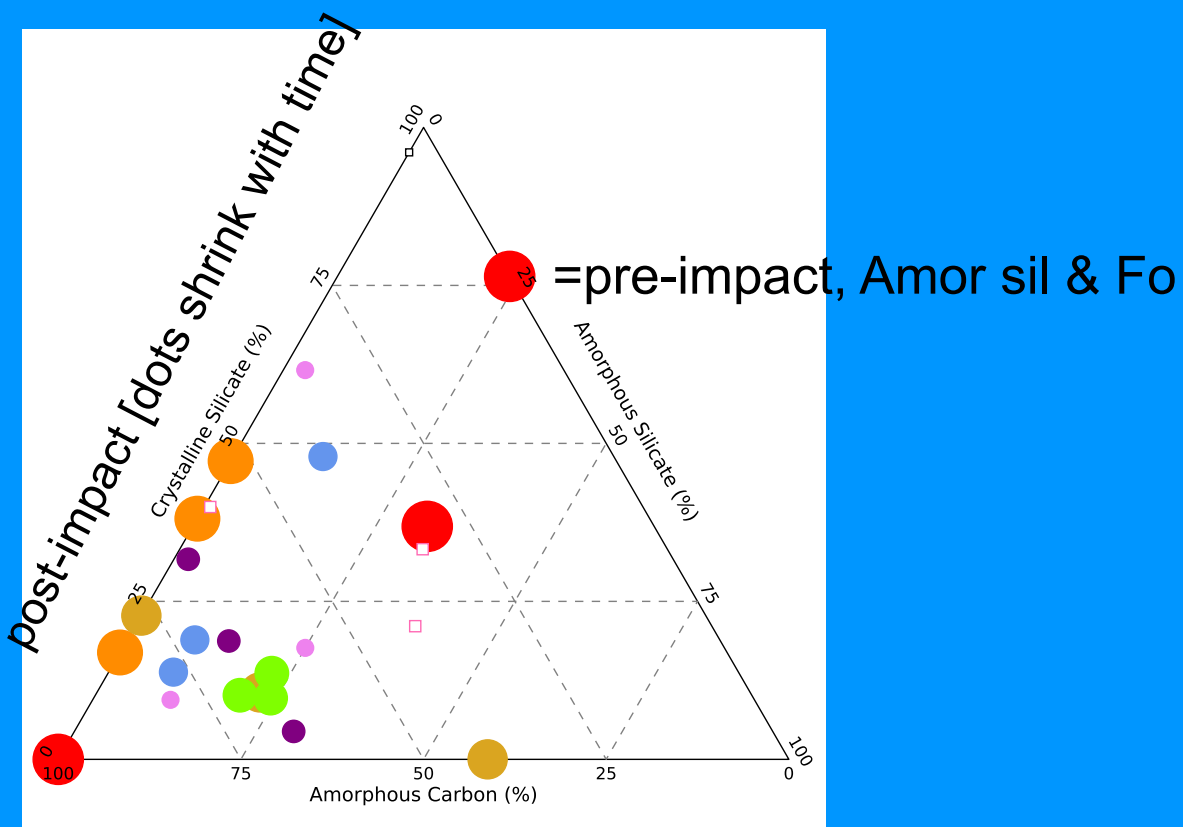
$\sim 0.5\text{--}1\mu\text{m}$ low porosity or solid grains, 'high' amorphous carbon relative to silicates



Comet 9P/Tempel 1 had a changing silicate-to-amorphous carbon ratio in the inner coma during +3 hr after Deep-Impact:
 (Gemini-N: Harker+05,
 Harker+07 (ternary diagram below)
 Subaru: Sugita+05)

103P/Hartley 2 has high amorphous carbon relative to silicates

103P/Hartley 2, Harker+18 AJ in press



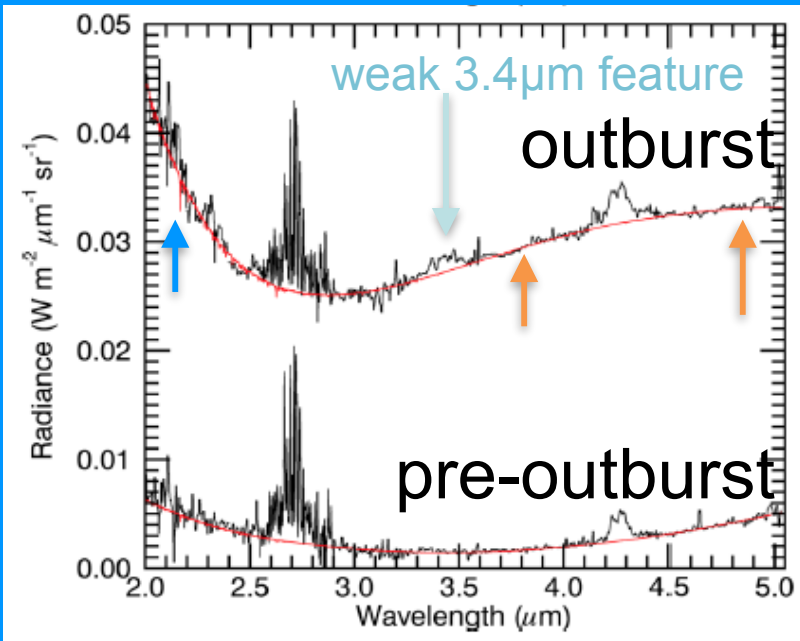
“Take home message”: Amorphous carbon versus silicates, and silicate crystalline fraction are not simply dependent on dynamical history of the comet (inner solar system evolution) or dynamical family (origin), i.e., not dependent on whether comet is a short-period ‘Jupiter Family’ or Ecliptic comet vs. long-period ‘Oort cloud’ comet or Isotropic comet.

Comet 67P had 2 **outbursts** of dust on 2015-09-13, 14 UT:

Reflected light increased at 2-2.5 μm and became bluer

Dust temperatures jumped from $\sim 300\text{K}$ to $\sim 600\text{K}$.

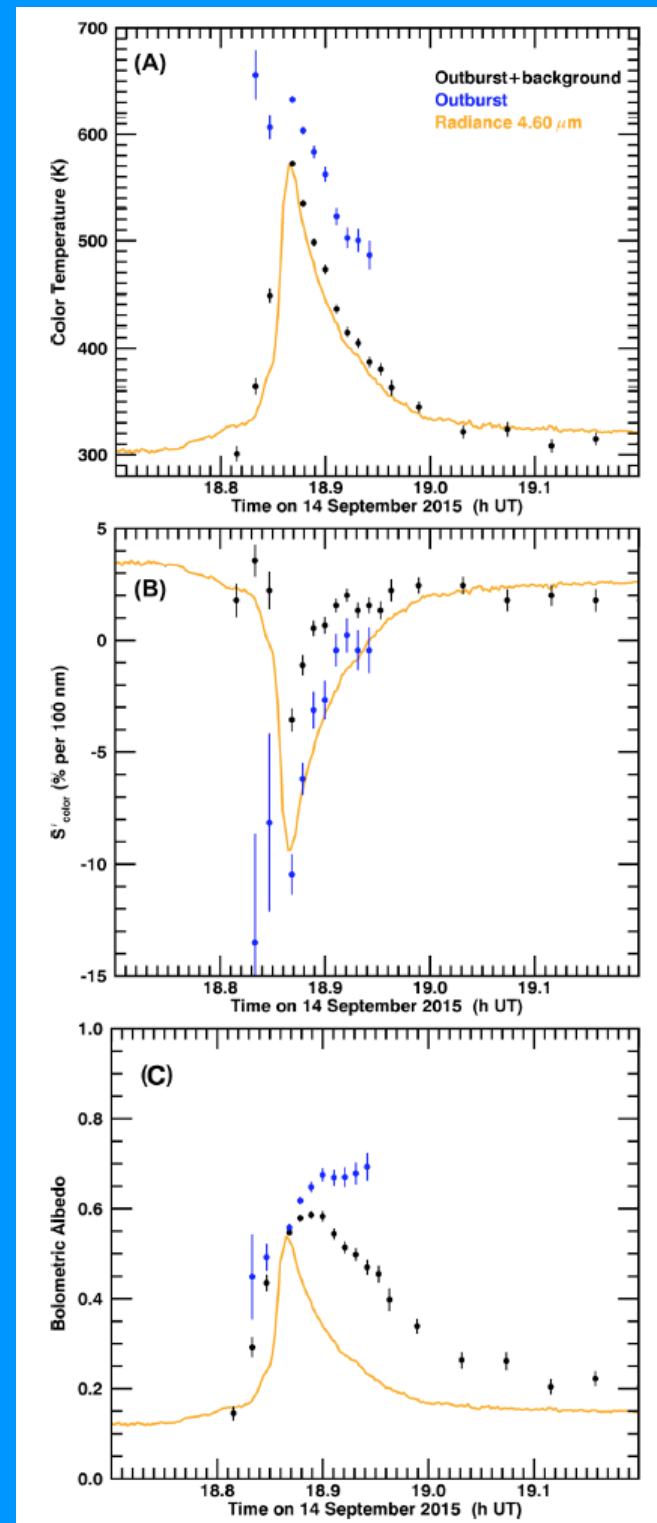
emission modeled with porous ($D=2.5$) 100nm-radii grains, mix of 66% amorphous carbon and 34 vol% amorphous Mg-Fe olivine or separate components (VIRTIS, Bockelee-Morvan+17)



“Both the colour and colour temperature measured at the peak of brightness of the September 14 outburst are satisfactorily reproduced with a population of carbon/olivine grains, constituted almost uniquely of small grains with a mean radius of $a_{\text{mean}} \sim 0.1 \mu\text{m}$. However, the high bolometric albedo ~ 0.6 is not explained.”

Olivine-only grains could explain the peak albedo but not the highest temperatures. Perhaps there are 2 grain components separately governing the scattered light and thermal emission, both $\sim 100 \text{ nm}$.

Changes with time could be progressively larger grains crossing field-of-view.



67P/C-G: 2015 Sep14 outburst

Deep Impact 9P/Tempel 1 had polarized light at leading edge of ejecta: dark particles!

- One possibility is that the carbonaceous grains are smaller than the silicate grains so that such carbonaceous grains got faster speeds due to acceleration by gas drag.
- Alternatively, suppose that the grains with the faster ejection velocity belonged to the surface layer.

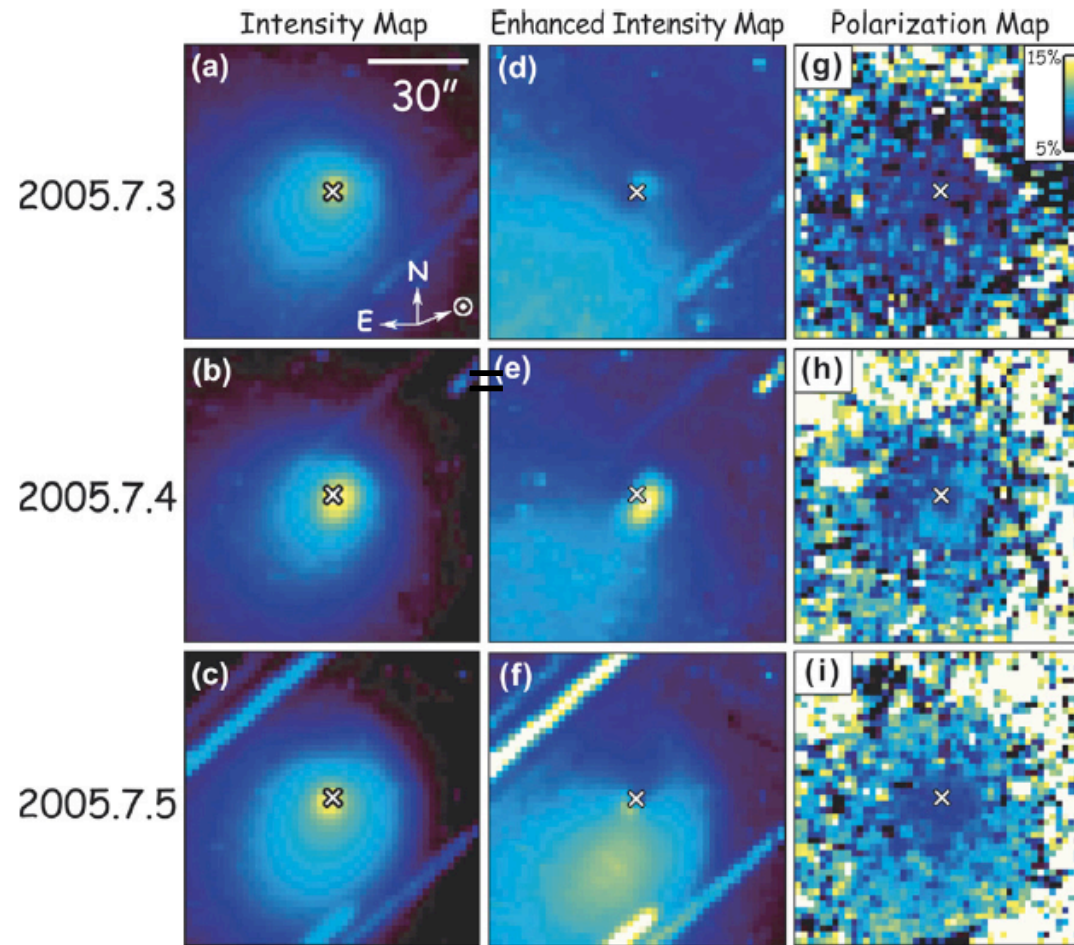


Fig. 1. The intensity, enhanced intensity, and linear polarization degree maps taken on July 3 (12:51–14:55 UT), 4 (12:12–14:48), and 5 (12:04–14:55). Up is the North, left is the East, and the area is 90×90 arcsec for each map. Cross mark denotes the optical center of the comet.

(Furusho+07)

1P/Halley: 'CHON' grains dominated flyby when VEGA, GIOTTO closer to nucleus and 19% of CHON are elemental C-only grains

Carbonaceous components in the comet Halley dust

M. N. FOMENKOVA,¹ S. CHANG,¹ and L. M. MUKHIN²

Geochimica et Cosmochimica Acta, Vol. 58, No. 20, pp. 4503-4512, 1994

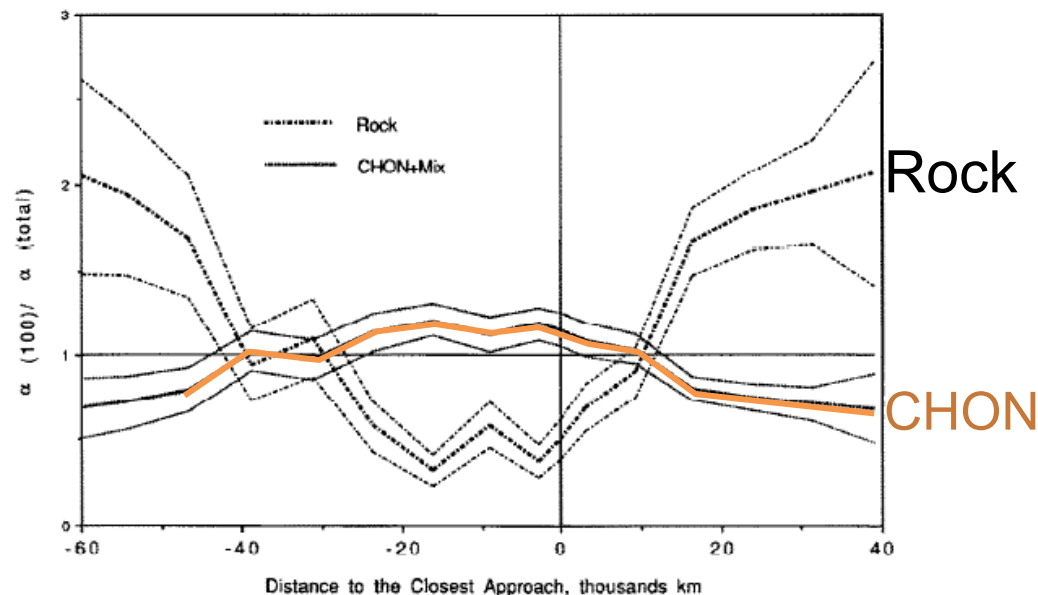


FIG. 1. Spatial variability of dust grain distribution in the coma (PUMA-1 data). For 100 second intervals along the trajectory, we considered $\alpha_{\text{org}}(100)$, the proportion of particles containing organic material (CHON and Mixed), and $\alpha_{\text{inorg}}(100)$, the proportion of particles lacking organic material (Rock):

$$\alpha_{\text{org}}(100) = \frac{N_{\text{CHON}} + N_{\text{Mixed}}}{N_{\text{CHON}} + N_{\text{Mixed}} + N_{\text{Rock}}}, \quad \alpha_{\text{inorg}}(100) = \frac{N_{\text{Rock}}}{N_{\text{CHON}} + N_{\text{Mixed}} + N_{\text{Rock}}}$$

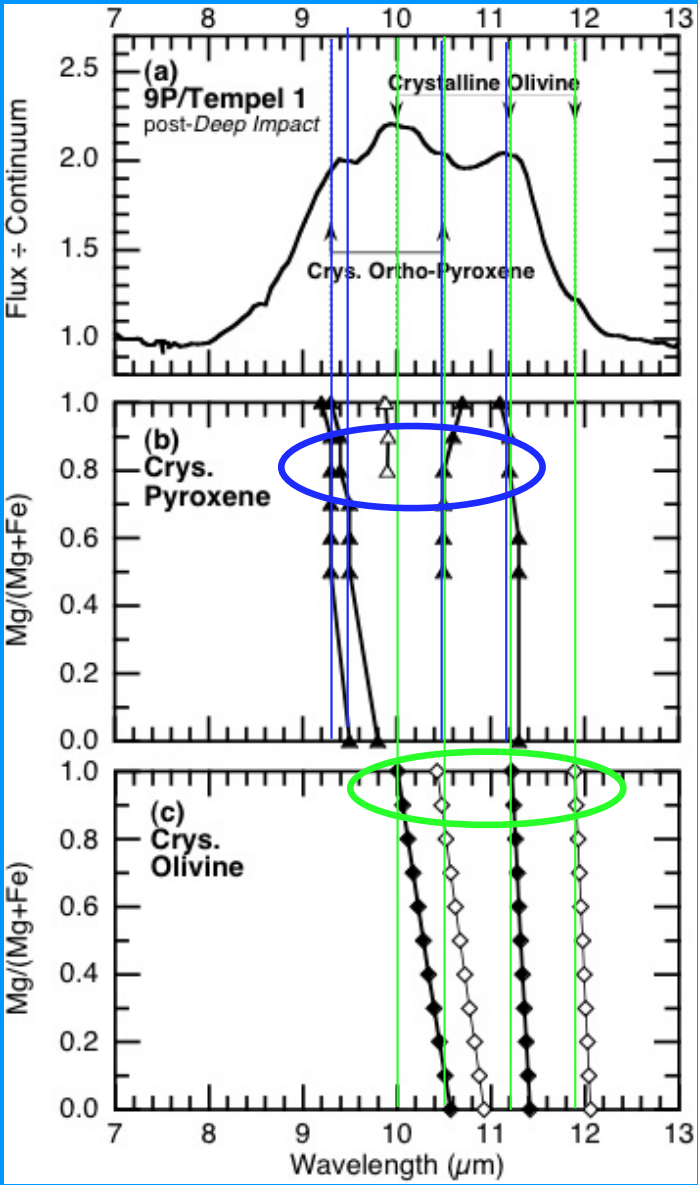
Table 2. Groups of CHON particles observed by cluster analysis.

# in PUMA-1	# in PUMA-2	H	C	N	O
I: [C]					
97	3	<0.004	0.99 ± 0.01	<0.005	<0.001
II: [H,C]					
1	8	0.12 ± 0.05	0.88 ± 0.05		
2	6	0.33 ± 0.06	0.67 ± 0.06		
3	17	0.52 ± 0.06	0.48 ± 0.06		
4	11	0.68 ± 0.03	0.32 ± 0.03		
	42				
III: [H,C,N]					
1	12	0.11 ± 0.04	0.87 ± 0.04	0.02 ± 0.01	
2	7	0.30 ± 0.03	0.67 ± 0.04	0.03 ± 0.02	
3	6	0.46 ± 0.05	0.48 ± 0.04	0.06 ± 0.05	
4	13	0.65 ± 0.04	0.34 ± 0.04	0.01 ± 0.01	
5	2	0.52 ± 0.17	0.23 ± 0.06	0.26 ± 0.11	
	38				
IV: [H,C,O]					
1	2	0.05 ± 0.07	0.87 ± 0.09		0.08 ± 0.02
2	5	0.57 ± 0.03	0.40 ± 0.05		0.03 ± 0.02
3	1	0.06 ± 0.02	0.48 ± 0.10		0.46 ± 0.09
4	4	0.66 ± 0.05	0.22 ± 0.03		0.12 ± 0.06
5	5	0.42 ± 0.03	0.23 ± 0.07		0.35 ± 0.05
6	3	0.60 ± 0.12	0.05 ± 0.03		0.35 ± 0.09
	1	0.29	0.67		0.04
	16				
V: [H,C,N,O]					
1	5	0.04 ± 0.02	0.86 ± 0.05	0.04 ± 0.02	0.06 ± 0.04
2	7	0.19 ± 0.03	0.74 ± 0.05	0.02 ± 0.01	0.05 ± 0.03
3	7	0.47 ± 0.08	0.50 ± 0.06	0.005 ± 0.004	0.03 ± 0.02
4	7	0.61 ± 0.05	0.26 ± 0.03	0.01 ± 0.005	0.12 ± 0.06
5	8	0.73 ± 0.03	0.23 ± 0.02	0.01 ± 0.01	0.03 ± 0.03
6	9	0.09 ± 0.05	0.62 ± 0.06	0.03 ± 0.02	0.26 ± 0.05
7	2	0.05 ± 0.01	0.41 ± 0.01	0.01 ± 0.01	0.53 ± 0.03
8	11	0.35 ± 0.06	0.41 ± 0.06	0.015 ± 0.01	0.23 ± 0.08
9	6	0.43 ± 0.03	0.19 ± 0.05	0.01 ± 0.003	0.37 ± 0.04
10	5	0.27 ± 0.07	0.18 ± 0.05	0.005 ± 0.005	0.55 ± 0.07
11	8	0.62 ± 0.06	0.08 ± 0.04	0.02 ± 0.02	0.28 ± 0.06
12	8	0.45 ± 0.10	0.33 ± 0.07	0.10 ± 0.05	0.12 ± 0.06
13	6	0.31 ± 0.09	0.21 ± 0.06	0.08 ± 0.03	0.40 ± 0.07
14	2	0.07 ± 0.05	0.31 ± 0.10	0.42 ± 0.11	0.20 ± 0.15
	91				
VI: no H					
1	10		0.90 ± 0.04	0.10 ± 0.03	
2	3		0.86 ± 0.08	0.02 ± 0.01	0.12 ± 0.06
3	4		0.82 ± 0.09		0.18 ± 0.09
4	5		0.62 ± 0.10	0.03 ± 0.03	0.35 ± 0.12
	22				

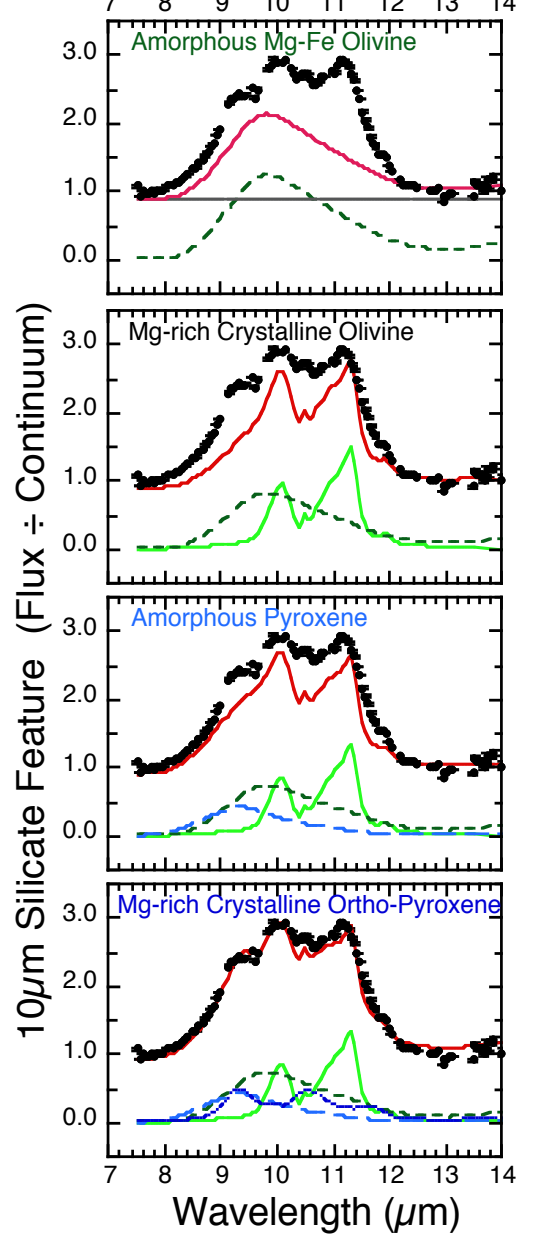
1) CHON particles dominated by carbon and/or organics represent ~22% of measured comet Halley dust grains (by number) and reveal a wide variety of compositional types. Decomposition of these particles in the coma may provide extended sources of some gaseous species.

3) Elemental carbon grains, various kinds of hydrocarbons, and probably polymers of cyanopolynes and multicarbon monoxides appear to be distinct contributors to the particle population. They represent, correspondingly, 19, 10, 2, and 1% of all CHON grains.

Mg-rich crystalline silicates produce strong 10μm features when coma is dominated by submicron silicate grains

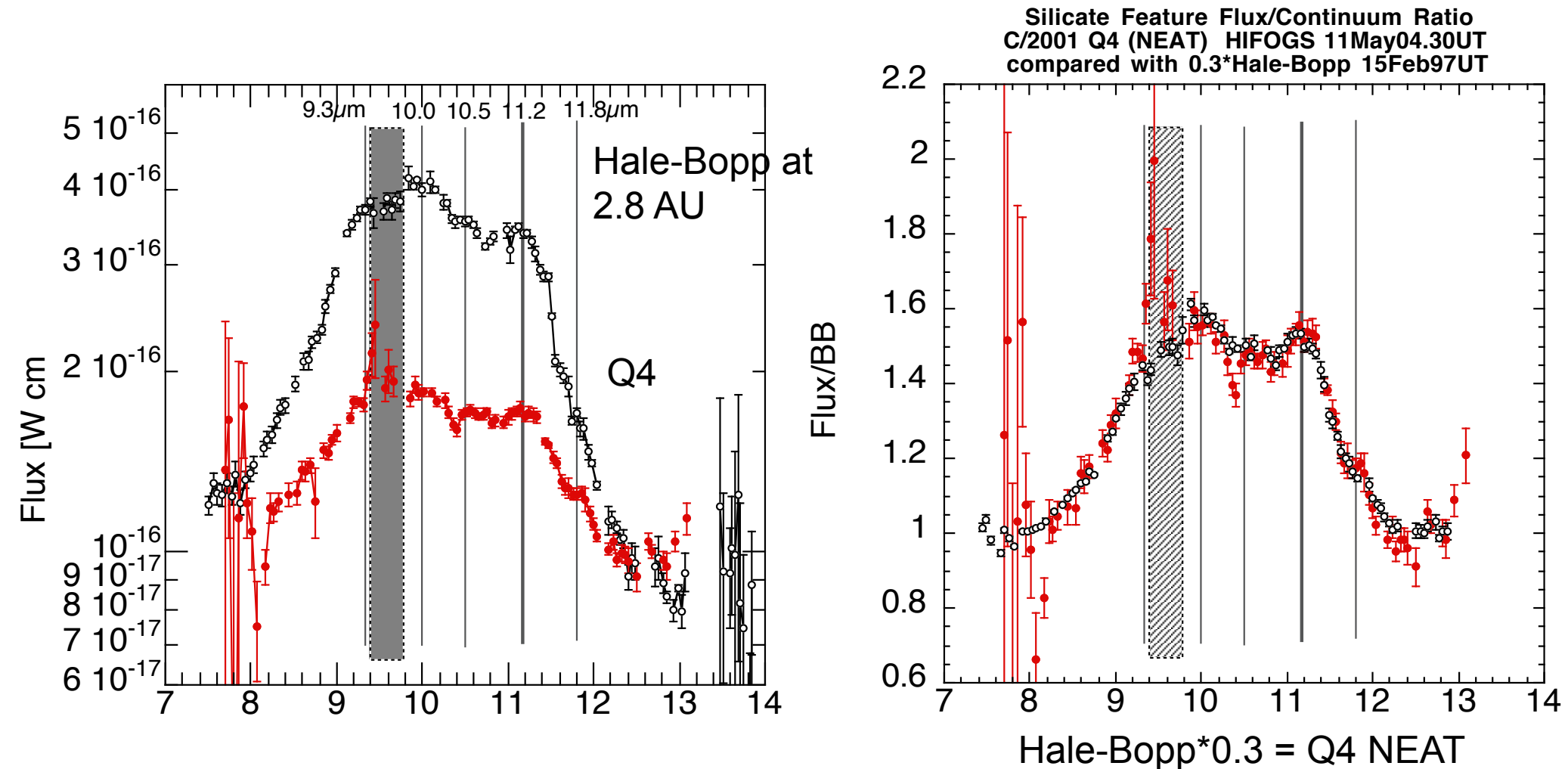


Hale-Bopp at perihelion

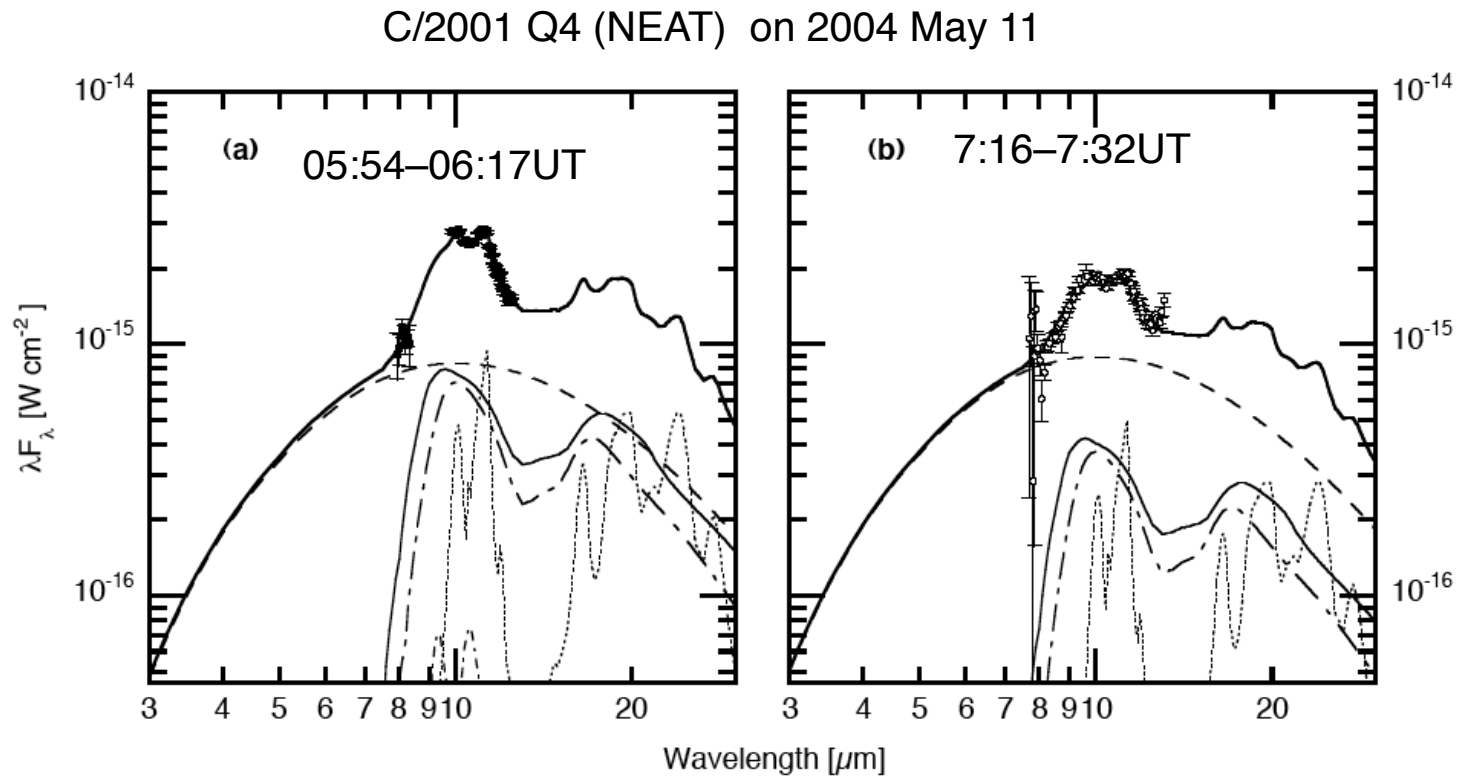


Oort cloud comets C/2001 Q4 (NEAT) & Hale-Bopp have similar silicate mineralogy; both have strong jet activity and abundant Forsterite crystals
 $f_{\text{crystal}} = \text{crystal}/(\text{amorphous}+\text{crystalline}) \approx 0.7$

C/2001 Q4 has variable silicate-to-amorphous carbon ratio, which lowers the contrast (height) of the silicate feature (next slide)



C/2001 Q4's silicate **feature drops in contrast** (height) over 1.5 hours, as jets move grains through beam and dust composition changes: there are **fewer silicate grains relative to amorphous C grains** (right).



Is this true? Assertion: Amorphous Carbon is a separate grain component from the silicates in this comet.

Outer icy bodies require darkening materials on their surfaces, and amorphous carbon is used in models.

~40-90% amorphous carbon

Object Class	Object Name	Amorphous Carbon	Titan Tholin [a]	Tritan Tholin [b]	Ice Tholin [c]	Kerogen Type II [d]	Water Ice	Olivine	A [e]	Refs
Centaur	2001 PT ₁₃	0.7 10 μm	0.15 7 μm		0.12 10 μm			0.03	0.09	4
Centaur Epoch1,2	2001 PT ₁₃	0.7, 0.9	0.15, 0.05		0.12, 0		0, 0.05	0.03, 0	0.09 0.06	4, 13, 2
Centaur	1998 SG ₃₅					0.97	0.02	0.01		4, 13, 10
Centaur	2000 QC ₂₄₃					0.96	0.03	0.01	0.04	13, 11
Centaur	2001 BL ₄₁	0.73		0.17	0.10				0.08	4, 13, 14
Centaur Epoch1,2	1999 UG ₅	0.66, 0.41	0.14, 0	0, 0.42		CH ₃ OH ice 0.03, 0	0.13, 0.17	0.04, 0	0.05	13, 1
Centaur	Pholus	carbon black	YES				YES +CH ₄ ice		0.06	13, 6
Centaur	Chariklo	YES	YES	YES			~0.02			13, 12
Centaur	Asbolus	0.73		0.17	0.10				0.08	13, 19
Centaur	Chiron						YES when inactive 1996-2001			13, 16
TNO	2000 EB ₁₇₃	YES	YES					Jarosite? [f]		4, 9
TNO	1999 TC ₃₆	0.10	0.67		0.25		0.08			4, 11
TNO	1996 GQ ₂₁	0.50	0.15		0.35					4, 11
KBO	1996 TO ₆₆ <i>Active</i>						YES strong			18
KBO	1999 DE ₉	yes		organics	yes		yes			18, 3, 14
KBO	2001 BL ₄₁	yes	yes				yes			18
Trojan Asteroid Model1 Model2 Model3	Hektor	YES; G=graphite 0.2 0.01 0.4+0.15G						pyroxene, serpentine 0.4, 0.4 0.29, 0.7 0.45, 0		8, 7

Can cometary dark materials provide clues to the abundance of this material and to its composition?

Comet samples can contain up to 45 wt% C (90 vol%).

Challenge: Tholins and IOM are relatively transparent !

Amorphous carbon darkens and then organics are added to get absorption bands (Cristina Dalle Ore, private communication)

Notes: [a] Titan Tholin N₂:CH₄=0.9:0.1 [15]; [b] Tritan Tholin: N₂:CH₄=0.999:0.001 [17]; [c] Ice Tholin H₂O:C₂H₆ [15]; [d] Kerogen Type II []; [e] A means Albedo at 0.55 μm; [f] Jarosite KFe₃(SO₄)₂(OH)₆

Refs: 1: Bauer et al. 2002; 2: Barucci et al. 2002; 3: Boehnhardt et al. 2002; 4: Boehnhardt et al. 2003, EMP 92; 5: Brown et al. 1997; 6: Cruikshank et al. 1998; 7: Cruikshank et al. 2001; 8: Cruikshank & Dalle Ore 2003, EMP 92; 9: de Bergh et al. 2003; 10: Dotto et al. 2002; 11: Dotto et al. 2003a; 12: Dotto et al. 2003b; 13: Dotto et al. 2003c, EMP 92; 14: Doressoundiram et al. 2003; 15: Khare et al. 1984; 16: Luu et al. 2000; 17: McDonald et al. 1994; 18: Meech et al. 2003, EMP 92; 19: Romon-Martin et al. 2002; 20: Sagan & Khare 1979.

Table that Diane assembled in 2008.

Cometary carbonaceous 'domains' are diverse in abundance and forms

- Carbonaceous matter in comets is highly variable in abundance, and has different forms of carbon with organic and possibly inorganic C
- not all organics are like insoluble organic matter (IOM)
- some organic matter is highly labile (soluble organic matter)
- some elemental carbon is seen (with names highly disordered carbon, poorly graphitized carbon, or amorphous carbon)
- different cometary IDPs have different characteristics:
 - chondritic porous IDPs can have high C as amorphous carbon or IOM-like (high molecular weight organic matter), Forsterite and Enstatite crystals
 - Giant IDPs have Olivine with range of Fe contents and IOM-like
 - IDPs with higher concentrations of Mg-rich crystals (Enstatite in particular) have higher C abundances (Thomas+93 GCA)
- Ultra Carbonaceous Antarctic Micrometeorites (UCAMMs, likely cometary) have high contents of carbonaceous matter (90% by volume).
- Thermal modeling of IR spectra of comets show a large variation in the ratio of dark absorbing grains [near-IR continuum] to silicates, i.e., 'amorphous carbon'-to-'silicate' ratios
- Cometary organics are more diverse than meteoritic organics (IR spectra and XANES), in functional groups and ratio of -CH₂ to -CH₃ in aliphatics
- **Is there link between organics in samples and dark particles spectrally seen in cometary coma?**
- **What role may FeS play in darkening surfaces compare to organics? We need better FeS optical constants.**

Intermission or Coda

» Details on minerals follow, for those who are interested

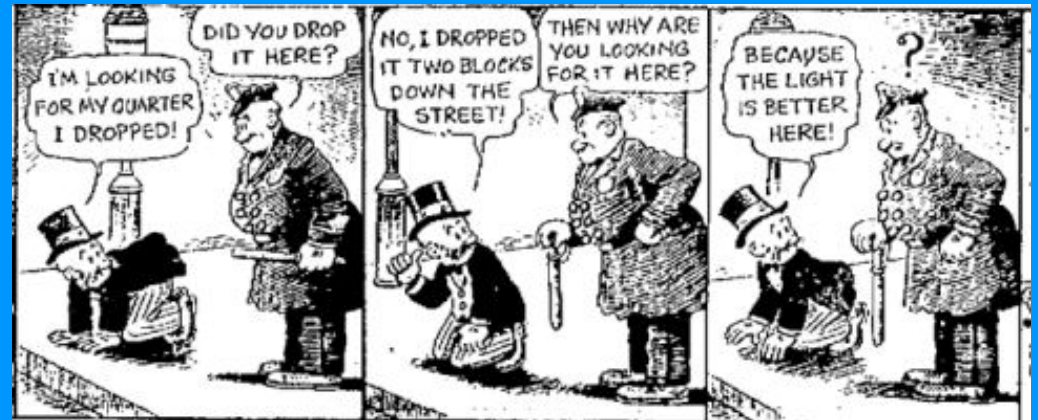
Organics and refractories in comets and meteorites?

What are primitive materials?

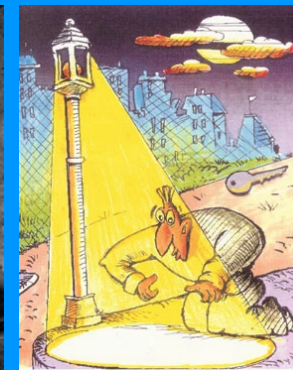
What are possible source regions?

Can we define primitive materials and consider different bodies that contain them?

Many details are discussed in:



remote sensing, flyby measurements



PHILOSOPHICAL
TRANSACTIONS A

rsta.royalsocietypublishing.org



Cometary Dust: The Diversity
of Primitive Refractory Grains

D. H. Wooden¹, H. A. Ishii² and M. E.
Zolensky³

¹NASA Ames Research Center, Moffett Field, CA
94035-0001, USA

Stardust

anhydrous IDPs carbonaceous
Cluster IDPs chondrites
Giant IDPs

“There is more than one street lamp.” To bridge the conversation, we discuss the sources & ideas in WIZ2017. (Open Access to main and suppl.)

Regime of Crystalline Silicate Condensation

When & Where

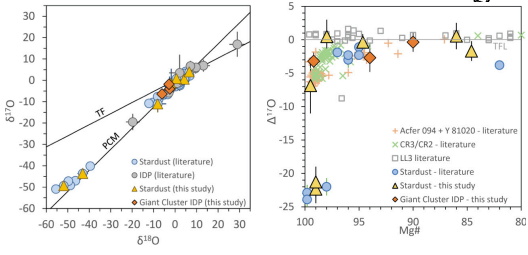
Transport outward (comets & Trojans & ?) ^{JUST}

LIME Low Iron Mn-Enriched / "Mg-rich" Olivine Forsterite Enstatite
 100% ≤ Mg ≤ 98% (Fo₉₈)
 160-rich ← "early"

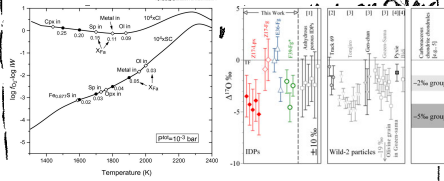
100% ≤ Mg ≤ 90%

Models Fedkin & Grossman

can be condensates of dust-enriched 10⁴ "aqueously-altered (CS)"
 fO₂ increases slightly so need water vapor



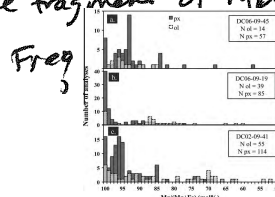
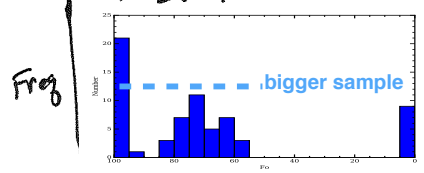
early 160-rich reservoir



CHONDRULE FORMATION

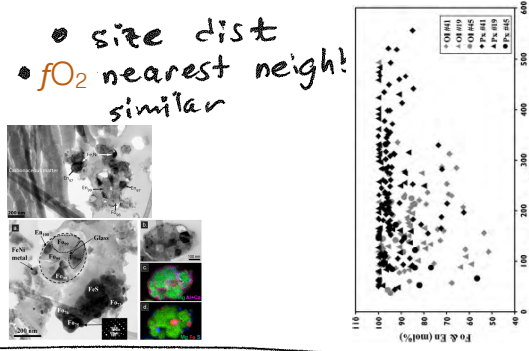
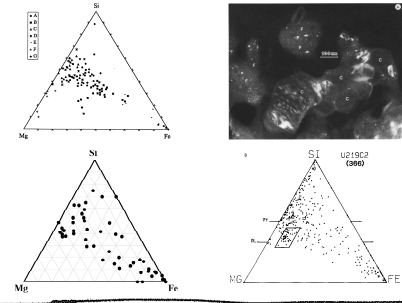
Regime of Fine-Grained Chondrule Formation

'Iris' in Stardust is an igneous system "mini"
 ~12% Fe ↔ chondrule fragments of type II



100% Frank et al '14 Stardust
 Brownlee 0%
 16 Giant IDPs

100% Dobrica UCAMMs 0%



• size dist
 • fO₂ nearest neigh! similar

Association of Carbon with Mg-mineral crystals

Abundance Range

Some CP IDPs
 50% by volume

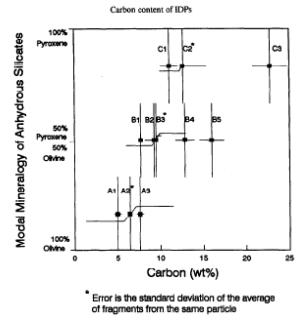
UCAMMs
 Halley

Stardust

little carbon capture-destruct.

very high carbon

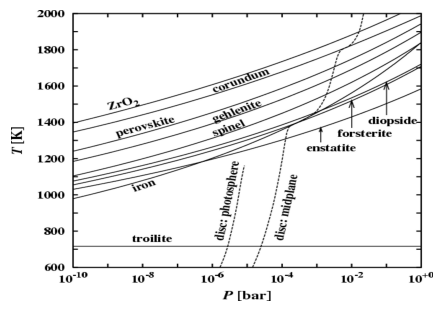
Thomas et al 1994-95 studies
 retention or destruction of carbon



Enstatite-rich IDPs have more carbon

GEMS-rich IDPs have more Mg-rich crystals and little Fe-rich crystals

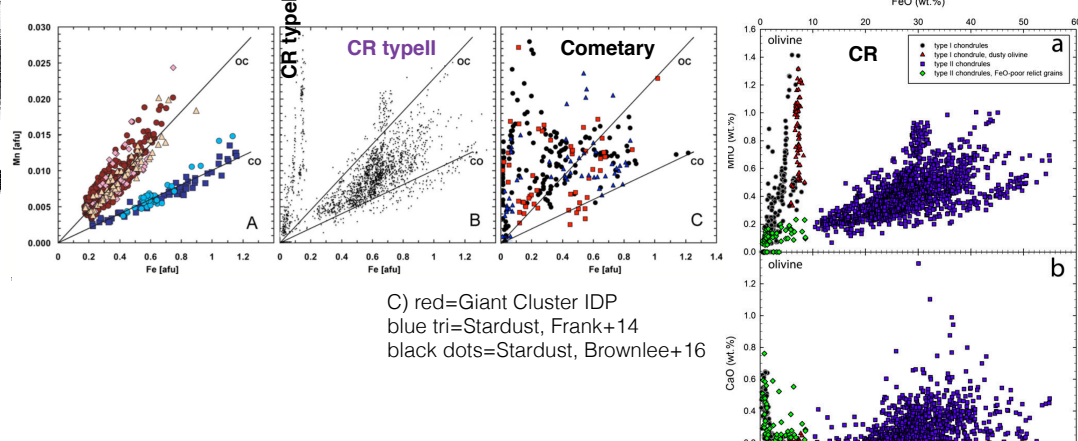
Do GEMS-rich IDPs have more carbon? Is survival of amorphous silicates and carbonaceous matter correlated?



Mn-story

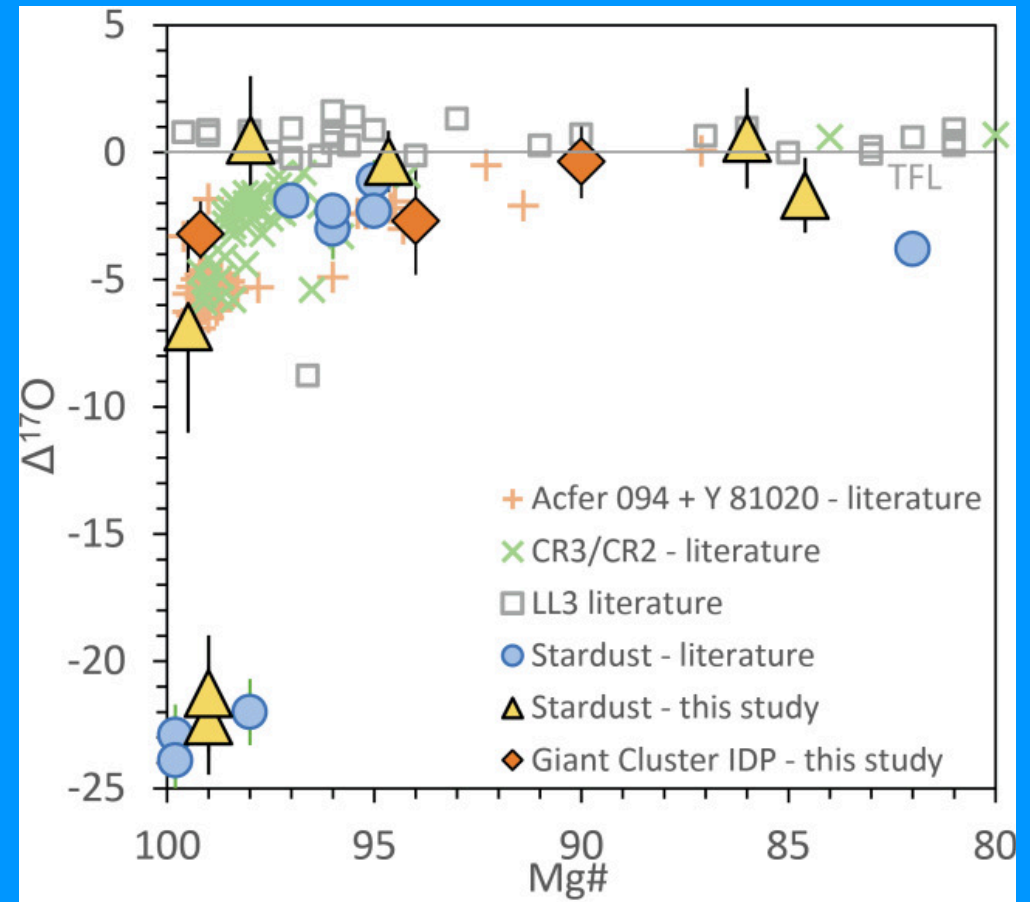
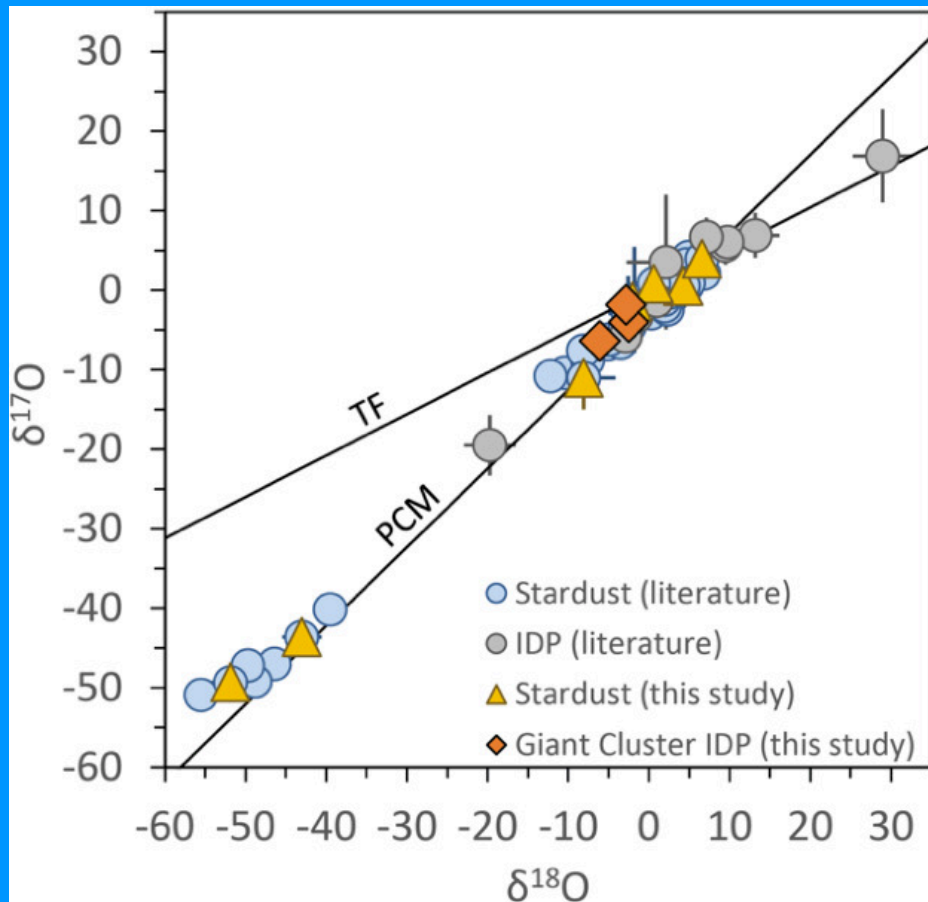
Type II < CR are assemblages of mini igneous systems

- Stardust & Giant IDPs have LIME ↔ CR-like radial transport, particles heated for a while CAI time=0 ~25 Myr ~3M yr
- Radial transport efficient enough over this huge time range
- particle size x similar 5-30 µm
- comets have ≤ matrix-size & matrix-composition olivine



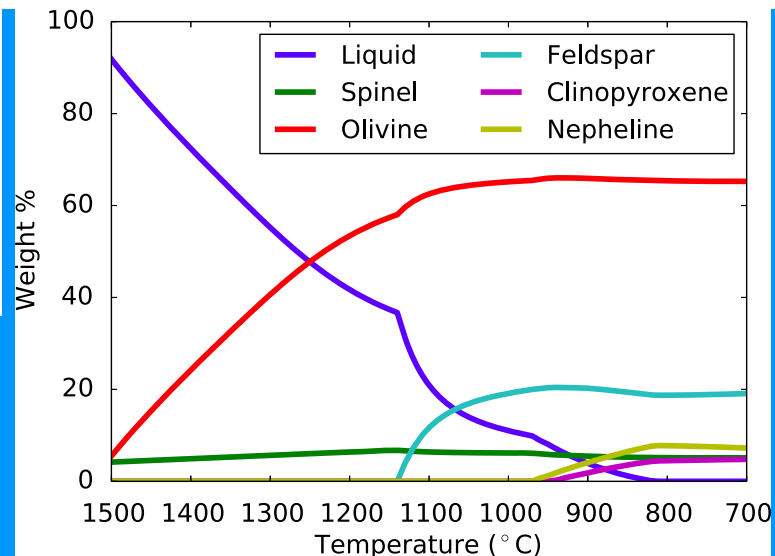
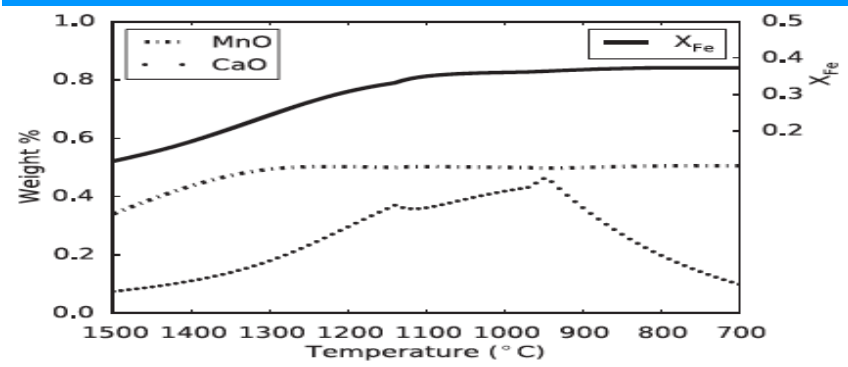
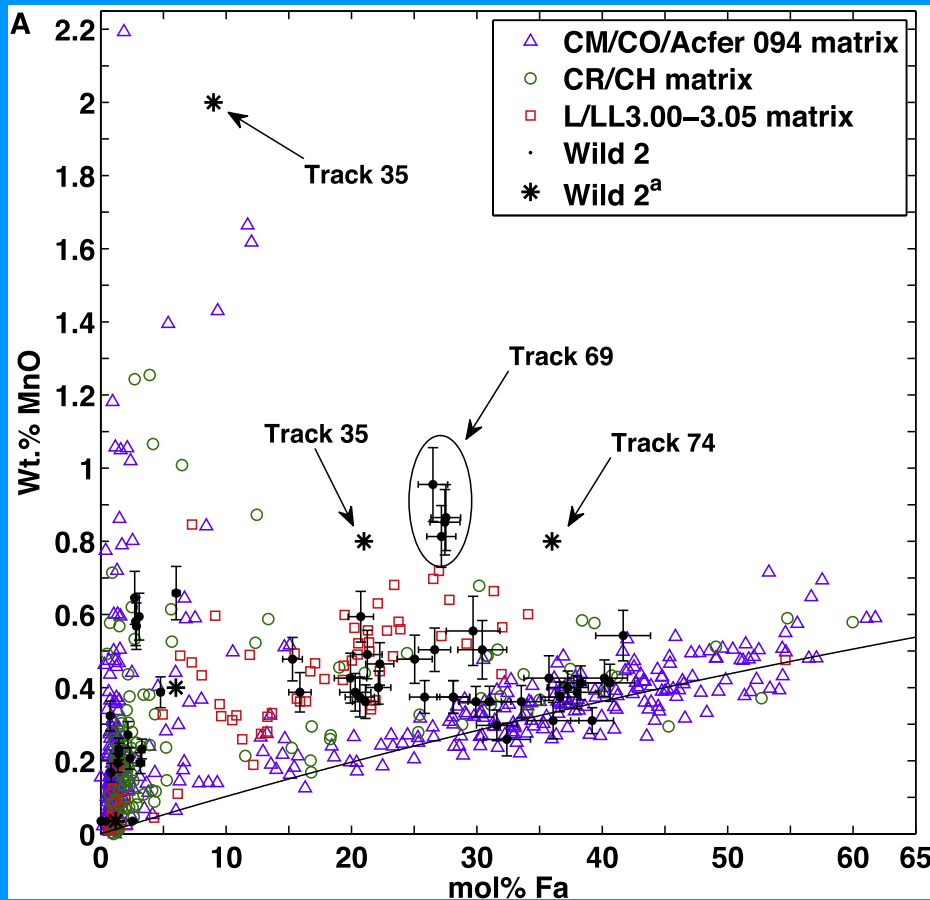
C) red=Giant Cluster IDP
 blue tri=Stardust, Frank+14
 black dots=Stardust, Brownlee+16

a story that emerges from Defouilloy+16LPSC, Defouilloy+17:
high Mg-content olivines are early **condensates** because
Fo100-Fo98 have ^{16}O -enrichments (like AOAs and CAIs)



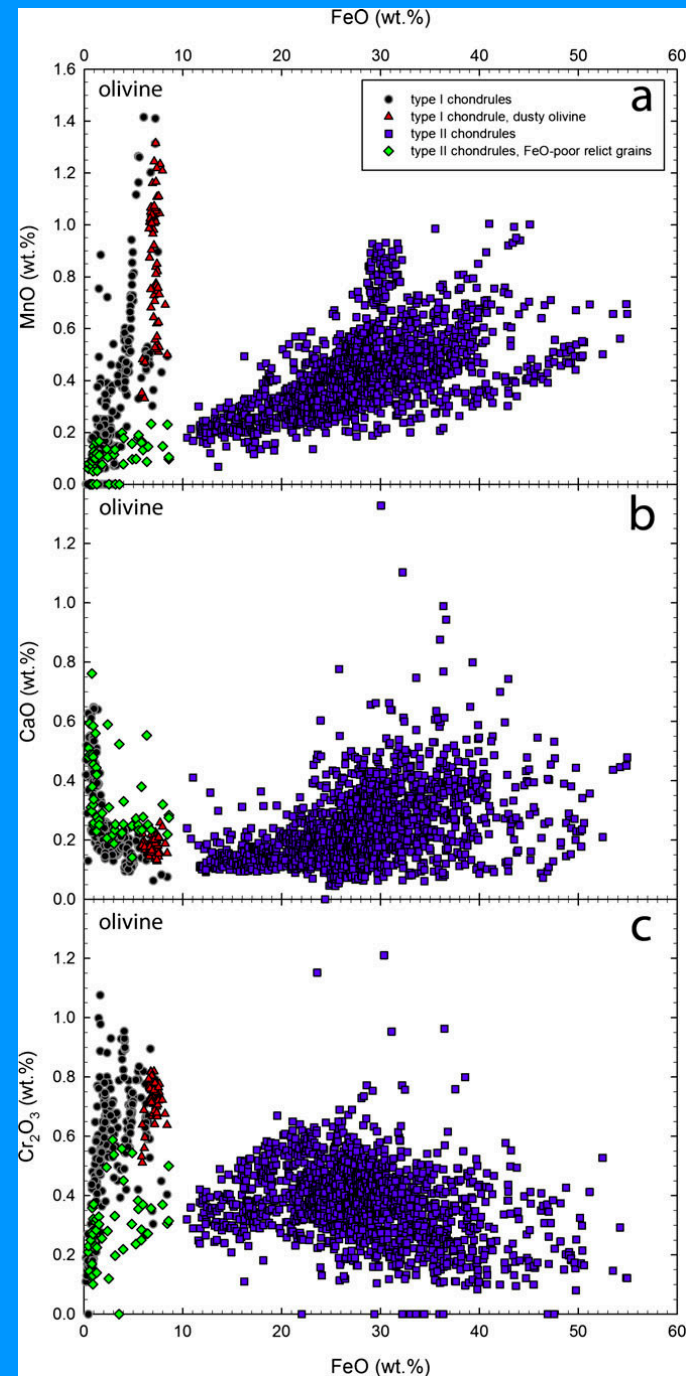
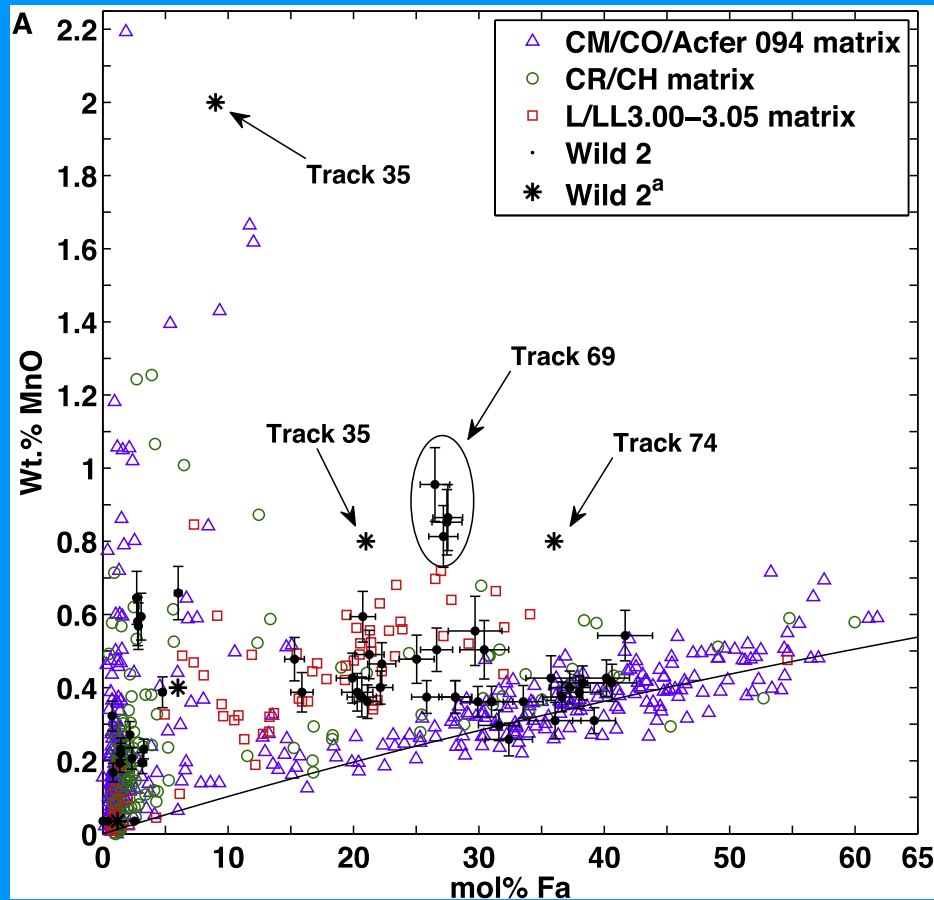
Stardust's olivines with Fe>10% are μ chondrules like 'Iris'

Iris (Fo60, $X_{Fe} \approx 0.4$) formed from a melt (droplet) in high oxygen fugacity gas. Iris is an 'igneous' particle, not a condensate.

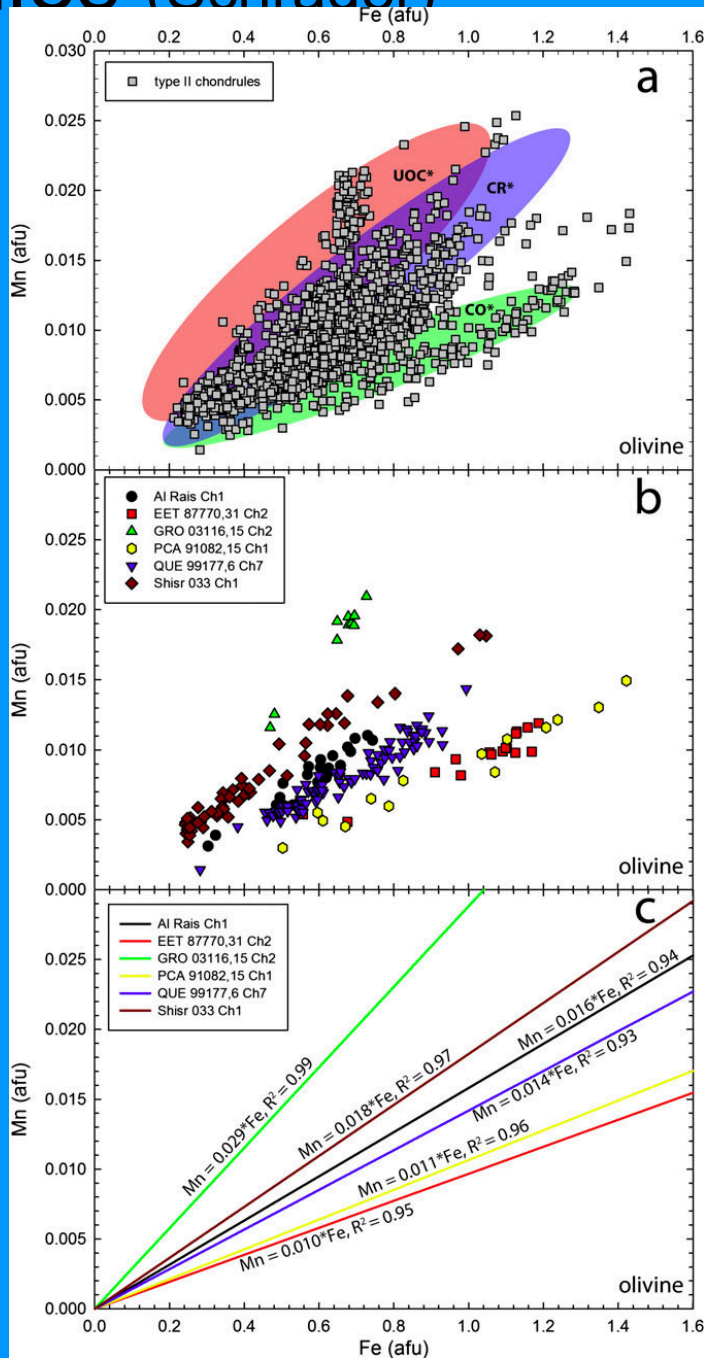


Iris: $\log(fO_2) = -13.3$ (IW-0.25 at 1000 C), at a pressure of 1 bar or less

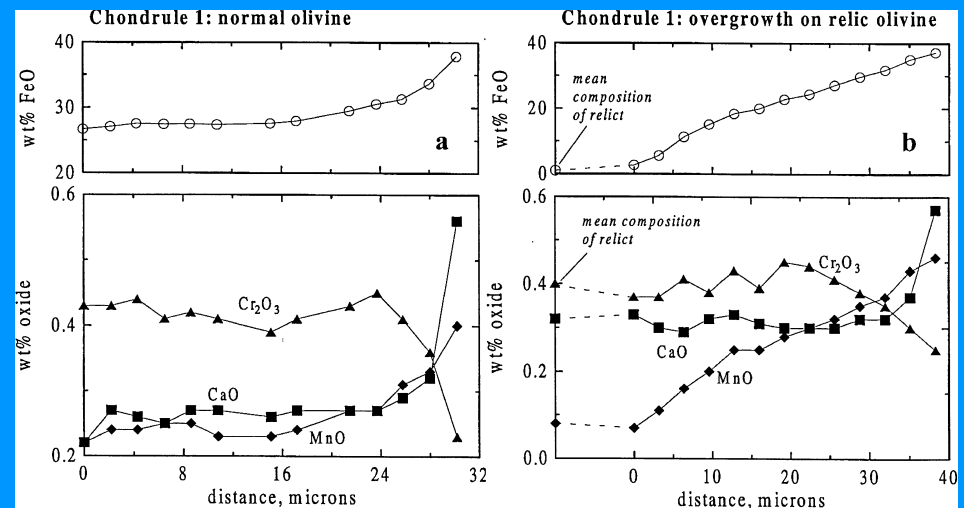
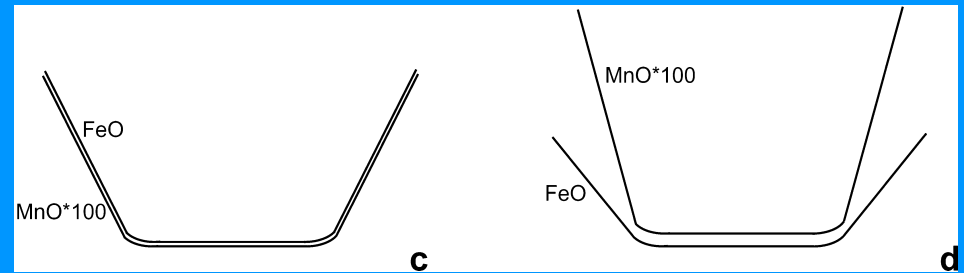
Stardust's olivines can be compared to CR chondrules (Schrader)



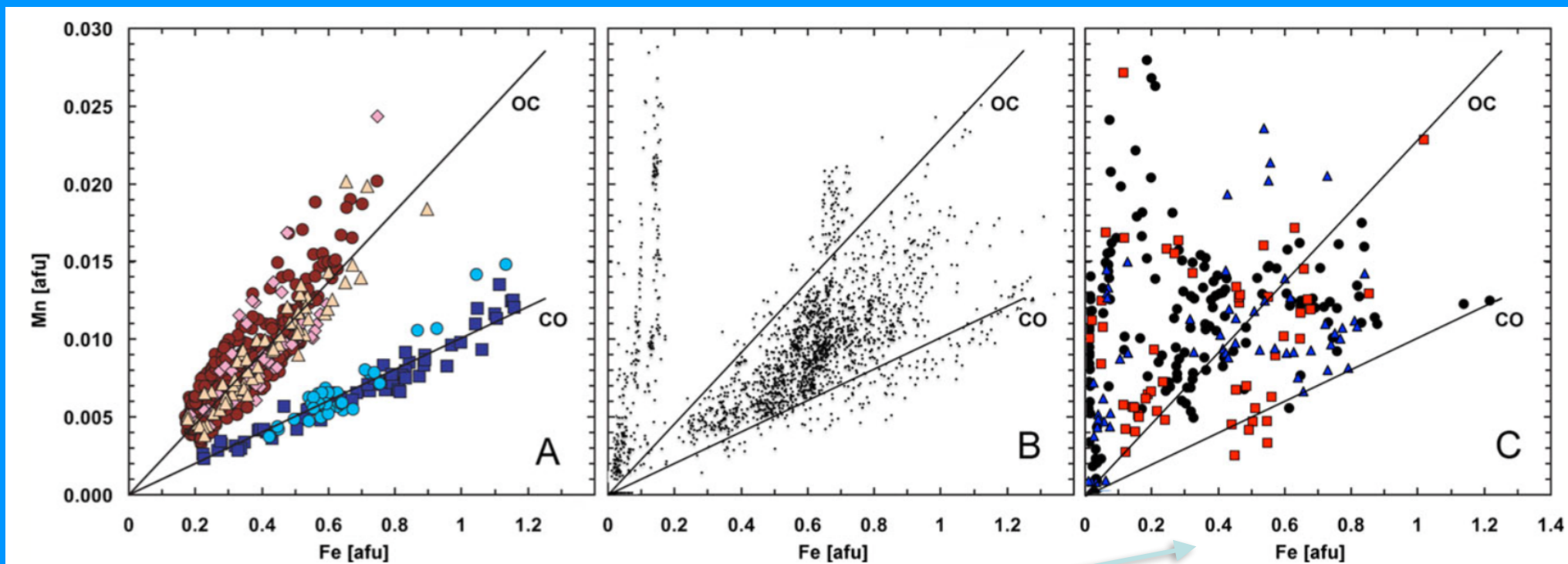
Stardust's olivines can be compared to CR chondrules (Schrader)



Range of increasing Mn-Fe lines could be 'zoning' or Schrader suggests 'discrete igneous systems' (like Iris)

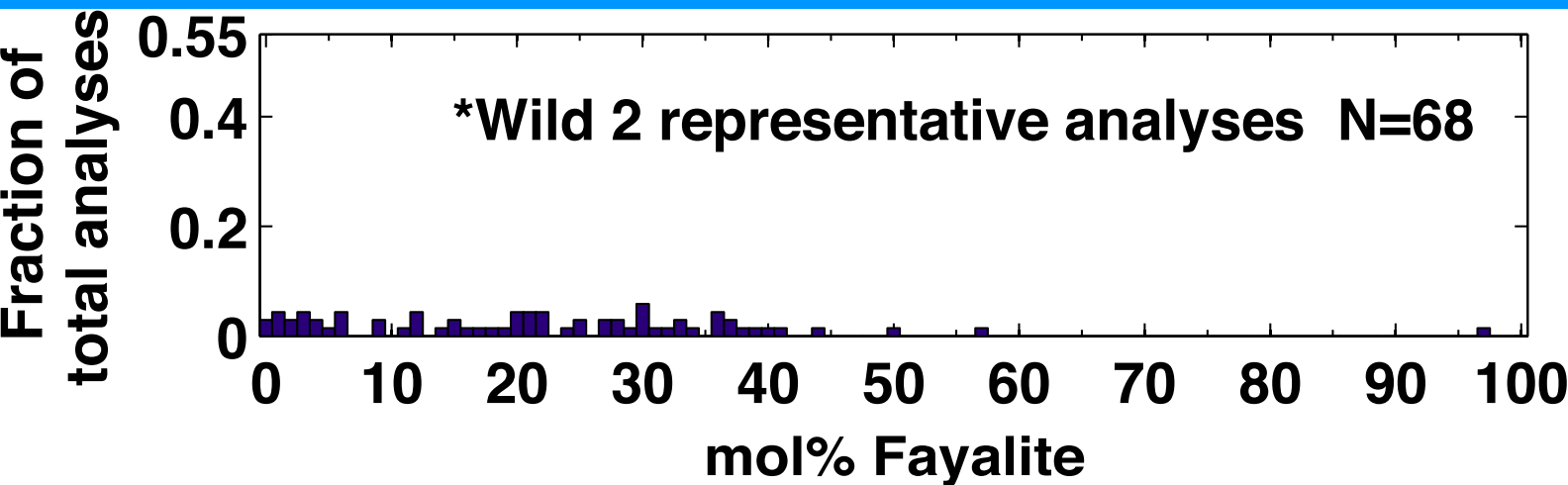
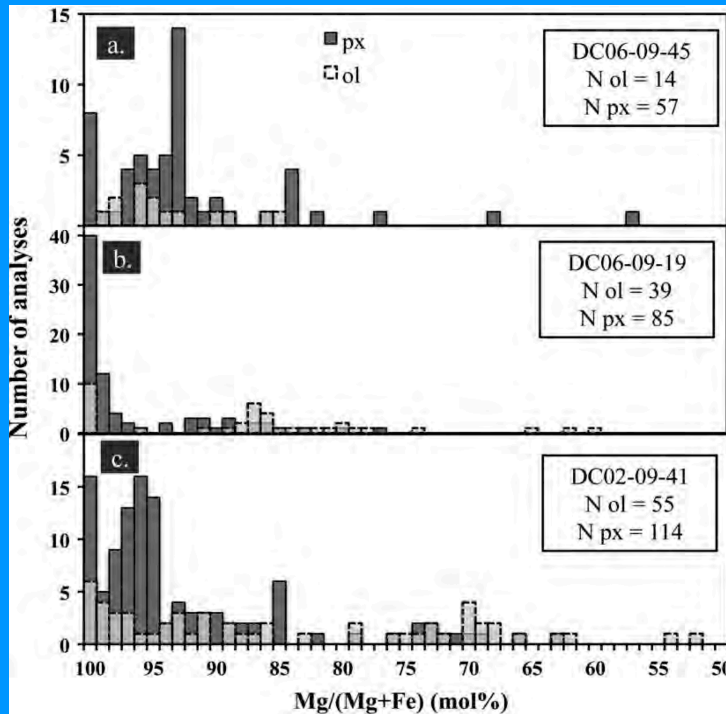


minor element Mn contents show ‘genetic’ relationship between olivines in Stardust and in Giant IDPs (‘C’) and carbonaceous chondrites (‘A’) and CR (‘B’)



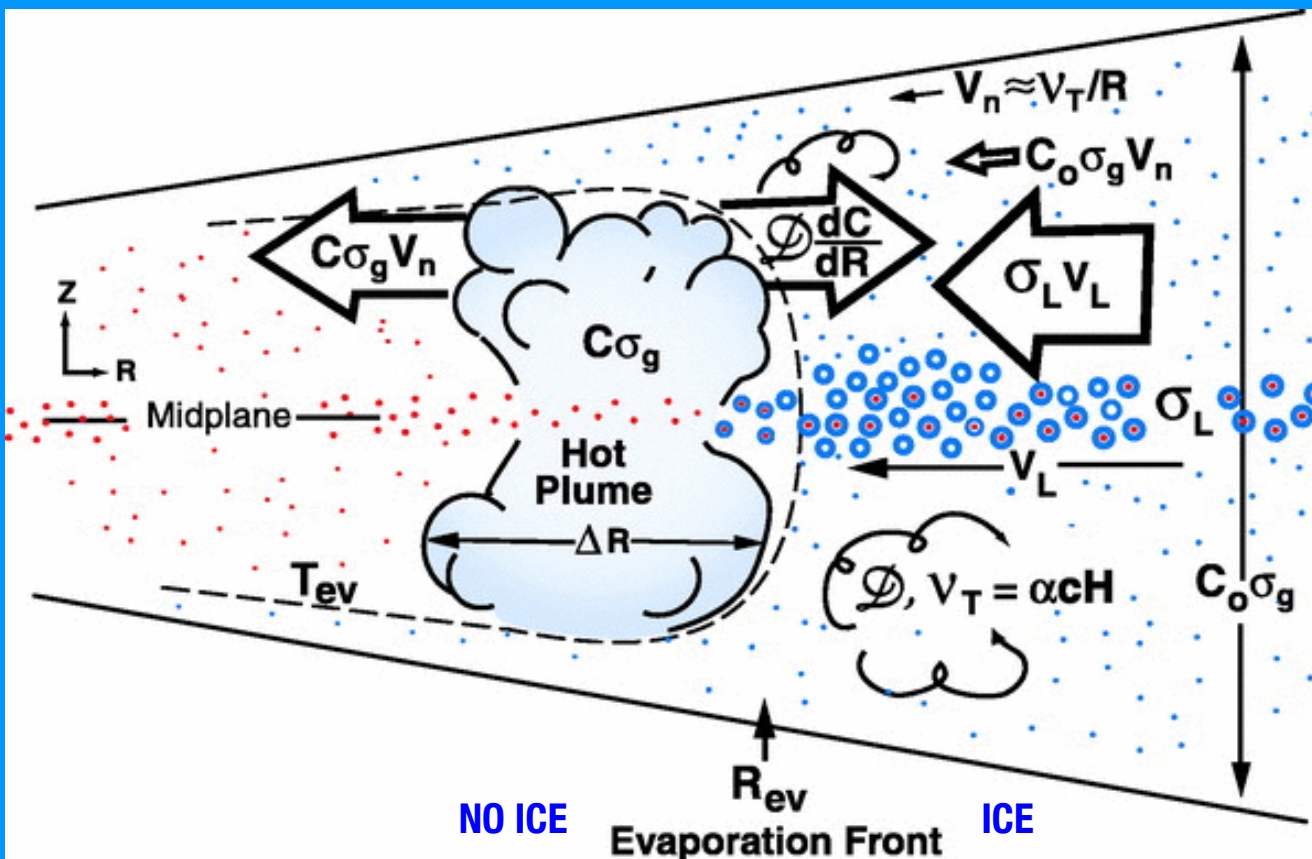
Cometary Wild 2 (Stardust = dots, triangles = Brownlee; Frank) and a Giant IDP (red squares) show comet olivines sample more conditions than any single primitive carbonaceous chondrite. Don Brownlee calls this a “decline in diversity” but I think it is more diversity. Words?

olivines Fo90 – ~Fo50 are not condensates,
they are μ chondrules



- Condensation of Fe-bearing silicates requires high oxygen fugacity in the solar nebula:
 - drive in silicate dust (silicates donate oxygen)
 - drive in ice grains (H_2O donates oxygen)

Cuzzi and Zahnle 2004



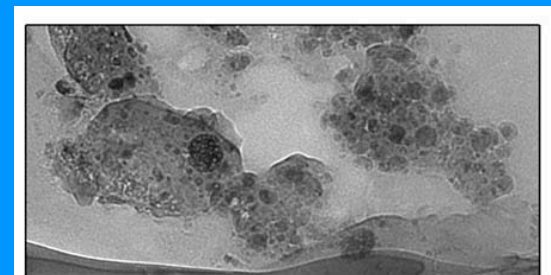
- Inward migration of cometsimals
- Outward transport of Fe-bearing silicates
- While comet grains are aggregating & before or during nuclei accretion

Other wild possibilities?

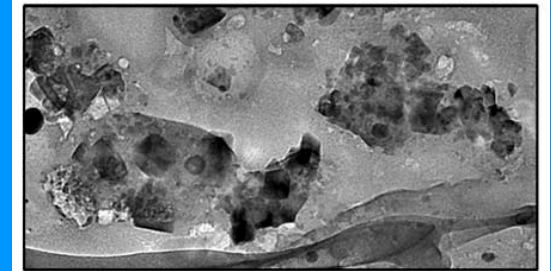
- » Could some of the dust ‘bunnies/rhinos’ that were heat-zapped to form chondrules have GEMS-like precursors?

Brownlee et al. 2005 LPSC COOKED GEMS — INSIGHTS INTO THE HOT ORIGIN OF CRYSTALLINE SILICATES IN CIRCUMSTELLAR DISKS AND THE COLD ORIGIN GEMS.

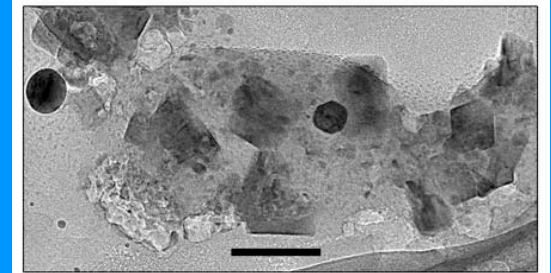
At just about 700 °C the typical GEMS texture of silicate glass with fine embedded metal and sulfides transforms to an igneous-like texture of silica rich glass and prominent subhedral to euhedral grains of moderately iron rich olivine and pyroxene. At such a temperature, this remarkable transformation occurs by sub-solidus processes.



Initial - U217B19 GEMS13

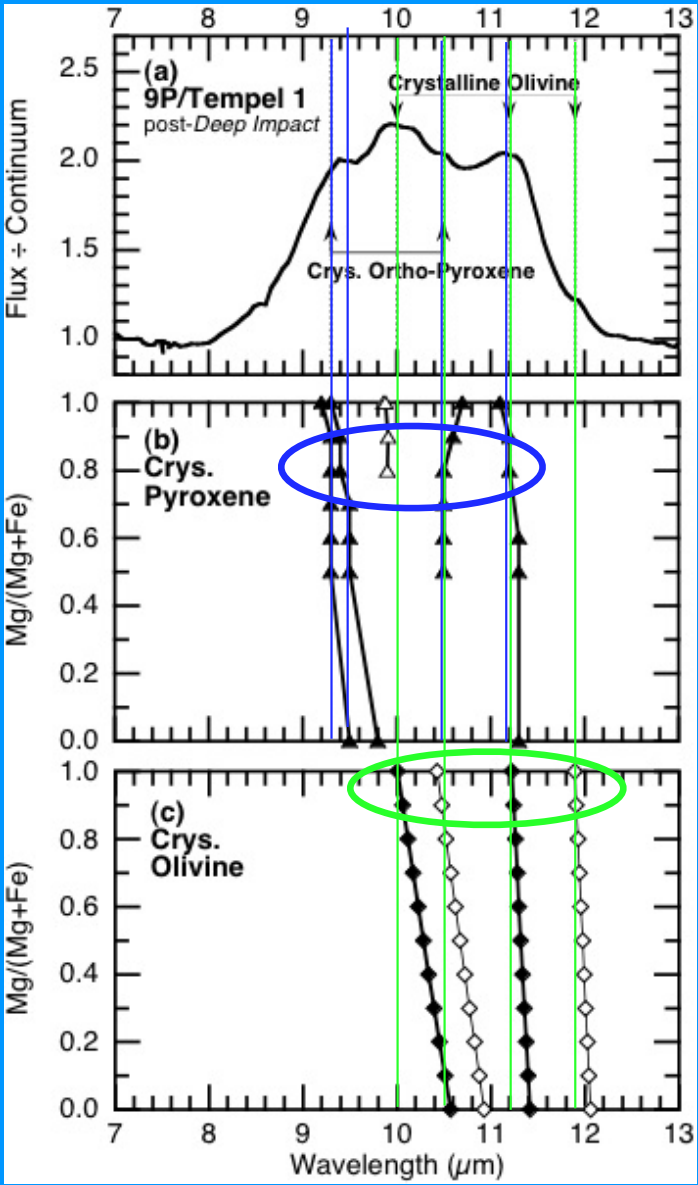


After heating to 970K



Enlargemen of above bar = 100nm

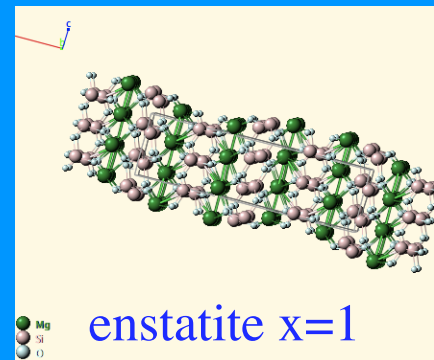
Mg-rich crystalline silicates dominate 10μm spectra of comet Hale-Bopp and are seen at some level in most all comets



Fo100 or Fa0
Forsterite

Fo0 or Fa100
Fayalite

- Mid-IR wavelength positions of crystalline resonance peaks show high Mg-contents:
 - crystalline pyroxene: $(Mg_x, Fe_{1-x}) SiO_3$ $0.7 \leq x \leq 0.9$
 - crystalline olivine: $(Mg_y, Fe_{1-y})_2 SiO_4$ $0.9 \leq y \leq 1.0$



Olivine: Koike et al. 2003, A&A 399, 1101
Pyroxene: Chihara et al. 2002, A&A 391, 267